ABSTRACT

PANZA, NICOLE MARIE. Modeling Follicle Wave Dynamics in the Menstrual Cycle. (Under the direction of James F. Selgrade.)

Though the discovery of the hormones that are critical to endocrine control of the human female reproductive system was made over eighty years ago, more recent technological advancements have provided additional information as to the mechanisms controlling the menstrual cycle. With ultrasound technology, scientists have been able to confirm the existence of ovarian follicle waves. It was long believed that a cohort of follicles is recruited once per cycle and from that cohort one follicle is selected to ovulate. It is now known that recruitment of more than one cohort of follicles occurs at regular intervals during each cycle. Each cohort is known as a follicle wave. Follicle waves were discovered in humans after their earlier discovery in animals, most notably horses and cows. The most prominent work in human follicle waves was conducted by Baerwald et al. [9, 10, 12]. The work was the first to measure follicle growth in conjunction with corresponding hormone concentrations. The results showed that none of the subjects had fewer than two follicle waves per cycle. It also showed that for every rise in the levels of follicle-stimulating hormone (FSH), a follicle wave emerges. Thus, follicle waves are a common occurrence and their emergence is a one-to-one relationship to rising levels of follicle-stimulating hormone. Any previous assumptions and work should be updated to include this phenomenon for biological accuracy and to help address any potential medical concerns that follicle waves may cause. One such work is the mathematical model for endocrine control of the human menstrual cycle.

Original work on the mathematical modeling of the human female reproductive cycle was done by Schlosser and Selgrade [87, 90], Harris-Clark et al., [30], Pasteur [78] and Pasteur and Selgrade [77]. Two sets of data compiled from the works of McLachlan et al. [66] and Welt et al. [98] were used for these models. The original model is a system of thirteen nonlinear, delay differential equations modeling five of the hormones that create a feedback loop between the hypothalamus-pituitary and the ovaries. It was later expanded to sixteen differential equations to allow for the inclusion of a sixth hormone. The original models were created under the assumption that recruitment and growth of the cohort of follicles occurs once each cycle. This work successfully builds upon the original five-hormone and six-hormone models to include two follicle waves per cycle for normally cycling women. The work is completed by first modeling just the ovarian component of the hormone loop and then taking the results and merging them with the pituitary component for a complete feedback system. The five-hormone system is successfully expanded to two waves for both the Welt and the McLachlan data sets in both the ovarian component and the full merged model. In addition, the six-hormone system is also

successfully expanded to two waves for the Welt data for the ovarian and merged models. In total, optimized parameters are obtained for six two-wave models. Sensitivity analysis is conducted on the merged five-hormone system parameters.

Though much research is needed on the biological ramifications of follicle waves, some ideas have arisen. One is that women who experience more than two follicle waves per cycle may reach menopause earlier than those who only have two waves each cycle. The hypothetical hormone interactions that could yield three follicle waves per cycle are tested in the ovarian and pituitary component models. The numerical experiment succeeded as the ovarian component produced three follicle waves per cycle and both component models yield the hypothesized hormone profiles as a result. It is also possible that follicle waves could cause a rare form of superfecundation, the fertilizing of two oocytes at two different points in time during one menstrual cycle resulting in dizygotic twins. Potentially if each follicle wave in one cycle ovulates both could be fertilized yielding two zygotes. Here the five-hormone merged model fit to the McLachlan data is successfully amended to show an ovulating follicle in each wave with appropriate corresponding hormones. Though there is still much to learn biologically, the mathematical model for endocrine control of the female menstrual cycle with follicle waves not only more accurately represents what is going on in the body but it also gives direction for future mathematical and biological research.

Modeling Follicle Wave Dynamics in the Menstrual Cycle

by
Nicole Marie Panza

A dissertation submitted to the Graduate Faculty of
North Carolina State University
in partial fulfillment of the
requirements for the Degree of
Doctor of Philosophy

Applied Mathematics

Raleigh, North Carolina

2015

APPROVED BY:

John Franke	Donald Martin
Mette Olufsen	James F. Selgrade Chair of Advisory Committee

BIOGRAPHY

Nicole was raised in Pittsburgh, Pennsylvania and graduated from Shaler Area High School in 2004. She went on to attend Westminster College in New Wilmington, Pennsylvania for her Bachelors of Science in Mathematics with minors in Computer Science and Secondary Education. In 2008, she graduated magna cum laude with college honors in mathematics. While there, she acquired her Pennsylvania Department of Education teaching certification for mathematics grades 7-12. Upon graduation she moved to Raleigh, North Carolina to attend North Carolina State University. She earned her Masters in Applied Mathematics in 2011 and her Doctorate in Applied Mathematics with minor in Statistics in 2015.

ACKNOWLEDGEMENTS

It is impossible to reflect on this journey without thinking about the people who loved and supported me along the way. I am forever grateful for the support from friends, family, peers and mentors. First and foremost, many thanks to my research advisor Dr. James Selgrade. Whether I needed a boost of confidence or a change in direction, I knew I could count on you for a kind word, a smile and an abundance of patience. I have learned so much from you as a researcher, a teacher and a mathematician. To my advisory committee, Dr. John Franke, Dr. Donald Martin and Dr. Mette Olufsen, your time, effort, support and expertise steered this work to an outcome even better than I had envisioned. I would not be writing this if it was not for the support from my Westminster family as well. I am grateful to Dr. Warren Hickman for asking if I had ever thought about going to graduate school. That conversation may have been simple for you, but it was life-changing for me. To Dr. Barbara Faires for always encouraging me to broaden my horizons and to try new things whether I wanted to or not and to Dr. Carolyn Cuff for nudging me into computer science, throwing me headfirst into my honors thesis and making the best brownies to help me get through it all. I am blessed to have been mentored by so many brilliant minds, supportive souls and kind hearts.

To my friends and family, each and every one of you knows me and knew exactly what to do to help me accomplish this goal. To Julie, Beth and Mandy, whether near or far, I knew I could count on a hug, a smile and a laugh to help me along the way and that we will always pick right back up from where we left off. To my Grandma Chulack who is the greatest example of hard work and to my Grandma Panza who is the most giving person I know. You both passed the best of what you are down to your grandchildren. To my Aunt Sharon and Uncle Bud, I can always count on a warm bed and something sweet from the oven on my journey home, a good kick on the tires and a mailbox full of greeting cards to make sure I am well taken care of. To Jeff, thanks for giving me hugs even though you do not like them. A truer friend and better brother would be hard to find. To my dear father, you taught me that hard work, logic and grace go a long way in work and in life. Thanks for always making sure I "take a break and then get right back to work." To my beautiful mother, you are the most stunning example of a strong, independent woman and I carry that example close to my heart. You may have struggled when you took calculus, but you helped me to reach way beyond it and to teach it to others. Each one of you has left an imprint on this work and my life forever.

Finally to my four-legged baby, Woodstock, you cannot even read this but I am grateful for your hugs and kisses, your unconditional love and for reminding me that a walk or a squeaky toy makes everything just a little bit better.

TABLE OF CONTENTS

LIST OF TABLES

LIST OF FIGURES

Chapter 1

Introduction

The number of women in the United States suffering from reproductive system disorders is of concern. In a study by the United States Center for Disease Control and Prevention (CDC) [26], in 2006-2010, it was predicted that 6% of all women between the ages of 15 and 44 are infertile and 12% of women in the same age group suffer from impaired fecundity. Infertility is defined as actively attempting to become pregnant each month over a twelve-month period of time with the same partner with no resulting pregnancy. Impaired fecundity is more broadly defined as difficulty in either becoming pregnant, carrying a pregnancy or delivering a live baby. It is also estimated that 12% of women aged 15-44 have used some form of fertility assistance in the process of becoming pregnant [27]. Though some countries provide public funding for assisted reproductive technologies (ART) to help these women achieve their goals, the United States provides next to nothing in terms of public support [31]. This along with the overall higher healthcare costs in the United States compared to other countries makes the United States the most expensive country for ART treatments. One cycle of in vitro fertilization (IVF) in the United States was estimated to cost just over $12,000 in a 2009 study [25]. Reproductive system disorders extend beyond fertility. Many life-threatening diseases attack the female reproductive system. The CDC [97] reports in its last data collection in 2011 that over 20,000 women had been diagnosed with ovarian cancer, over 12,000 with cervical cancer and over 220,000 with breast cancer. All of these issues, their resulting side effects and their remedies can be specifically linked to the endocrine control of the human female reproductive system.

Though the basics of the female reproductive system have been known for ages, the endocrine control of the menstrual cycle is a young area of research in comparison. This history is summarized in Table 1.1. It was originally stated in the fifth century B.C. by Hippocrates that male sperm and female menstrual blood formed a fetus [12]. A century later, Aristotle deemed the ovary an organ with no physical purpose [6]. It was not until the 1500's that the research on the reproductive system became more engaged. In Italy in the 16th century the study was

taken up again and passed down from mentor to mentee [40]. First, Vesalius through dissection discovered what is now known as ovarian follicles and the corpus luteum. His student Fallopius discovered the connection between the ovaries and the uterus known today as the Fallopian tubes. Finally, the student of Fallopius, Fabricus, discovered the organ in birds that houses their eggs and named it the ovary. Another student of the same university, William Harvey published the first book on the anatomy and physiology of reproduction claiming 'ex ova omnia', that all lifeforms start as an egg [12, 40]. Though it seems ovarian follicles were identified earlier, it was not published until 1672 in "New treatise concerning the generative organs of women," by Regnier de Graaf, a Dutch physician [6]. He believed the follicles themselves were the eggs and the ovary produced them. Ovarian follicles were later known as graafian follicles [40]. Not long after this publication, he became embattled with one of his peers and one of his professors who claimed they published the same findings weeks earlier [6]. A committee was assembled to look into the matter and their findings were that a third independent party published this result before everyone else. De Graaf was also the first to describe the corpus luteum in publication [40]. However, Marcello Malpighi is credited with giving it its name in papers that were discovered after his death and after de Graaf's publication. This anatomical knowledge stayed relatively the same until the early 1800's when Karl Ernst von Buer discovered during a hysterectomy on a dog that the follicles house the eggs and are not the eggs themselves equating the follicles to the shell on a bird's egg [6].

It was at this point in time that the endocrine contributions to the female reproductive system came to light. In the mid 1800's Carl Ludwig took note of how menstruation ends after a hysterectomy [105]. By the end of the century, it had been determined that chemicals from the ovaries were the cause of all of the changes. Edgar Allen's studies on mice and rats gave indication that the follicles themselves produce these chemicals. Edward Doisy and his research group isolated estrogen while George Corner isolated progesterone, the former in work on the follicles and the latter from the corpus luteum. As more and more reproductive health issues became linked to the pituitary, the 1930's saw the beginnings of the research to show their link. In Fevold et al. [38], the link was established in the discovery of luteinizing hormone and follicle-stimulating hormone. Around this time another link was being made with cycle disruptions. It seemed that stress was disturbing a woman's cycle which turned an eye toward the nervous system [105]. The gonadotropin-releasing hormone was discovered as the trigger from the hypothalamus on the hormone release from the pituitary. Ernest Knobil linked the frequency and pattern of these hormone pulses from the hypothalamus to the release of the luteinizing and follicle-stimulating hormones from the pituitary [74]. In the mid 1960's, Treloar [94] collected menstrual cycle data on the back of a postcard for women over the course of their lifetime beginning in their early twenties. He discovered that any cycle outside of the length of 21 to 35 days should be assumed abnormal.

Table 1.1 A historical summary of studies of the female reproductive cycle.

Date	Researcher	Contribution	Reference
400's B.C.	Hippocrates	Believed male sperm and female menstrual blood formed a fetus.	[12]
300's B.C.	Aristotle	Believed the ovary had no physical purpose.	[6]
1500's	Vesalius	Discovered ovarian follicles and corpus luteum through dissection.	[40]
1500's	Fallopius	Discovered the Fallopian tubes.	[40]
1500's	Fabricus	Determined the bird eggs are housed in the ovary.	[40]
1600's	Harvey	Published the first reproductive physiology textbook which claimed all life starts as an egg.	[12, 40]
1600's	De Graaf	Published "New treatise concerning the generative organs of women." Described ovarian production.	[6]
1600's	Malpighi	Discovered and named the corpus luteum.	[40]
1800's	Von Buer	Discovered that eggs are housed in ovarian follicles.	[6]
1800's	Ludwig	Linked end of menstrual cycle to hysterectomy.	[105]
1920's	Allen	Determined that follicles release hormones.	[105]
1920's	Doisy	Isolated follicle secretion of estrogen.	[105]
1920's	Corner	Isolated corpus luteum secretion of progesterone.	[105]
1930's	Fevold	Linked pituitary hormone secretion to reproductive health.	[38]
1960's	Treloar	Determined normal menstrual cycle length.	[94]
1960	Rajakoski	Discovered multiple waves of follicle recruitment and growth in the bovine estrous cycle.	[84]
1970's	Knobil	Linked hormone pulses from hypothalamus to release of pituitary hormones controlling reproductive health.	[74]
1996	Gougeon	Established stages of ovarian follicle growth.	[45]
2003	Baerwald	Linked follicle waves in humans with corresponding hormone concentrations.	[9, 10]

There was only so much that could be gleaned from the methods available to this point in history. Endocrinology could be performed with little harm to the research subjects. Hysterectomies could give information about the mechanisms in the organs at the time they were removed. Knowing what happens over the course of the cycle was hard to piece together without being able to look at a live person or animal with organs in tact.

In 1960, Rajakoski [84] published work stating that the bovine estrous cycle had two waves of follicular growth per cycle. This work was considered groundbreaking as to the previous belief that follicles grew once per cycle. However in the years following, conflicting results were obtained from researchers trying to substantiate his claims [6]. Some found only one wave of growth, some found up to four and some even believed that new growth was continuously occurring. The lack of technology to view live ovaries created a thirty year disagreement.

Finally in the late 1970's researchers took their first live look at ovaries using transabdominal ultrasound [12]. This tool was able to illustrate follicle growth and atresia. In 1984, Pierson and Ginther [80] were the first to use ultrasound technology to confirm the existence of follicle waves in the bovine estrous cycle. By the late 1980's, the transvaginal ultrasound provided a look at the smaller follicles in growth. Ultrasound technology confirmed that follicle waves occur, but not every wave ovulates [6]. It shows that a wave is chosen, from that wave one follicle is selected to grow larger than the rest while the others undergo atresia and this large, dominant follicle ovulates which suppresses the further growth of any follicles at this time. Work by Gougeon [45] in 1996 established a classification for the stages of growth of ovarian follicles. In 2003, Baerwald et al. [9, 10] was the first research group to identify follicle waves in humans with hormone profiles. Later works have shown that these waves continue through the menopause transition and are more pronounced with women undergoing ovarian stimulation therapy [12]. To glean this information, all three areas of study, histology, endocrinology and ultrasonography, give the full picture as to what is happening in the female reproductive system. Knowing all of the intricacies of the cycle is important in the effort of helping women maintain their reproductive health.

Many substances, known as endocrine disrupting compounds, and behaviors can cause cycle abnormalities potentially resulting in health concerns. Endocrine disrupting compounds are natural or synthetic substances that disrupt the normal endocrine operation of physiological processes [32]. Endocrine disrupting compounds have been found in food, detergents, solvents, pesticides, plastic additives, food wrappers and cans and water supplies [102]. A listing of common endocrine disruptors is included in Table 1.2. Many endocrine disrupting compounds are byproducts of industrial progress such as Dichloro-diphenyl-trichloroethane (DDT) which was created in 1924 as a pesticide [65]. It is now classified as an unsafe endocrine disruptor and it was banned in the United States in the 1970's. Diethylstilbestrol (DES) was created to mimic estrogen to help prevent miscarriages. Its use was discontinued in 1971 after studies showed that

the daughters of mothers who took DES had higher rates of cervical, vaginal and breast cancers, infertility and early menopause [32, 65]. Behaviors, lifestyle habits and physical characteristics such as stress, amount of physical activity, age, weight, sexually transmitted diseases, caffeine consumption, eating particular foods and smoking habits can also disrupt the cycle [23, 28].

Table 1.2 Endocrine disruptors alter a woman's normal menstrual cycle. Some endocrine disruptors are chemicals known as endocrine disrupting compounds that are found in items such as food, pollutants, household cleaners and food wrappers. Other disruptions can be caused by behaviors and actions that a woman does or does not take part in. The following table addresses both common compounds and behaviors that can cause serious cycle disorders [23, 32, 65, 102].

Chemical Substances	**Lifestyle habits**
Benzene	Lacking physical activity
Diethylstilbestrol (DES)	Consuming caffeine
Polychlorinated biphenyls (PCBs)	Contracting a sexually transmitted disease
Dichloro-diphenyl-trichloroethane (DDT)	Eating foods high in insulin, trans fats and proteins
Bisphenol A (BPA)	Smoking

These endocrine disrupting compounds can directly affect the synthesis, release and clearance of hormones from both the pituitary and the ovaries and how they interact with each other [23]. A table of medical concerns due to endocrine disruptors is included in Table 1.3. In a study of 48 endocrine disrupting compounds, 79% were shown to be carcinogenic, 52% to be immunotoxic and 50% to be neurotoxic [29]. The most frightening information about endocrine disruptors is that when more than one compound is affecting a woman, its combined influence is greater than the sum of the individual parts so a compounding effect may occur [65]. Women's health is of great concern with so many substances in common household items and in environmental pollutants silently affecting the ability to reproduce. Developing methods to address these concerns is vital to women's health studies.

Fertility is a growing concern for women. The percentage of women who experience fertility issues jumps from 10% for women in their early twenties to 30% for women in their early forties [28]. Most women who seek reproductive assistance in the United States are typically married, older, non-Hispanic white, well-educated and with a good socioeconomic status [27]. Lack of public support for these treatments in the United States likely excludes much of the population. As of 2014, only fifteen states require health insurance to cover them. The Family Act of 2013 was proposed but never passed in the United States Senate and House of Representatives calling

Table 1.3 Health consequences of endocrine disrupting compounds for women [32, 102].

Polycystic ovarian syndrome (PCOS)
Irregular menstrual cycles
Anovulatory cycles
Reduced quality and quantity of follicles and eggs
Premature ovarian failure
Endometriosis
Cancers
Heart disease
Osteoporosis
Alzheimer's disease

for a tax credit to families seeking medical assistance for reproduction [1].

Perhaps as more studies are done on the cycle, these treatments may become more affordable. Ovarian stimulation by follicle-stimulating hormone increases the number of dominant follicles [93]. In a recent study, it was shown that synchronizing the follicle-stimulating hormone treatment with each follicle wave a woman has increases the number of dominant follicles that develop and thus the estrogen concentration [14]. Unfortunately, after insemination no improvements to the previous pregnancy rates were observed. Studies like these help pinpoint more precise cycle mechanisms and hone the treatments available to address cycle disruptions.

Over the past century, much has been learned about how the cycle works and what problems could arise affecting the cycle. One method of studying the cycle in a cost-effective and noninvasive way is by mathematically modeling the endocrine control of the menstrual cycle. As in all mathematical biology scenarios, the biological research helps to develop and improve the mathematical model and the mathematical model can be used to test hypothesis and treatments in the most ethical way possible giving direction for further biological studies. Much of the initial work modeling the cycle was done by Schwartz [89], Bogumil et al. [20, 21] and Plouffe and Luxenberg [81]. The original model of the cycle that this work is based on was developed by Schlosser and Selgrade [87, 90] and has gone through many improvements and upgrades from its initial form.

This work will expand the model to include ovarian follicle waves for biological accuracy and for use in hypothesis testing for medical concerns. Ovarian follicle waves should be included in the model because in a study by Baerwald et al. [9], all women in the study had no fewer than two waves per cycle. Medical concerns that the follicle wave model could help address are the plausibility of follicle wave superfecundation and the discovery of the specific hormone

balance needed for more than two follicle waves per cycle which could lead to early menopause. Women's reproductive health has become an important area of research due to the gravity of the issues affecting fertility and long term health. The physical, emotional and financial costs of attempting to remedy these situations are staggering. With infertility and cancer, even if one can afford all of the costs no guarantees can be made as to the outcome. Mathematical modeling of endocrine control of the human female reproductive system including follicle waves can give an accurate representation of what is happening in the body and the opportunity to test ideas on a computer simulation instead of on a person.

The following chapters will discuss the mathematical model for endocrine control of the menstrual cycle with follicle waves and its uses:

Chapter 2: An in-depth biological background including discussion on follicle selection, follicle waves and the data sets available for normally cycling women sets the scene for how the model was developed.

Chapter 3: The five-hormone, two-wave model is discussed with results for two different data sets. Parameter sensitivities are examined for the exploration of model behavior.

Chapter 4: The six-hormone, two-wave model is discussed with results for one data set.

Chapter 5: The working models are used to examine two proposed biological consequences of ovarian follicle waves, early menopause and follicle wave superfecundation.

Chapter 6: Concluding thoughts and ways to continue this work are discussed.

Chapter 2

Biological Background

Each human menstrual cycle, one follicle ovulates out of all the follicles left in a woman's ovarian follicle reserve. Follicle selection is a two part process. The first is the recruitment of a cohort of approximately a dozen follicles to grow larger to compete to be the ovulating follicle. The second is the selection of a dominant follicle to ovulate from that cohort. It was originally believed that the first part of the process, recruitment, occured once per cycle. But that was based on the known fact that the selection of the dominant follicle and subsequent ovulation only occurs once per cycle. Now it is known that recruitment occurs more than once per cycle in what are now known as follicle waves. This chapter addresses three issues necessary to building a mathematical model for endocrine control of the human menstrual cycle with follicle waves. The first is the process of follicle selection. The second is the biology of follicle waves and how waves expand the previous beliefs on follicle selection. The third is the data for normally cycling women that will later be used for modeling purposes. The aim of this chapter is to provide the biological foundation needed to understand how the cycle should be modeled.

2.1 Follicle Selection

The purpose of endocrine control of the female reproductive system is to select and release oocytes for potential fertilization. Folliculogenesis is the process of development and selection of an oocyte for ovulation [63]. The menstrual cycle is the process of doing so repeatedly until a fertilization event occurs. A woman typically has 36 years for which the ovaries can complete this task [8]. The cycle repeats during that time until the body exhausts the pool of oocytes [51]. After one year of anovulation due to a greatly reduced pool of oocytes, menopause has occurred [75]. Oocytes are only created during gestation in a process called oogenesis [100]. The number generated can range from six to seven million in total [16]. At birth however, only one to two million will have survived due to apoptosis or programmed cell death. The oocytes

are stored in somatic cells, both granulosa and theca, and together are known as follicles [74]. Understanding folliculogenesis answers the questions of how one follicle is selected for ovulation and what happens to the remaining millions of oocytes a woman had at birth.

The menstrual cycle is known as the interval between the start of menses [68]. The event of ovulation, releasing the oocyte from a follicle, splits the cycle into two parts, the follicular phase and the luteal phase. Figure 2.1 illustrates the cycle phases. On average, a typical cycle length is 28 days with a follicular phase lasting 14.6 days and the luteal phase lasting 13.6 days [36]. Approximately 400 oocytes are released during the reproductive years [74].

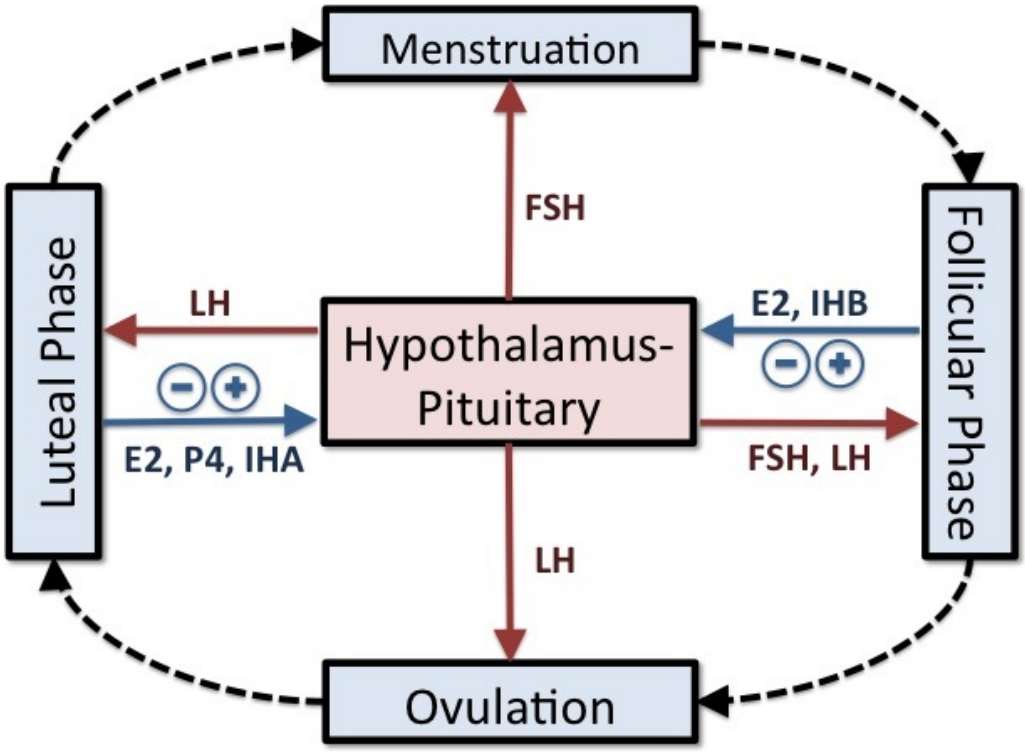

Figure 2.1 The hypothalamus-pituitary and ovaries create a hormone feedback loop for the female reproductive system. Two hormones, FSH and LH, are secreted by the pituitary to stimulate growth of follicles in the ovaries. The follicles and subsequent corpus luteum in the ovaries in turn produce E2, P4, IHA and IHB which regulate the synthesis and release of FSH and LH. The cycle begins at menstruation with follicle recruitment. Follicle growth continues in the follicular phase with the influx of FSH and LH. Ovulation is triggered by the LH surge. The corpus luteum grows during the luteal phase and secretes ovarian hormones. If fertilization does not occur, the corpus luteum degenerates and the cycle begins again. Because ovarian hormones can both feedback positively and negatively on the pituitary, +/- are used to illustrate that behavior.

The menstrual cycle is a feedback system between the hypothalamus-pituitary and the ovaries. Figure 2.1 illustrates this process. The cycle begins in the hypothalamus which discharges gonadotropin-releasing hormone (GnRH) [51]. Gonadotropin cells in the pituitary produce lutenizing hormone (LH) and follicle-stimulating hormone (FSH) in response to pulses of GnRH from the hypothalamus [74]. GnRH triggers LH and FSH to be released from the pituitary [51]. Both LH and FSH are glycoproteins and are used to regulate the ovaries [74]. The ovaries in response to LH and FSH release their own hormones estrogen (E2) and progesterone (P4) which at normal levels feedback on the pituitary [51]. Thus, the release of FSH and LH are regulated not only by GnRH, but also by E2 and P4. Also secreted by the ovary is the peptide hormone inhibin. Inhibin is made up of an α-subunit and a β-subunit [56]. The β-subunit can be of two forms, βA, known as inhibin A (IHA), or βB, known as inhibin B (IHB). IHA and IHB also help regulate the pituitary hormones by a negative feedback process [100]. The feedback relationship between the pituitary and ovarian hormones is illustrated in Figure 2.1. The theca cells and granulosa cells on the follicles in the ovaries are responsible for the production of ovarian hormones [74]. The theca cells contain receptors that respond to LH secretions while the granulosa cells contain receptors for FSH. With these six hormones in constant harmony, folliculogenesis can occur.

Though ovarian follicles are created long before the cycle even begins, they are not fully prepared to release their oocytes at that time. Figure 2.2 illustrates this growth process. At about week five or six of gestation, germ cells begin to develop [51]. These germ cells are the oocytes and by birth have multiplied in number. No additional oocytes are created after birth. The oocytes are surrounded by flattened granulosa cells at this time and are called primordial follicles [60]. These flattened granulosa cells are sometimes called pre-granulosa cells [51]. The oocytes go into meiotic arrest until puberty [100]. Folliculogenesis begins with the growth of these primordial follicles. The first step of primordial follicle growth occurs when the flattened granulosa cells become cuboidal and begin dividing [60]. When more than one layer of granulosa cells surround the oocyte, the follicle is known as preantral.

The number of layers of granulosa cells on the preantral follicle continue to increase as the follicle grows [104]. As layers of granulosa cells are added, fluid begins to emerge between the cells [79]. These preantral follicles also have FSH receptors in the granulosa cells, making them available to future growth if an influx of FSH occurs [100]. When the number of layers of granulosa cells on the preantral follicle is between six and seven, a layer of theca cells emerges. A follicle with both granulosa and theca cells is known as a small antral follicle. A small antral follicle is typically between 2 and 4 mm in diameter [15]. Theca cells have receptors for LH, so the small antral follicle has the opportunity to develop further contingent on the availability of LH and FSH [74]. Since the receptors for LH and FSH are not present until later in development, little presence of hormones is needed for the development to the small antral stage. To grow

beyond the small antral stage, higher concentrations of FSH and LH are necessary. All follicles not receiving hormones to further stimulate growth undergo atresia. Atresia entails both follicle cell and egg death [100]. Primordial follicle growth is constantly occurring, but small antral follicle growth is periodic, dependent on FSH and LH [64].

Periodic follicle recruitment starts from the small antral stage of follicle growth. Recruitment is defined as a handful of small antral follicles growing in response to an influx of FSH to become antral follicles [86]. Antral follicles are known for their antral cavities that form when the fluid between the granulosa cells gathers in the center of the follicle [79]. It is believed that recruitment occurs when FSH reaches a particular concentration called the FSH threshold [24]. The FSH window or gate is the length of time the FSH concentration is above the threshold [15]. When FSH rises above the threshold, recruitment occurs and the selected small antral follicles continue to grow [51]. If recruitment does not occur, the small antral follicles that have developed are not able to grow beyond that stage and will undergo atresia. In the very early follicular phase, IHB is high suppressing FSH [68]. Then, IHB levels decrease allowing FSH to rise and if it surpasses the threshold, recruitment occurs. Thus, at follicle selection, FSH is high but it has been shown that E2 is low so there is an inverse relationship between their levels [100]. Ovarian hormones E2 and P4 also determine the pattern of LH concentrations [73].

After recruitment occurs, FSH levels are still high enough to maintain growth of this cohort. Folliculogenesis is the process of developing and selecting one follicle for ovulation. This follicle is known as the dominant follicle because it grew larger than the rest. In the late follicular phase, FSH levels begin to decrease due to a rise in E2 and IHB [86]. The larger the cohort grows, the more theca and granulosa cells available to secrete even more E2 and IHA triggering the pituitary to slow the release of FSH [100]. The rise in E2 designates the selection of the dominant follicle [10, 42].

At the point in which FSH is once again below its growth threshold, the FSH window has closed and follicle growth is no longer possible for the remainder of the follicles not selected as the dominant follicle [74]. Thus, the rest of the cohort undergoes atresia. It is believed that the dominant follicle does not need as much FSH to continue its growth, so while the FSH levels have decreased enough so that the rest of the cohort cannot maintain growth, the dominant follicle has just enough to maintain its course [100]. It is also believed that the dominant follicle has more granulosa cells with more FSH receptors making it more sensitive to FSH needing less than before to continue its growth. No order or pattern has been found as to which ovary, the left or the right, contains the dominant follicle during any given cycle [36]. It is believed that the width of the FSH window may play a part in how many and which follicles are recruited and promoted for growth [15]. If the window is wide enough, more than one dominant follicle could be selected for ovulation which could potentially result in multiple births if fertilized [86]. Schipper et al. [86] has shown that the width of the window may affect how many dominant

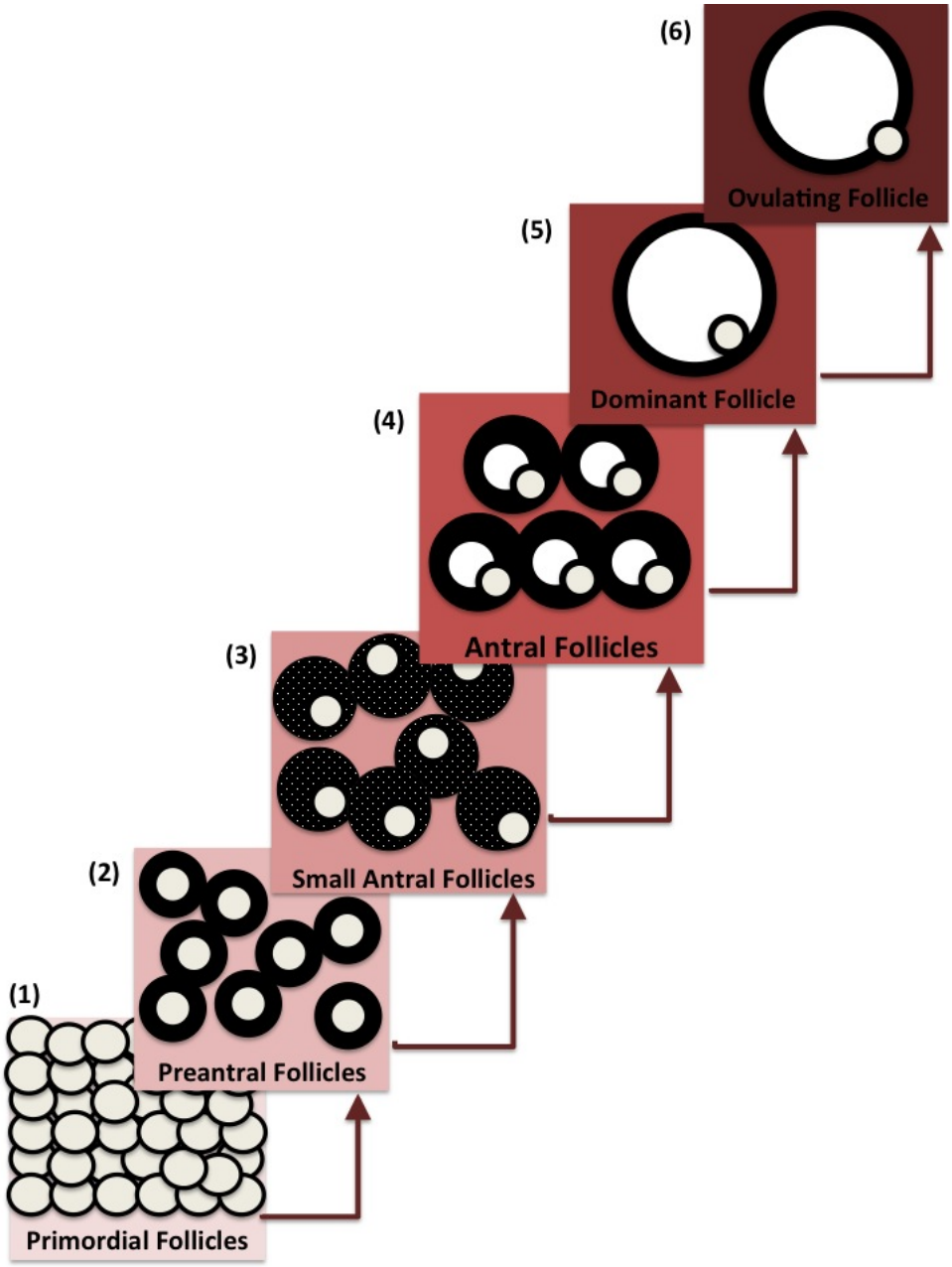

Figure 2.2 The process of folliculogenesis is illustrated here: **(1)** Primordial follicles are oocytes surrounded by flattened granulosa cells and are the follicles a woman is born with which are dormant until puberty. **(2)** Preantral follicles have more than one layer of granulosa cells that have turned cuboidal. **(3)** Small antral follicles have many layers of granulosa cells, a layer of theca cells and antral fluid between cells. **(4)** Antral follicles are cohorts of follicles selected to grow larger and are marked by the fluid between cells gathering to form a cavity in the center of the follicle. **(5)** One dominant follicle is chosen to grow larger than the rest. **(6)** The dominant follicle ovulates.

follicles are selected even more so than if the amount of FSH is very much higher than the threshold.

At this point, the dominant follicle that was selected has been growing for about five cycles as it prepares for ovulation [46]. The dominant follicle is on average 6mm in diameter at recruitment, 10mm when chosen as the dominant follicle and around 21mm at ovulation [43]. FSH is continuing to decrease after the selection of the dominant follicle as E2 continues to increase. IHA has a similar release pattern to E2 so in the late follicular phase, its level is high [100]. Also, P4 is on the rise.

Ovulation occurs at the end of the follicular phase. The rising levels of E2 and a slight increase in P4 trigger the LH surge, a spike in the concentration [75]. The LH surge occurs about eighteen hours prior to and causes ovulation, the release of the oocyte from the dominant follicle and the luteal phase begins [100]. Once the oocyte has been released, the remainder of the follicle becomes the corpus luteum which secretes ovarian hormones in preparation for pregnancy if the oocyte is fertilized. The corpus luteum has an interior fluid filled cavity that grows after ovulation [11]. As with follicle growth, the larger the corpus luteum grows, the higher concentration of ovarian hormones secreted [72]. FSH is again suppressed at this time due to the higher ovarian hormone levels [104]. If the oocyte is not fertilized, the corpus luteum and consequentially the ovarian hormones it produces to support a pregnancy are no longer needed [51]. The corpus luteum degenerates and as it becomes smaller the ovarian hormone levels decrease. As these levels drop, GnRH pulses increase and subsequently allow FSH to increase during the late luteal phase approximately four days prior to menses [69]. The rise of FSH once again marks the end of the luteal phase and the start of the next cycle [68].

2.2 Follicle Waves

Though many biological process have been long known, advances in technology are allowing scientists to reexamine what we previously believed to be true. For the menstrual cycle, the groundbreaking discovery of FSH and LH was made over 80 years ago and yet there is still much to learn about how the cycle works [38]. One of the most current research breakthroughs is the discovery of ovarian follicle waves. A follicle wave occurs every time follicle recruitment takes place [10]. The word wave suggests recruitment occurs constantly and periodically throughout the cycle. It was originally assumed that follicle development was strictly a follicular phase event because luteal phase progesterone from the corpus luteum would suppress development of more follicles however some reports of luteal growth refute this idea [9].

It was first thought that a woman experiencing luteal phase recruitment must be suffering from an abnormal cycle or a medical issue [9]. Original conclusions were drawn from interpolating hormone results or from ovarectomy examinations due to the lack of technology available at

the time. With the development of transabdominal ultrasound in the 1970's and transvaginal ultrasound in the 1980's, visuals of follicle growth in women were available for the first time [12]. It was used to confirm that most women experience more than one wave of follicle growth per cycle. Besides the lacking technology, data collection practices may also account for overlooking follicle waves.

Many animals such as cattle, horses, sheep, goats, deer and primates have been shown to exhibit follicle waves [12]. Follicles in cattle, mares and sheep grow to dominance and ovulate throughout the entire cycle similar to women [39]. Ginther et al. [43] has spent much time comparing mares with women while Adams et al. [5] has compared cattle with women. Animal studies help direct human studies, but because of ethical and logistical restrictions on human studies no exact relationships are known for certain [12]. Horses exhibit multiple follicle waves and like women have only one follicle reach dominance per cycle regardless of how many waves a mare has per cycle [44]. Women and horses have follicles that grow proportionately in size and have similar growth times, growth diameters and cycle interval lengths [43].

Much research has been done on bovine follicle waves. Two waves of follicle growth in cattle were first proposed by Rajakoski [84]. The idea was not corroborated until the late 1980's when ultrasound technology improved [92]. Two or three follicle waves per cycle are now known to occur regularly per estrous cycle [19]. A bovine follicle wave is defined as a cohort of between 8 and 41 follicles that grow for two days before one is selected to become dominant and the rest undergo atresia caused by progesterone [3]. Each bovine follicle wave has one follicle reach dominance, but only one wave per cycle ovulates. Adams et al. [6] reported that most cattle exhibit two or three follicle waves per cycle and that regardless of the number of waves per cycle, the first wave emerges at ovulation. It was found that for two-wave cycles the second wave emerges 9 or 10 days after ovulation. For three-wave cycles, the second wave emerges 8 or 9 days after ovulation and the third wave emerges 15 or 16 days after ovulation. Two-wave cycles are three days shorter than three-wave cycles on average [53]. When the corpus luteum from the previous ovulating follicle begins to regress, the next ovulating follicle wave emerges [6]. Thus, since the corpus luteum in the two-wave case regresses earlier than in the three-wave case, the lifespan of the corpus luteum may dictate the number of follicle waves per cycle [53]. Also, since the dominant follicle suppresses further follicle growth as it gets larger, the time it takes to develop can delay the growth of subsequent waves and thus dictate the number of waves per cycle [5].

No differences in resulting fertility and health were noted between cattle with two versus three follicle waves per cycle [101]. Many different factors have been examined as to the cause of two versus three follicle waves. Heat stress, parity and nutrition were shown to cause more follicle waves per cycle but age, breed and season of the year were not [6, 18]. The number of waves per cycle can switch from cycle to cycle [53, 83, 85]. Thus, cattle may not consistently

have two waves or three waves each cycle over the course of their lifespans. It has been shown that 70% of cycles repeated the same pattern while 30% switched between two and three waves per cycle [53]. It has also been shown that the wave emerges concurrently in both the left and right ovary and that the ovary from which the dominant follicle is selected is random [41].

Cauterization of cattle dominant follicles has shown that lower E2 and inhibin causes an FSH surge approximately one day later and thus causes an earlier emergence of the next wave [4]. Lower FSH and IHA levels have been found in anovulatory waves from three-wave cows versus two-wave cows and may imply that these hormones affect the number of waves per cycle as well [76]. When immunizing cows for IHA, the levels of FSH were able to increase and a subsequent increase in the number of waves per cycle was indicated [67]. Thus, FSH has been shown to influence wave recruitment in addition to dominant follicle selection [4]. It was later shown that for every surge of FSH, a follicle wave emerges [2].

Both equine and bovine follicle waves have taught researchers much about follicle development in women. Table 2.1 compares and contrasts bovine and human follicle waves. In the late 1980's, two follicle waves per cycle with longer cycle lengths were reported after using transabdominal ultrasound [34, 47]. Baerwald et al. [9, 10] was the first to use transvaginal ultrasound to detect ovarian follicle waves while measuring for hormone levels. Ultrasound images were collected daily from the women in the study while blood was drawn every three days [9]. The blood was drawn from women by staggering the days so that some women had day 1, day 4, day 7, etc., others had day 2, day 5, day 8, etc. and so on [10]. This procedure ensures that blood measurements were collected for every day of a cycle but prevents any woman from having blood drawn daily which is considered unfavorable from test subjects. Though the ultrasound is now able to give a glimpse of growth and atresia of antral follicles, it cannot detect small antral follicles or previous stages of growth, typically anything under 2mm in diameter.

Table 2.1 A comparison of bovine and human ovarian follicle waves [3, 9, 10, 12, 19, 34, 47, 53].

	Bovine	**Human**
Number of Waves per Cycle	Two or three	Two or three
Number of Waves per Cycle with Dominant Follicles	All	One
Number of Waves per Cycle that Ovulate	One	One
Two-Wave vs. Three-wave Cycle Length	Three-wave cycle longer than two-wave cycle	Three-wave cycle longer than two-wave cycle
Cause of Follicle Waves	Rise in FSH	Rise in FSH

In the study, 63 women who were deemed premenopause and healthy were selected for daily ultrasounds from one ovulation to another [9]. Only 50 were included in analysis because 13 others had cycle or ovarian disruptions. Two waves, a follicular phase wave resulting in ovulation and a luteal phase anovulatory wave were discovered in 68% of the women. The other 32% had three waves per cycle, a very early follicular phase, nonovulatory wave, the standard follicular phase ovulatory wave, and an anovulatory luteal phase wave. No women had one follicle wave per cycle. An increase in FSH was detected prior to the emergence of a wave [9].

Figure 2.3 from Baerwald et al. [12] shows that the two-wave follicle growth is accompanied by the hormone levels that have been long considered normal for healthy women [12]. The three-wave hormones concentrations were quite similar but not exactly the same as the two-wave case. Though close in concentration levels, these minor differences as seen in Figure 2.4 could have monumental consequences. Again, from the hormone levels we can see that the two-wave case has two surges of FSH and the three-wave case has three surges of FSH which is consistent with the bovine results. No size differences were observed in follicle diameter based on the number of waves per cycle [10]. As in bovine wave studies, it was shown that the length of the human cycle is based on the follicle growth dynamics as well [9]. Thus like cattle, the more waves per human menstrual cycle implies the longer the cycle length [10]. The left and right ovaries were examined as a whole, because there were no differences or patterns detected between the left and right ovaries based on wave emergence and dominant follicle emergence. The number of waves per cycle was not dictated by age, physical characteristics, environmental conditions or social factors. Like horses, only one follicle per cycle grew to be dominant due to the luteal levels of E2 and P4 [12]. IHA, IHB and anti-müllerian hormone (AHM) are also believed to prohibit the luteal phase wave from achieving a dominant follicle [48]. However, it has been shown that selection of a dominant follicle may occur more than once per cycle, but only one ovulates per cycle [9]. The presence of P4 in the luteal phase does not allow the luteal phase wave to ovulate because it prevents another LH surge [10]. No difference has been reported in hormone secretion or the size of the corups luteum in two-wave versus three-wave cycles [11]. It also seems that the more waves that occur, the higher the concentration of luteal E2 present but the source of the E2 is unknown as both the corpus luteum and a luteal wave could be responsible [12]. E2 has also been shown to increase earlier in three-wave situations than in two-wave cases [9].

More research should be done as to specific environmental and biological factors causing these waves [12]. It is hypothesized that the number of waves per cycle may indicate an earlier arrival at menopause and knowing how many waves a woman experiences each cycle may increase the opportunities for fertility treatments and optimize the chances for conception. Though the discovery of follicle waves debunks the century-old belief that follicle recruitment only occurs once per cycle, the recruitment class that ovulates, it is clear that knowing more

about these waves could have drastic impacts on women's reproductive health.

2.3 Data

Two sets of data have historically been used to model the menstrual cycle and are used here to model ovarian follicle growth waves. Table 2.2 summarizes the similarities and differences in both data sets. The first set was collected in an experiment by McLachlan et al. [66]. The goal of this experiment was to study the relationship between the pituitary hormones and inhibin with the hope of determining how it is controlled and secreted. Thirty-three women between the ages of 21 and 35 were subjects in the study undergoing daily blood draws. The women were deemed to have normal cycles and to be in good health under a number of specific criteria such as normal blood chemistry, basal body temperature and luteal P4 levels used to determine if ovulation occurred. The data seen in Figure 2.5 shows the average FSH, LH, E2, P4 and IHA centered around ovulation (denoted by day 0). Note the data in Figure 2.5 has been scaled for illustration. The data later used in modeling are adapted from Selgrade [91] and are shown in their entirety for all 31 days in Appendix A. The error bars (scaled for illustration in Figure 2.5), were obtained using *grabit* in MATLAB on the figures from the McLachlan et al. [66] publication.

The second set of data was collected in a study conducted by Welt et al. [98]. The purpose of the study was to to examine IHA and IHB to determine their interaction with the pituitary and their importance in the menopause transition. Forty-four women were selected for the study and broken into two groups based on age, 23 were between 20 and 34 years of age and the remaining 21 were from 35 to 46 years of age. The age at which the groups were split was chosen since 35 years is typically when it is first possible to notice the rise in FSH levels marking the start of the menopause transition. Again, the women were determined to be in good health and have normal menstrual cycles under various specifications. Blood was drawn on each day of the cycle for each subject and measurements for FSH, LH, E2, P4, IHA and IHB were recorded. The average cycle was standardized to 28 days using the area under the curve and centered around ovulation. The data for the younger women, scaled for illustration, is shown in Figure 2.6. The values are also included in Appendix A as taken from Pasteur [78]. The error bars (scaled for illustration in Figure 2.6), were obtained using *grabit* in MATLAB on the figures from the Margolskee [62].

The benefit of modeling these two data sets is that blood samples were taken daily. Due to financial constraints and reluctance of test subjects, many studies only take samples every few days or stagger the draw days for women in the study so a data point for each day is collected but not from each woman [10]. Thus, we have two complete sets of data for normally cycling women. Having daily values for each woman studied results in less error in the data. The

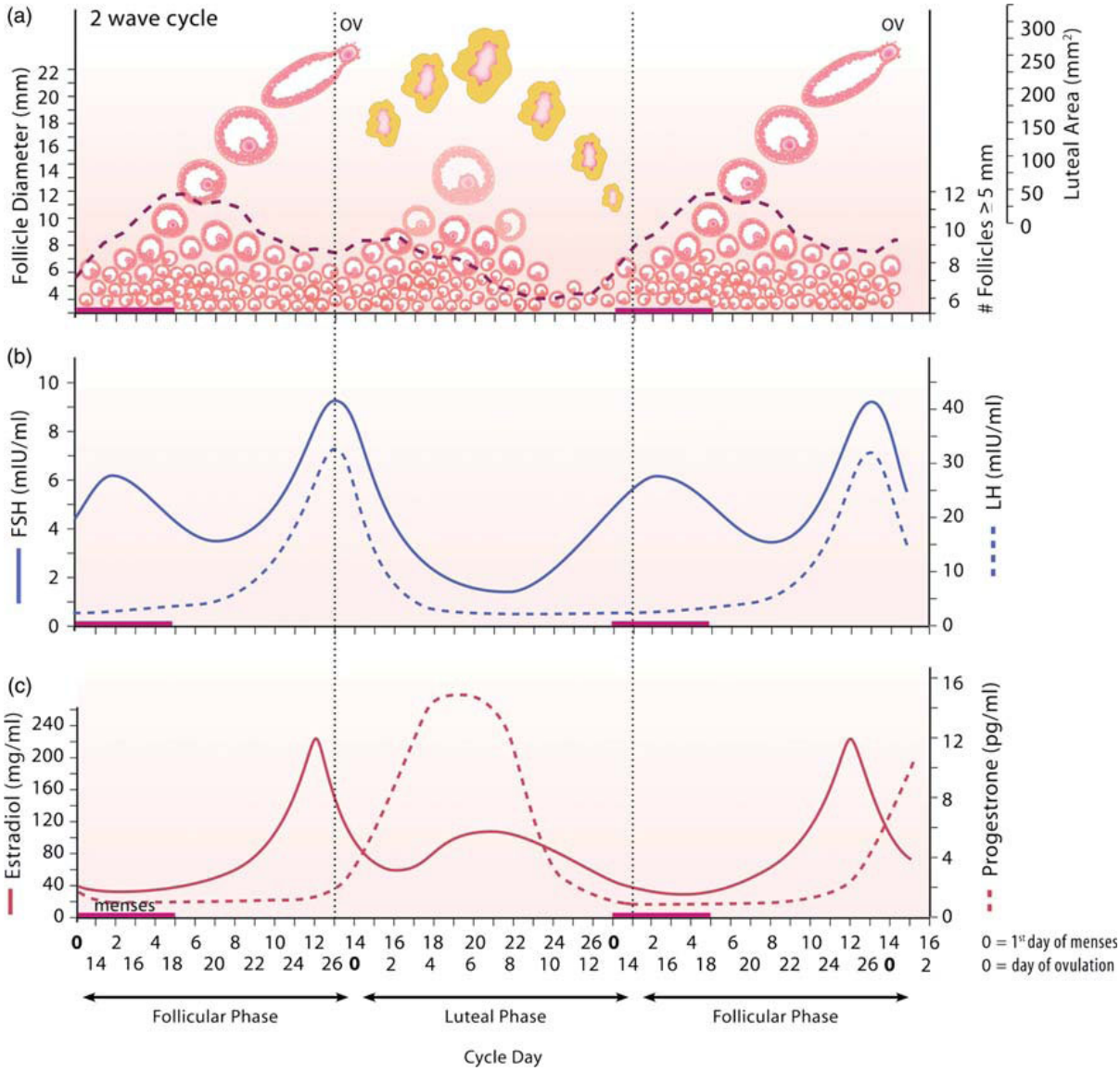

Figure 2.3 Figure from Baerwald et al., (2012) [12] based on results from Baerwald et al. (2003a,b) [9, 10]. Two-thirds of the women in the study exhibited two follicle waves per cycle and the results pertaining to those falling in this category are illustrated in this figure. Follicle diameter (panel **(a)**) and hormone concentrations (LH and FSH in panel **(b)**, E2 and P4 in panel **(c)**) were studied. The two-wave hormone levels resemble the hormone levels for normally cycling women for all four hormones measured. Note that two follicle waves per cycle corresponds to two rises in FSH. From A. R. Baerwald, G. P. Adams, and R. A. Pierson, Ovarian antral folliculogenesis during the human menstrual cycle: a review, *Human Reproduction Update*, 2012, volume 18, issue 1, pages 73-91 by permission of Oxford University Press. *Human Reproduction Update* is published on behalf of the European Society of Human Reproduction and Embryology (ESHRE).

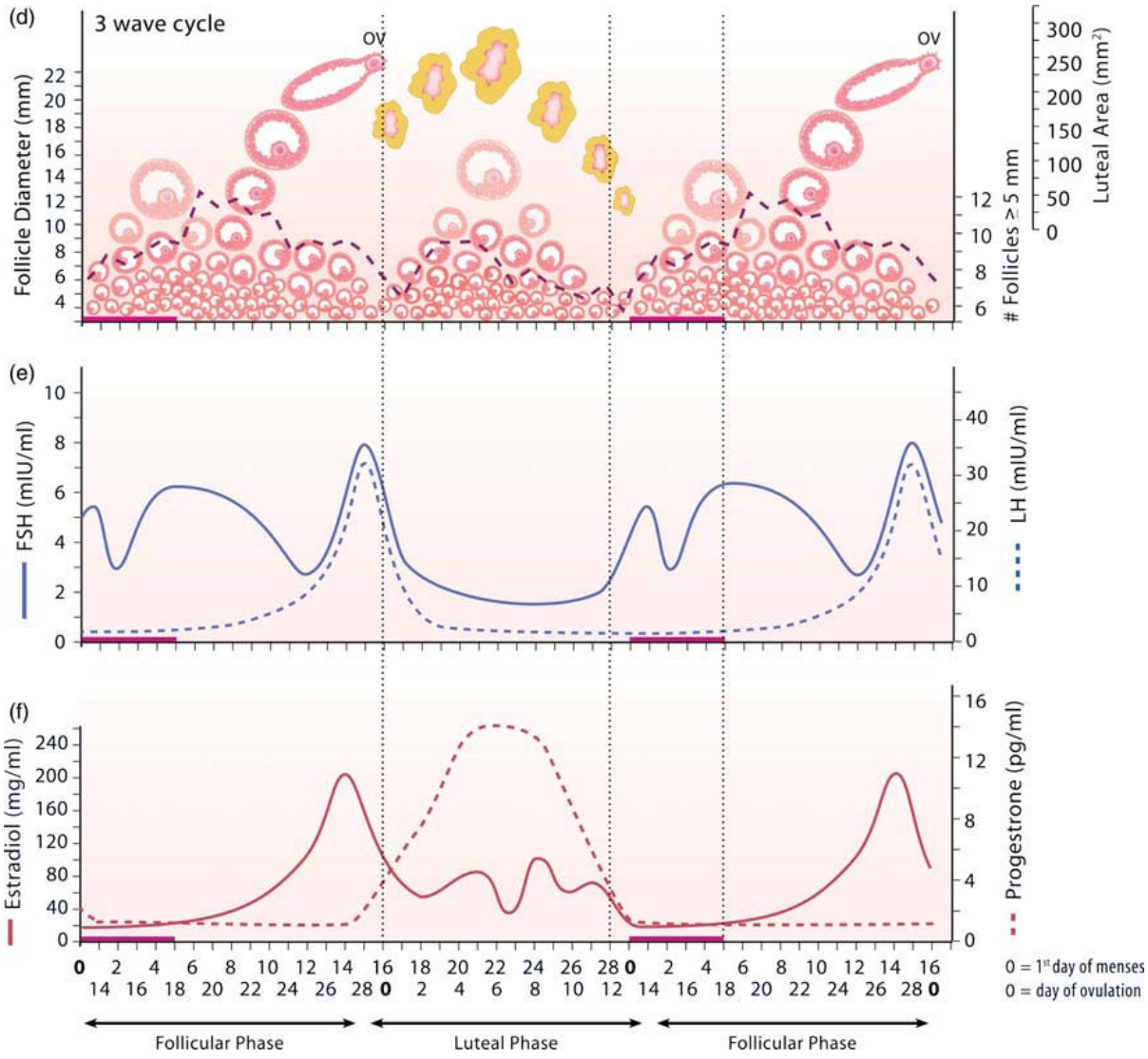

Figure 2.4 Figure from Baerwald et al., (2012), [12] based on results from Baerwald et al. (2003a,b) [9, 10]. Approximately one third of women participating exhibited cycles with three follicle waves per cycle and the results pertaining to those falling in this category are illustrated here. The hormones of these women were averaged together centered around ovulation. Follicle diameters for these women are in panel **(d)**. The hormone measurements for FSH and LH are in panel **(e)** while E2 and P4 are shown in panel **(f)**. Note that here the hormone patterns are different than those from the two-wave results and vary from hormones of normally cycling women. Of importance, here FSH has three distinct rises that correspond to three follicle waves. From A. R. Baerwald, G. P. Adams, and R. A. Pierson, Ovarian antral folliculogenesis during the human menstrual cycle: a review, *Human Reproduction Update*, 2012, volume 18, issue 1, pages 73-91 by permission of Oxford University Press. *Human Reproduction Update* is published on behalf of the European Society of Human Reproduction and Embryology (ESHRE).

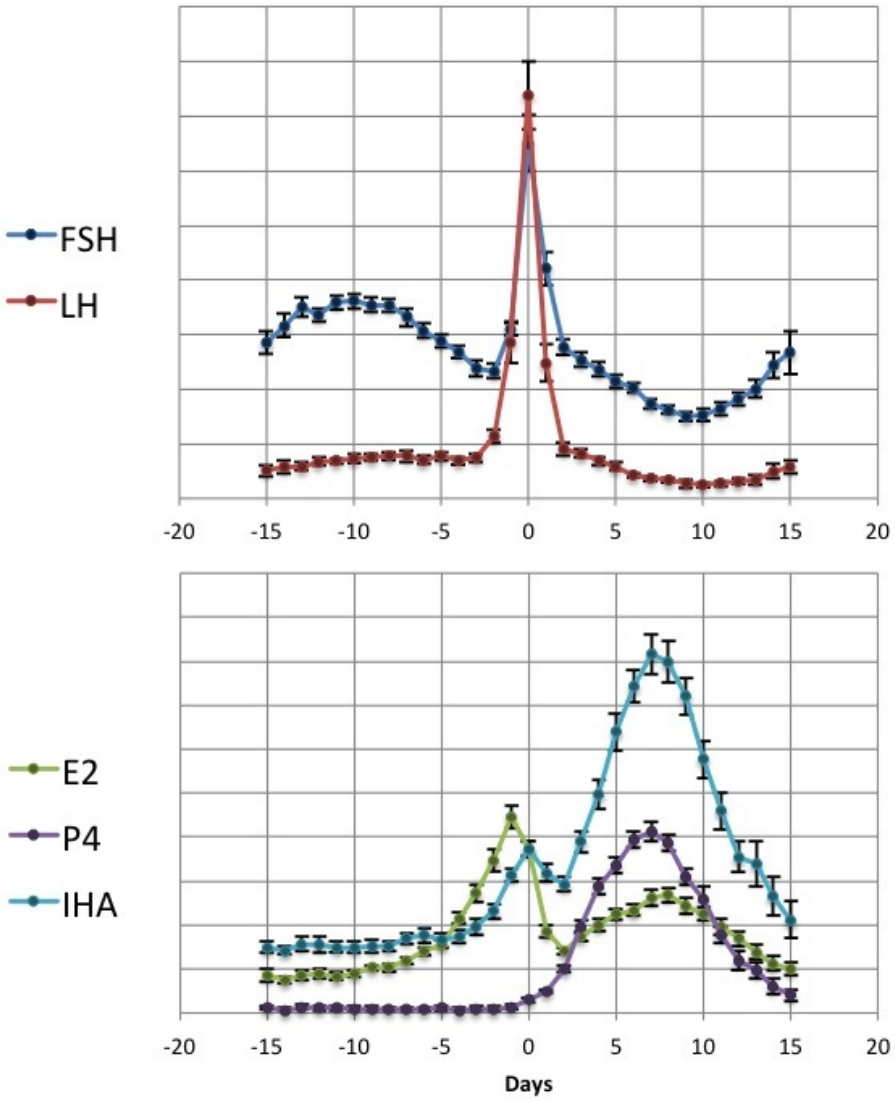

Figure 2.5 Data from by McLachlan et al. [66] for normally cycling women as recorded in Selgrade [91]. Hormone concentrations for E2, P4, IHA, FSH and LH were measured daily for thirty-three women. The resulting cycle length averaged to 31 days. Here, day 0 represents ovulation and values were scaled for illustration. The data as recorded in Selgrade [91] is included in Appendix A.

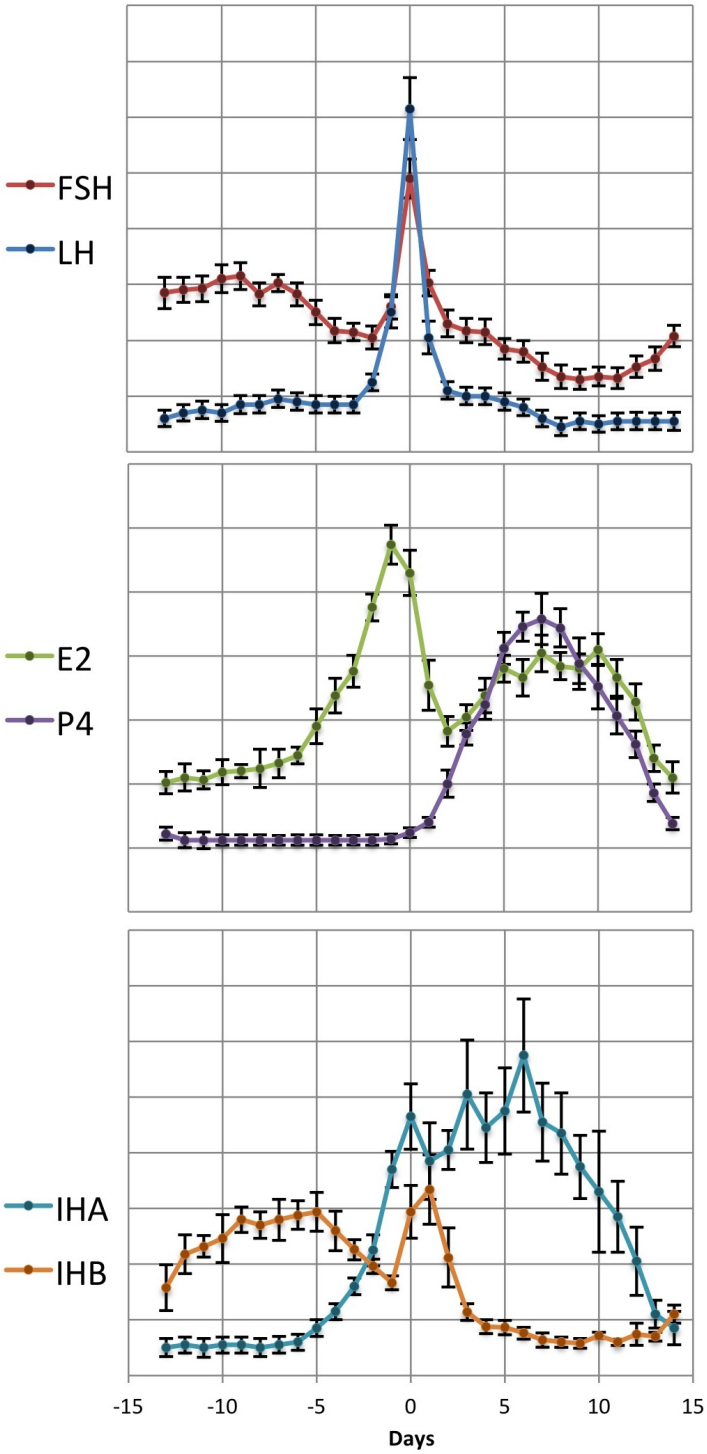

Figure 2.6 Data collected by Welt et al. [98]. The data is from the younger age group, 20 to 34 years of age, studied and hormone levels were found from daily blood draws. Hormones collected were FSH, LH, E2, P4, IHA and IHB. The data collected for each woman was centered at ovulation and the values were averaged together. Here, day 0 denotes ovulation and the values are scaled for illustration. Full data values can be found in Appendix A as taken from work by Pasteur [78].

Table 2.2 A comparison of the McLachlan and Welt data sets [66, 98].

	McLachlan	**Welt**
Average Cycle Length	31 days	28 days
Hormones Collected	FSH, LH, E2, P4, IHA	FSH, LH, E2, P4, IHA, IHB
Number of Subjects	33 women	23 women
Ages of Subjects	21-35 years of age	20-34 years of age
When Blood Draws Occurred Per Subject	Daily	Daily

Welt data for younger women is used in this work as the menopause transition has abnormal behaviors. Averaging the values for these women in both data sets does result in greater error on each end of the cycle. Since these women may have cycles that ranged from 25-35 days in length and were centered around ovulation, the first few days and last few days of the cycle are a little more variable than the the days around ovulation. Most peak or surge values for the hormones have larger error because peak amounts vary per woman. This can be seen in Figures 2.5 and 2.6. Finally, to model the cycle consistently for many periods, the data is repeated. The McLachlan data ranges from day 0 to day 30. Thus, day 31 is the same as day 0 and the cycle repeats. For the Welt data that ranges from day 1 to day 28, day 29 is the same as day 1 and again the cycle repeats. The wealth of data available for normally cycling women enabled the creation of a model including ovarian follicle waves.

Chapter 3

Two-Wave, Five-Hormone Model

The main purpose of this work is to model the endocrine control of the menstrual cycle with more than one follicle wave per cycle. The data available for normally cycling women has an FSH profile with two rises. To show a correspondence between the rises in the FSH profile and the number of follicle waves per cycle, we use data to optimize parameters of the model equations. In this chapter, we discuss the five-hormone model and the parameters with fits for both the McLachlan and Welt data sets. We review the original model and the three step process of how its model was developed. We then discuss the two-wave model and the resulting parameters. Finally, we discuss the behavior of the system using sensitivity analysis.

3.1 Original Model Development

The mathematical model for endocrine control of the human female reproductive system was developed in three steps:

1. **Pituitary Component Model:** The first step involves modeling the hypothalamus-pituitary axis. The pituitary component is a system of four delay differential equations for the pituitary hormones LH and FSH. Here, exponential functions that fit the data for ovarian hormones E2, P4 and IHA are used as fixed inputs into the system to represent the ovarian half of the loop.

2. **Ovarian Component Model:** The second involves modeling the follicle growth and resulting hormones of the ovaries. A system of nine differential equations represent the stages of ovarian follicle growth and three equations that are the proportional sums of these stages represent the ovarian hormones. Again, exponential functions that fit the data for LH and FSH are used as fixed inputs into the system to represent the pituitary part of the loop.

3. **Merged Model:** The third and final step involves merging those two pieces into one feedback cycle. The result is a system of thirteen delay differential equations (the four from the pituitary component and the nine from the ovarian component) and the three ovarian hormone equations with no input functions.

Modeling the hypothalamus-pituitary and the ovaries as separate component models in steps one and two is a benefit because each simulates the full feedback process on a smaller scale using fixed functions representing the other half of the loop as inputs into the system. The full merged model is much larger. The parameters found in steps one and two provide a good starting point for finding parameters in step three for a more accurate result and reduced computation time. Since the follicle waves being modeled reside in the ovaries, steps two and three are of vital importance to this work.

The original components for the hypothalamus-pituitary axis and the ovaries were presented by Schlosser and Selgrade [87, 90]. In Harris-Clark et al., [30], the merged model taking the two components and putting them together, was presented. Both of these works used the data from McLachlan et al. [66] for modeling. As seen in the previous chapter, the model was written based on the five hormones measured in that paper, E2, P4, IHA, LH and FSH. Later, in Pasteur [78] and Pasteur and Selgrade [77] the same three step process was used to find parameters for the system using the E2, P4, IHA, LH, and FSH data from Welt et al. [98]. The model was later expanded to include the sixth hormone IHB. These fundamental models and available data sets represent the cycles of normally cycling women. However, the models were developed under the assumption that recruitment only occurs once during a menstrual cycle. Using these models as a basis, the goal is to add a second follicle wave per cycle for these normally cycling women during the luteal phase.

3.1.1 Pituitary Component

The pituitary model represents the synthesis, release and clearance of LH and FSH from the pituitary and into the bloodstream. LH and FSH are each represented as a two compartment model with two time-dependent, delay ordinary differential equations. The steps of the component model are illustrated in Figure 3.1. The two components for the LH system are:

- $\mathrm{RP}_{\mathrm{LH}}(t)$ which represents the amount of LH produced in the pituitary and stored there until its release.
- $\mathrm{LH}(t)$ which represents the concentration of LH released into and cleared from the bloodstream.

Similarly, the two components for the FSH system are $\mathrm{RP}_{\mathrm{FSH}}(t)$ and $\mathrm{FSH}(t)$. LH and FSH synthesis and release are determined by ovarian hormones. E2, P4 and IHA are represented

as time-dependent inputs into these systems of differential equations. These functions used as inputs into differential equations in component models will henceforth be referred to as input functions. These input functions are exponential functions that approximate the data for the hormones in the data set being used. Thus, the McLachlan and the Welt sets have different input functions for E2(t), P4(t) and IHA(t) in the pituitary component model.

The differential equations for the compartment models can be simply thought of as the rate of change of hormone in the pituitary and the rate of change of hormone in blood serum.

- The pituitary concentration changes in two ways, how much is produced and how much is released from the pituitary.
- The serum concentration changes in two ways, how much enters the bloodstream and how much clears from the bloodstream.

The difference here between the amount released from the pituitary and the concentration in the bloodstream after the release is the blood itself. Upon release from the pituitary, we have the exact amount sent forth but it becomes part of the overall volume of blood, a proportion dictated by the blood volume V. The basic equations are as follows and will be expanded upon:

$$\frac{d}{dt}\mathrm{RP_{LH}} = synthesis_{\mathrm{LH}} - release_{\mathrm{LH}} \tag{3.1}$$

$$\frac{d}{dt}\mathrm{LH} = \frac{1}{V} \cdot release_{\mathrm{LH}} - clearance_{\mathrm{LH}} \tag{3.2}$$

$$\frac{d}{dt}\mathrm{RP_{FSH}} = synthesis_{\mathrm{FSH}} - release_{\mathrm{FSH}} \tag{3.3}$$

$$\frac{d}{dt}\mathrm{FSH} = \frac{1}{V} \cdot release_{\mathrm{FSH}} - clearance_{\mathrm{FSH}} \tag{3.4}$$

From previous work and using Figure 3.1 as a guide we determine the synthesis, release and clearance actions of the system:

Synthesis E2 positively influences hormone production for LH while P4 inhibits LH production and IHA inhibits FSH production, so $synthesis_{\mathrm{LH}}(\mathrm{E2}, \mathrm{P4})$ and $synthesis_{\mathrm{FSH}}(\mathrm{IHA})$. The synthesis terms are rational functions in which production effects are in the numerator and inhibitory effects are in the denominator.

Release The release of LH and FSH are inhibited by E2 and promoted by P4. The amount of LH or FSH released from the pituitary is also determined by how much has been produced and stored so $release_{\mathrm{LH}}(\mathrm{E2}, \mathrm{P4}, \mathrm{RP_{LH}})$ and $release_{\mathrm{FSH}}(\mathrm{E2}, \mathrm{P4}, \mathrm{RP_{FSH}})$.

Clearance The rate of clearance is proportional to the amount that is in the blood, so $clearance_{\mathrm{LH}}(\mathrm{LH})$ and $clearance_{\mathrm{FSH}}(\mathrm{FSH})$.

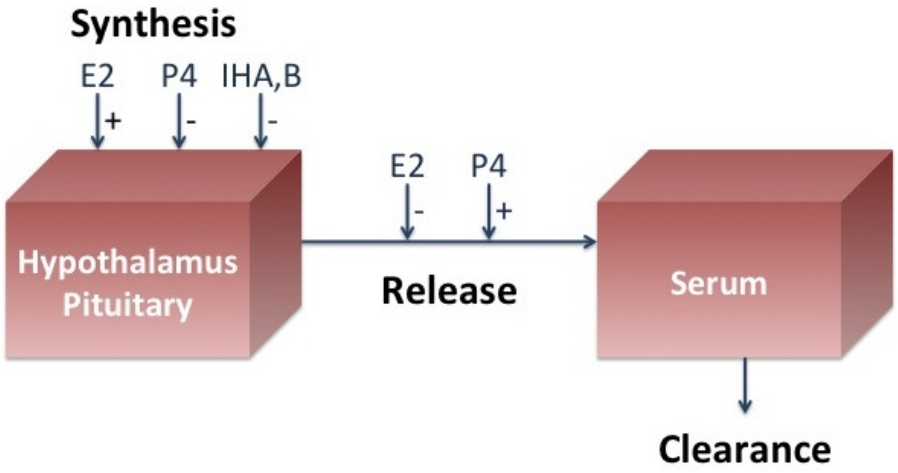

Figure 3.1 Illustration of the compartment model for the pituitary. The compartment model is split into three pieces, synthesis of hormones in pituitary, release of hormones from pituitary into the blood and clearance of hormones from the blood. E2 promotes synthesis of LH, P4 inhibits synthesis of LH and IHA inhibits synthesis of FSH. P4 promotes pituitary hormones to be released into the blood while E2 inhibits it.

These expand the previous equations to the following:

$$\frac{d}{dt}\mathrm{RP_{LH}} = synthesis_{\mathrm{LH}}(\mathrm{E2}, \mathrm{P4}) - release_{\mathrm{LH}}(\mathrm{E2}, \mathrm{P4}, \mathrm{RP_{LH}}) \tag{3.5}$$

$$\frac{d}{dt}\mathrm{LH} = \frac{1}{V} \cdot release_{\mathrm{LH}}(\mathrm{E2}, \mathrm{P4}, \mathrm{RP_{LH}}) - clearance_{\mathrm{LH}}(\mathrm{LH}) \tag{3.6}$$

$$\frac{d}{dt}\mathrm{RP_{FSH}} = synthesis_{\mathrm{FSH}}(\mathrm{IHA}) - release_{\mathrm{FSH}}(\mathrm{E2}, \mathrm{P4}, \mathrm{RP_{FSH}}) \tag{3.7}$$

$$\frac{d}{dt}\mathrm{FSH} = \frac{1}{V} \cdot release_{\mathrm{FSH}}(\mathrm{E2}, \mathrm{P4}, \mathrm{RP_{FSH}}) - clearance_{\mathrm{FSH}}(\mathrm{FSH}) \tag{3.8}$$

Time delays are incorporated into the ovarian hormones to represent the time span between changes in their hormone levels and the effect on the synthesis of the pituitary hormones. The delays are d_E, d_P and d_{IHA} and are only included in synthesis terms. The full equations for the

two compartment model for LH and for FSH are as follows:

$$\frac{d}{dt}\mathrm{RP_{LH}} = \frac{v_{0LH} + \dfrac{v_{1LH} \cdot E_2(t-d_E)^a}{Km_{LH}^a + E_2(t-d_E)^a}}{1 + \dfrac{P_4(t-d_P)}{Ki_{LH,P}}} - \frac{k_{LH} \cdot (1 + c_{LH,P} \cdot P_4) \cdot \mathrm{RP_{LH}}}{1 + c_{LH,E} \cdot E_2} \tag{3.9}$$

$$\frac{d}{dt}\mathrm{LH} = \frac{1}{V} \cdot \frac{k_{LH} \cdot (1 + c_{LH,P} \cdot P_4) \cdot \mathrm{RP_{LH}}}{1 + c_{LH,E} \cdot E_2} - a_{LH} \cdot \mathrm{LH} \tag{3.10}$$

$$\frac{d}{dt}\mathrm{RP_{FSH}} = \frac{v_{FSH}}{1 + \dfrac{\mathrm{IHA}(t-d_{IHA})}{Ki_{FSH,IHA}}} - \frac{k_{FSH} \cdot (1 + c_{FSH,P} \cdot P_4) \cdot \mathrm{RP_{FSH}}}{1 + c_{FSH,E} \cdot E_2^2} \tag{3.11}$$

$$\frac{d}{dt}\mathrm{FSH} = \frac{1}{V} \cdot \frac{k_{FSH} \cdot (1 + c_{FSH,P} \cdot P_4) \cdot \mathrm{RP_{FSH}}}{1 + c_{FSH,E} \cdot E_2^2} - a_{FSH} \cdot \mathrm{FSH} \tag{3.12}$$

The release terms for LH and FSH are almost identical except for the exponent on E2. As in Tsai and Yen [96] the inhibitory effect by E2 is stronger on FSH than on LH, so the exponent is one on LH and two on FSH. Also note the Hill function on the synthesis of LH. The levels of E2 when high induce the rapid synthesis of LH for its surge which makes the Hill function appropriate. Most values in the system are parameters that need solved for through optimization. However, four values are either known or have been derived:

- Blood volume in liters is a known constant at $V = 2.5$.
- From Harris et al. [30], the derived clearance rate for LH is $a_{LH} = 14$ (1/day)
- Also from Harris et al. [30], the derived clearance rate for FSH is $a_{FSH} = 8.21$ (1/day).
- The Hill function Hill coefficient a was derived to be 8 [30]

3.1.2 Ovarian Component

The ovarian component model is a system of nine time-dependent ordinary differential equations for the five hormone system. Recall from Chapter 2 that the follicles and corpus luteum in the ovaries secrete E2, P4 and IHA at different times throughout the cycle based on the current stage of growth. Thus, these nine differential equations represent nine of the stages of growth in the ovaries. This growth depends on hormones LH and FSH from the pituitary. Here, FSH and LH are used as inputs into the ovarian follicle differential equations. The stages are as follows:

- (RcF) Recruited Stage: FSH induced recruitment from the preantral pool

- (GrF) Growing Stage: FSH sustaining growth of cohort
- ($DomF$) Dominant Stage: Selection of a dominant follicle
- (OvF_1) First Ovulatory Stage: Follicle ovulation
- (OvF_2) Second Ovulatory Stage: Follicle luteinization
- (Lut_{1-4}) Luteal Stages: Four stages of corpus luteum decay

The stages of growth represent the mass of the follicles, singular follicle or corpus luteum at that point in time. The stage increases until it reaches its full mass for that phase of growth and then decreases as that stage ends and a new one begins. The mass is transferred from one stage to another. Thus, to get to the growing stage one must come from the recruited and so on. The transfer of mass is exhibited in the differential equations as a decay term from one stage and the same exact term is used as a growth term in the following stage. The differential equations for the stages of growth are as follows:

$$\frac{d}{dt}RcF = b \cdot \mathrm{FSH} + c_1 \cdot RcF \cdot \mathrm{FSH} - c_2 \cdot \mathrm{LH}^{\alpha} \cdot RcF \tag{3.13}$$

$$\frac{d}{dt}GrF = c_2 \cdot \mathrm{LH}^{\alpha} \cdot RcF + (c_3 \cdot \mathrm{LH}^{\beta} - c_4 \cdot \mathrm{LH}) \cdot GrF \tag{3.14}$$

$$\frac{d}{dt}DomF = c_4 \cdot \mathrm{LH} \cdot GrF - c_5 \cdot \mathrm{LH}^{\gamma} \cdot DomF \tag{3.15}$$

$$\frac{d}{dt}OvF_1 = c_5 \cdot \mathrm{LH}^{\gamma} \cdot DomF - d_1 \cdot OvF_1 \tag{3.16}$$

$$\frac{d}{dt}OvF_2 = d_1 \cdot OvF_1 - d_2 \cdot OvF_2 \tag{3.17}$$

$$\frac{d}{dt}Lut_1 = d_2 \cdot OvF_2 - k_1 \cdot Lut_1 \tag{3.18}$$

$$\frac{d}{dt}Lut_2 = k_1 \cdot Lut_1 - k_2 \cdot Lut_2 \tag{3.19}$$

$$\frac{d}{dt}Lut_3 = k_2 \cdot Lut_2 - k_3 \cdot Lut_3 \tag{3.20}$$

$$\frac{d}{dt}Lut_4 = k_3 \cdot Lut_3 - k_4 \cdot Lut_4 \tag{3.21}$$

Due to the fast clearance rates of ovarian hormones from the blood, it is sufficient to write the ovarian hormone equations not as differential equations but as the direct proportional sums of the stages of growth that contribute to them. They will be referred to as auxiliary equations

and are as follows:

$$E_2 = e_0 + e_1 \cdot GrF + e_2 \cdot DomF + e_3 \cdot Lut_4 \tag{3.22}$$

$$P_4 = p_0 + p_1 \cdot Lut_3 + p_2 \cdot Lut_4 \tag{3.23}$$

$$\text{IHA} = h_0 + h_1 \cdot DomF + h_2 \cdot Lut_2 + h_3 \cdot Lut_3 + h_4 \cdot Lut_4 \tag{3.24}$$

3.1.3 Merged Model

The merged model combines the pituitary component model with the ovarian component model. In the previous two steps, exponential input functions were used to represent the hormones stimulating growth in that component model. In reality, the pituitary affects the ovaries which in turn feedback onto the pituitary. The component models with set input functions do not exhibit this feedback behavior because one half of the loop is fixed. The merged model allows the grand total of thirteen differential equations and three ovarian hormone equations to work together and rely on each other instead of relying on the input functions. Before embarking on the two-wave model, we tested that the model produced the correct one-wave response and improved the system parameters for all components and data sets. An example of this work is in Figure 3.2. This figure illustrates a recreated merged model for the Welt five-hormone system. It illustrates how well the hormone profiles match the data. Figure 3.3 illustrates the ovarian follicle stages of growth that generate the hormones. Appendix B has the parameter values for the five-hormone, one-wave merged model for both the McLachlan and Welt data sets. The initial conditions for both of these models are included in Appendix C.

3.2 Two-Wave Model Development

This section shows how recent work on follicle waves and the FSH threshold concept can be used to improve the model. An exploratory attempt at including follicle waves into the model was conducted by Margolskee [62]. The biology of follicle waves dictates that two important aspects of waves must be executed in the model:

1. The FSH threshold needs to be represented in the recruited stage of growth. Regardless of whether we have one, two or even more follicle waves per cycle, the FSH threshold is a vital part of the cycle and should be represented as such. There is a one-to-one relationship between the number of rises in FSH and the number of follicle waves per cycle. With the threshold in the recruited stage, we expect that the normal FSH curve with two rises will result in two waves per cycle.

2. Typically, only one wave per cycle is a major wave resulting in the emergence of a dominant

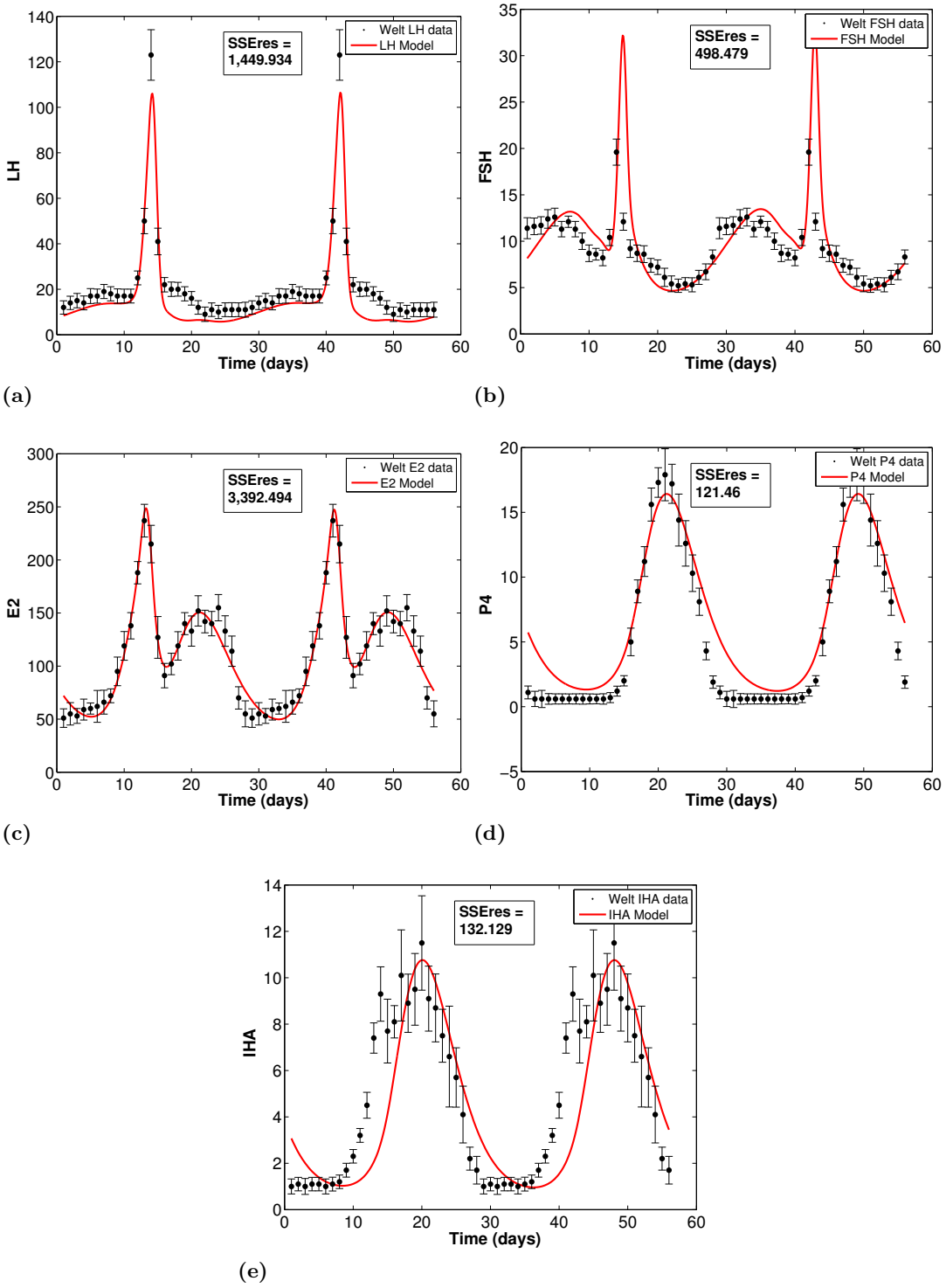

Figure 3.2 Hormone profiles for the five-hormone, one-wave merged model fit to the Welt data set using the original equations in Pasteur [78]. These parameters (Appendix B) serve as a baseline for the two-wave model. SSEres is the summed squared difference between the hormone and the data for one cycle (Equation (3.36)).

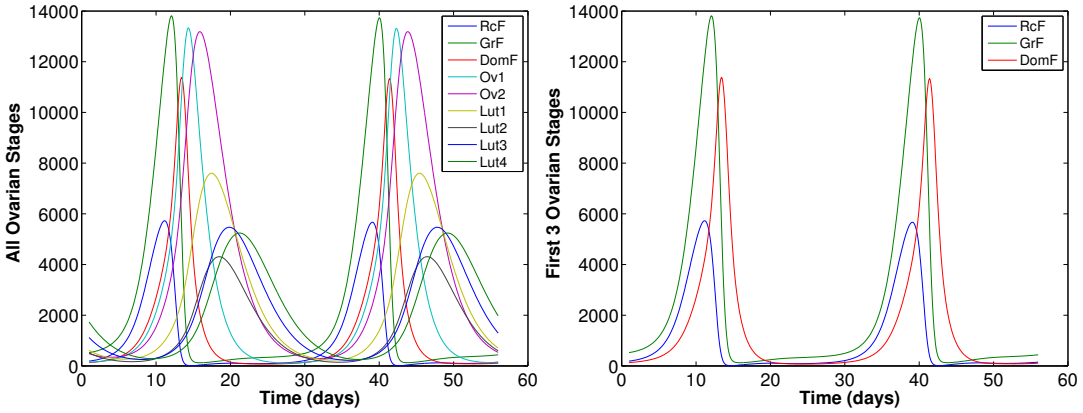

(a) (b)

Figure 3.3 Stages of ovarian follicle growth and development for the Welt data set. The stages here are produced from parameters resulting from the optimization process using the equations from Pasteur [78]. Since the original one-wave model is the starting point for the two-wave model, it made sense to recreate that model first as a baseline.

follicle. An atresia term is required to modify the stages such that every stage from the dominant through luteal have no second follicle wave per cycle.

The same three step component process used in the original, one-wave, model development will be employed for the two-wave model.

Pituitary Component: The pituitary component stays exactly as it was in the one-wave model outlined in the previous section. The follicle stages of growth are changed to accommodate a second follicle wave in the luteal phase but the hormone profiles did not change. FSH for normally cycling women should produce the ovarian hormone profiles and two follicle waves per cycle. E2, P4, IHA should look as close to the original profiles as possible despite the changes to the number of waves in the ovarian growth stages. If the ovarian hormone profiles do not change, there is no need to reexamine the pituitary component model at this time. The goal is to amend the ovarian component model to include the follicle waves but maintain the ovarian hormone profiles and then to show these waves are also possible in the full merged model.

Ovarian Component:

FSH Threshold: The first piece of the follicle wave puzzle that needs to be addressed is the second follicle wave. It is clear from the literature that follicle waves are a result of the FSH threshold and/or window. When the FSH concentration is high enough so that the threshold level is exceeded, recruitment occurs. We start by examining the recruited stage (Equation (3.13)). Two terms in the recruited stage are based on FSH as it is the catalyst for recruitment and growth of the follicles. The final term is the transfer of mass out of the recruited stage and

into the growing stage based on LH and should be left as is. The first term is the independent growth term based on the FSH levels at the time and again would do well to be left alone. The second term is based on not only FSH but also on how much mass is already achieved in the recruited stage. As this term takes in all factors, the FSH levels and the amount of mass the cohort currently has, it seems reasonable that it is a prime candidate for the follicle wave changes. The question is now, what should be used to represent the FSH threshold in this term? Hill functions are used to represent how cooperative a substance is binding to a receptor. The function is of the form:

$$V = V_{max} \frac{S^p}{Km^p + S^p}$$

Where:

- V is the velocity of the reaction
- V_{max} is the maximum velocity
- S is the substrate concentration
- Km is the Michaelis constant that represents the substrate concentration at which half of the maximum velocity is achieved
- p is the Hill coefficient which relates to the degree of cooperation of the substrate to its receptors.

If the Hill coefficient is equal to one, no cooperation is achieved. If it is less than one then there is negative cooperation and if it is greater than one there is positive cooperation. As FSH is released into the bloodstream, it was stated in Chapter 2 that the receptors on the follicles react to the FSH and the follicles undergo recruitment and growth. Thus, the Hill function is a logical choice for the FSH threshold (Equation (3.25)). Here the Hill coefficient, p, should be greater than one to indicate a positive cooperation which will cause the Hill function to look sigmoidal. Km_F is the concentration of FSH at which reaction velocity reaches half of its maximum in binding to the follicles. Note that c_1 now represents the V_{max}. The recruited equation now looks as follows to include the FSH threshold function (denoted in red):

$$\frac{d}{dt}RcF = b \cdot FSH + c_1 \cdot RcF \cdot \frac{\left(\frac{FSH}{Km_F}\right)^p}{1 + \left(\frac{FSH}{Km_F}\right)^p} - c_2 \cdot LH^{\alpha} \cdot RcF \tag{3.25}$$

Atresia: In theory, this FSH threshold function could trigger any number of follicle waves dependent of the amount of FSH coming out of the pituitary. The cascading transfer of mass from one follicle stage of growth to another should also pass whatever happens in the recruited

stage through to every subsequent stage of growth. The theory of follicle waves also hinges on the fact that the second follicle wave should not go through dominant follicle selection. With no dominant follicle, that wave cannot go through ovulation or luteinization. An atresia term can be included in the dominant follicle stage changing the original equation (Equation (3.15)) to stop the second wave at this stage and after.

The atresia term is a rational function decay term based on Dom_F to reduce the existing mass. The goal of this term is to maintain the first wave but eliminate the second. LH plays a large part in dominant follicle growth. It is required for a growing follicle to be selected to grow to dominance. LH has one surge that promotes dominant follicle selection and ovulation, but is relatively flat everywhere else throughout the cycle. Thus the shape of LH can be used to an advantage in the atresia term. We want the dominant follicle to be high when LH is high and low when LH is low. Therefore, using LH in the atresia term should suppress a luteal follicle wave because LH itself is suppressed in the luteal phase. The atresia term is an addition to the two existing terms that remain as they were originally written. The new dominant follicle equation is as follows (with atresia term in red):

$$\frac{d}{dt}DomF = c_4 \cdot LH \cdot GrF - c_5 \cdot LH^{\gamma} \cdot DomF - \frac{atr \cdot DomF}{1 + \left(\frac{LH}{Ki_{atr}}\right)^{pwr_{at}}} \tag{3.26}$$

The full system of equations for the ovarian stages of growth is listed below. No other equation changes are needed.

$$\frac{d}{dt}RcF = b \cdot FSH + c_1 \cdot RcF \cdot \frac{\left(\frac{FSH}{Km_F}\right)^p}{1+\left(\frac{FSH}{Km_F}\right)^p} - c_2 \cdot LH^{\alpha} \cdot RcF \tag{3.27}$$

$$\frac{d}{dt}GrF = c_2 \cdot LH^{\alpha} \cdot RcF + (c_3 \cdot LH^{\beta} - c_4 \cdot LH) \cdot GrF \tag{3.28}$$

$$\frac{d}{dt}DomF = c_4 \cdot LH \cdot GrF - c_5 \cdot LH^{\gamma} \cdot DomF - \frac{atr \cdot DomF}{1+\left(\frac{LH}{Ki_{atr}}\right)^{pwr_{at}}} \tag{3.29}$$

$$\frac{d}{dt}OvF_1 = c_5 \cdot LH^{\gamma} \cdot DomF - d_1 \cdot OvF_1 \tag{3.30}$$

$$\frac{d}{dt}OvF_2 = d_1 \cdot OvF_1 - d_2 \cdot OvF_2 \tag{3.31}$$

$$\frac{d}{dt}Lut_1 = d_2 \cdot OvF_2 - k_1 \cdot Lut_1 \tag{3.32}$$

$$\frac{d}{dt}Lut_2 = k_1 \cdot Lut_1 - k_2 \cdot Lut_2 \tag{3.33}$$

$$\frac{d}{dt}Lut_3 = k_2 \cdot Lut_2 - k_3 \cdot Lut_3 \tag{3.34}$$

$$\frac{d}{dt}Lut_4 = k_3 \cdot Lut_3 - k_4 \cdot Lut_4 \tag{3.35}$$

Solving the System: All work done with these equations was done in MATLAB. For the ovarian component model, ODE23 was used to solve the system with time dependent input functions. For this subsystem, the delay was subtracted off of the time in the input functions so no delay solver was needed. For the merged model, DDE23 was used to solve the system of delay equations without input functions.

Optimization: Optimization was used for finding the parameters that fit a particular data set using fminsearch. The fminsearch method finds a local minimum without using derivatives by employing a Nelder-Mead Simplex method. The fminsearch takes in an argument that we will refer to as a cost function which the method tries to minimize. The routine stops when there are no more parameter changes within set ranges that minimize the cost function or when other stopping criteria are met. Here, the cost function is the summed squared difference between the model solution and a data set. The fminsearch is a beneficial method because no numerical solutions or gradients are needed; however the downside is having to be meticulous in the methods used to prepare the system so the solver finds an acceptable local solution. There are many ways to encourage the optimizer to find a set of parameters that yields a stable solution. The following are many that were employed in the optimization process in this work. Though variations of each step or the order of the steps may change for each particular case

for which results are found, the following is a general method:

Begin from Previous Results. It helps to start from previous parameter results. In this case, the starting point for the ovarian component model would be previous one-wave parameters for the respective data sets. For the merged models, the starting parameters for the pituitary equations are the previous one-wave results and for the ovarian equations are the two-wave ovarian component parameters.

Adjust Parameters by Hand. Manually changing parameters by hand to give the system a general starting point typically helps.

Change Cost Function Length of Time. More than one cycle of data should be used in the cost function to promote the cyclic nature. If the model is yielding results that do not match the cycle length of the data, more cycles in the cost function can force the optimizer to find a solution in that time frame. For most results, two cycles worth of data were enough. Using too many can drastically extend the time it takes for the optimizer to complete.

Build Up Cost Function. Typically optimization is done in steps in which the cost function is built up over time. The cost function is a sum of the summed squared differences (SSE) between the hormone model and the data.

$$SSE(\text{hormone}) = \sum_{\text{start day}}^{\text{end day}} (\text{hormone model}(day) - \text{data}(day))^2 \tag{3.36}$$

Here, the model can be any of the hormones. Build up the cost function means to sum the summed squared differences for the hormones a hormone at a time. Typically P4 and IHA are the easiest to fit while E2 and FSH are harder to fit. Also, FSH is of vital importance to work with the wave. Using a particular order in how the cost function is built up is important.

- For the ovarian component model, it is best to start with a cost function of just $SSE(\text{E2})$ because it is the most difficult to fit and will have the highest cost. After the routine finishes and any manual adjustments have been made, the next cost function would be $SSE(\text{E2}) + SSE(\text{P4})$ and so on until all the ovarian hormones are included. Starting with P4 in this case does not help to optimize the more complex stages as it does by starting with E2. Starting with the total sum of all three hormones would be a poor choice as well. Because P4 and IHA are easier to fit, their piece of the cost function would be relatively small compared to E2. In this case, the optimizer will yield a solution that is better for E2 than it is for P4 or IHA.

By doing multiple optimizations and building up the cost function, the cost for E2 is brought down before P4 and IHA are included to level the playing field so each has a good chance of a nice looking fit.

- For the merged model, FSH was the top choice to start with and then E2, LH, P4 and IHA in subsequent steps. FSH was chosen first because the second follicle wave hinges on the FSH levels. The better FSH fits, the better the waves look. Typically, if FSH fits fairly well, the rest of the hormones are also fairly accurate.

Set Optimization Boundaries. There are no boundaries on the optimization routine itself, but boundaries can be set through the cost function. For example, if we desire that α stay under 0.4, we can require the optimizer to return a large cost value if it tries to make α larger than that value. Since the goal is to minimize the cost function, the routine will move back to whatever its previous step was and keep the parameter value within its acceptable range.

Match Model Peaks to Data Peaks. One final aid to optimizing, especially the merged model where the length of a model cycle may differ from the cycle length of the data, is matching a peak. Based on initial conditions, the solver does not find a stable solution immediately. There is a small amount of time where the solver has some 'runoff' solution that doesn't fit the hormone profile before it finds an attracting cycle. This runoff is typically not a full cycle length. Since the ovarian component model uses fixed input functions, there typically is no runoff for component models, only for merged models. To remedy this runoff, the time given to the solver must be a few cycles in length. It should not be too long because that will increase the overall time for optimization which is already long in the best of circumstances. The next step is to choose a hormone, typically, E2, LH, or FSH, something with a distinct peak. Then for the first cycle chosen to use for optimization, make sure the peak model value for that hormone lines up with the peak data point. For example, once the index is found for the peak of E2 data for the fourth cycle of the model, that cycle starts thirteen days earlier for the Welt data and that should be the starting index in the cost function. Another aid is to change the initial conditions to minimize the runoff. Though this helps find a stable solution faster, it does not entirely eliminate the runoff time, so matching peaks is still necessary. Not matching peaks encourages the optimizer to attempt to possibly match the model's luteal phase with the data's follicular phase.

In subsequent sections, this process will be referred to as optimization. The same process was used in each scenario and this serves as a general overview of the optimization process.

3.3 Results

3.3.1 McLachlan Ovarian Component Model

Input Functions: The ovarian component model depends on the input functions that match the McLachlan data set. The equations themselves represent one cycle length. When used in the differential equations, modular arithmetic (here for 31 days) is used to extend the input function to more than one cycle. The input functions were updated from those in Harris et al. [30] and are illustrated in Figure 3.4. The equations are as follows for the pituitary hormones:

$$\text{LH} = 35 + 340e^{-\frac{(t-15)^2}{1.2}} + 5e^{-\frac{(t-7)^2}{23}} + 20e^{-\frac{(t-25)^2}{40}} \tag{3.37}$$

$$\text{FSH} = 75 + 110e^{-\frac{(t-4.5)^2}{46}} + 210e^{-\frac{(t-15)^2}{0.75}} + 50e^{-\frac{(t-17.5)^2}{20}} - 12e^{-\frac{(t-25)^2}{10}} \tag{3.38}$$

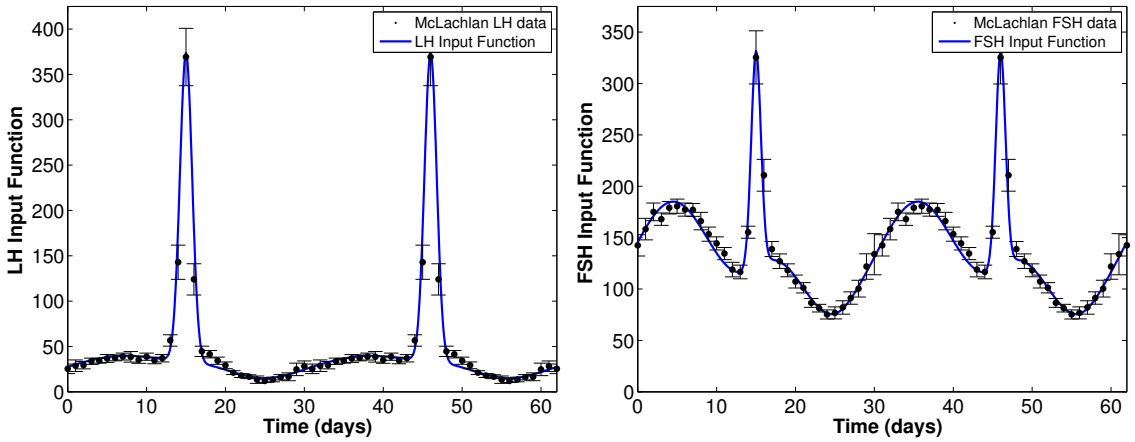

(a) (b)

Figure 3.4 Input functions that fit the McLachlan data set for the pituitary hormones LH and FSH. These input functions are used to solve and optimize the system of nine differential equations that model the stages of ovarian follicle growth with two follicle waves. With these stages, the auxiliary equations for the ovarian hormones can be solved.

Upon solving and optimizing the system using the steps outlined above, the parameters in Table 3.1 were found as an optimized minimum solution to the system's cost function. It is important to note that e_0, p_0, p_2 and h_2 all optimized to values very small and are deemed

negligible. These parameters should be assumed to be zero so they can be removed from the system to aid in the efficiency and accuracy of the optimizer.

Cycle Results: As can be seen in Figure 3.5, the recruited and growing stages of growth each have two follicle waves, the ovulatory follicular phase wave and the anovulatory luteal phase wave. It is also important to note that the dominant and subsequent stages only have one wave that follows from the follicular phase wave. Thus, the FSH threshold function successfully inserted a second follicle wave into the cycle while the atresia term prevented it from moving beyond the growing stage.

Parameter Results: Not only are the values that are listed in Table 3.1 for the five new parameters that control the wave and the atresia important, but some other original stage parameters were important to the wave as well.

- The parameter c_1 was always in the model but now takes on a different role as the maximum velocity of the Hill function and its value is now larger than one. Again, as a way to manipulate the model to include follicle waves, the original model was compiled based on results in Schlosser and Selgrade [87, 90] and Harris-Clark et al., [30]. The original value of c_1 was on the order of 10^{-3} so a 300 fold increase was needed.

- In the ovarian component model, the b parameter controls the height of the recruited stage. It can be manipulated by hand to make the recruited stage as large as possible. When the threshold function was included, the stage heights were reduced dramatically probably due to the fact that FSH was no longer just a multiplicative factor but a threshold on the current level of FSH. As a result, b is about 100 times larger to regain the height lost.

- Finally, c_2 and α were changed in concert. The transfer out term from the recruited stage contributes to the luteal wave height. This term is not only important to the recruited waves but also to the growing stage waves as it is the starting point for that stage as the mass is transferred in. The α parameter was cut by a little more than half and the c_2 parameter was increased by almost 0.1. By investigating these two parameters by hand, it seems that they are quite sensitive and will be explored further in a later section of this chapter. Thus if α is reduced too much, increasing c_2 helps offset some of that change. Changing one without the other led to a loss of the wave or an unstable solution.

To obtain a fit for the ovarian hormones, a series of steps were taken based on the optimization outline in the previous section. For the most part, the outline above was followed (two cycle lengths of data in the cost function, peak matching, etc.) but a few items of importance are pointed out here.

Adjust Parameters by Hand. First, a handful of parameter changes were made by hand. Changing the existing equations while using the original parameters is a start, but chang-

Table 3.1 Parameter results for the five-hormone, two-wave ovarian component model fitting the McLachlan data set. All of the following optimized parameters were truncated to two significant decimal digits.

Parameter	**Value**	**Units**
α	0.30	dimensionless
β	0.067	dimensionless
γ	0.010	dimensionless
b	0.42	L/day
c_1	1.62	1/day
c_2	0.49	$(\text{L}/\mu\text{g})^{\alpha}(1/\text{day})$
c_3	0.077	$(\text{L}/\mu\text{g})^{\beta}(1/\text{day})$
c_4	0.025	$(\text{L}/\mu\text{g})(1/\text{day})$
c_5	0.75	$(\text{L}/\mu\text{g})^{\gamma}(1/\text{day})$
d_1	0.50	1/day
d_2	0.52	1/day
k_1	0.47	1/day
k_2	0.49	1/day
k_3	1.33	1/day
k_4	0.59	1/day
e_1	0.022	1/kL
e_2	0.027	1/kL
e_3	0.047	1/kL
p_1	0.010	1/L
h_0	188.64	U/L
h_1	0.044	$(\text{U/L})/\mu\text{g}$
h_3	0.89	$(\text{U/L})/\mu\text{g}$
h_4	0.0060	$(\text{U/L})/\mu\text{g}$
Km_F	101.93	μg/L
p	26.27	dimensionless
atr	380.87	1/day
Ki_{atr}	5.20	μg/L
pwr_{at}	1.98	dimensionless

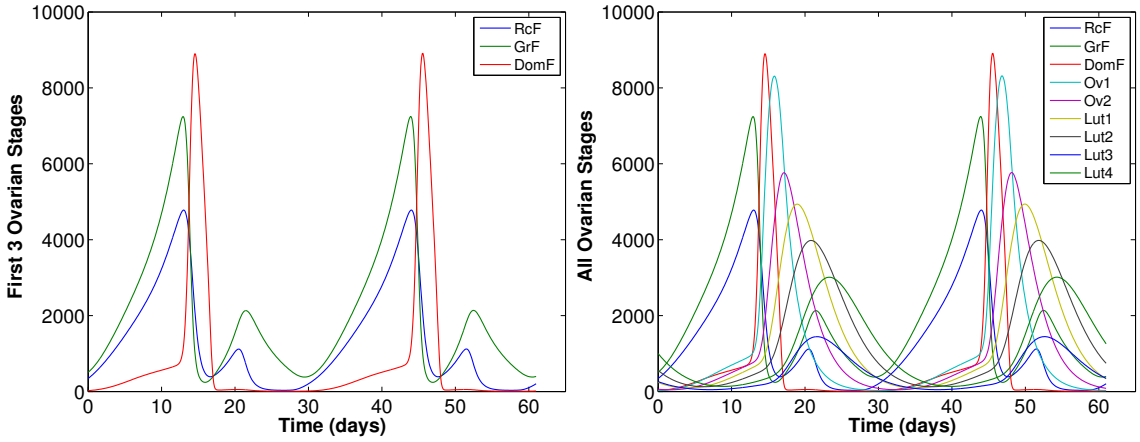

(a) **(b)**

Figure 3.5 Ovarian follicle stages of growth from the ovarian component, five-hormone, two-wave model fit to the McLachlan data set. The ovarian component model results come from optimizing system parameters for the stages of follicle growth and the ovarian functions based on input functions for FSH and LH. Here we see that the addition of a Hill function in the recruited stage of follicle growth causes a second follicle wave of recruitment to occur during the luteal phase. The first picture isolates the recruited, growing and dominant follicles for easier viewing and the second is of all nine stages of follicle growth.

ing some parameters intuitively by hand, most obviously the recruited stage parameters, gives the optimizer a better starting point. Also, the rise and fall of the height of all nine stages of growth can be forced by hand as well. By just changing b to be larger so the stages were all larger and increasing c_1 to be larger than one, the second wave of follicle growth emerged. As c_1 increased, the timing of the second wave became more accurate. Also, Km_F seemed to be quite sensitive which will be tested in a later section.

Set Optimization Boundaries. Once a sampling of parameter changes were made, optimization took place on the whole ovarian component system as outlined in the previous section. The optimizer gives more accurate stage heights. Though the goal is to have a second wave of follicle growth, the optimizer is only looking at matching ovarian hormones and does not care what the stages look like. In some instances the optimizer felt the better option was to eliminate the second wave of growth and though despite the fact that the FSH threshold function was included, the stages looked quite similar to the original model. In this case, a more drastic approach was needed. To eliminate the wave altogether, the optimizer reverted some of the parameters that were changed by hand before optimization. To aid in optimization, the cost function in the optimizer was given some limitations. For example, c_5 was limited to stay below 0.76. This was because the

optimizer was making that value too large which greatly reduces the size of the dominant follicle because too much is transferring out. In the original model, a large value for c_5 would have been acceptable but now that it is not the only decay term on the dominant follicle with the inclusion of the atresia term, a large value would be too much for the system. Likewise, a restriction on γ was made as well since those two parameters are partners on the transfer of mass.

Word of Caution - Retain Results, even Seemingly Unfavorable Ones. In the case that the optimizer reduced the height or completely eliminated the second wave of growth, the results were retained and that round of optimization was not considered a failure. Those results were then changed by hand to regain the second follicle wave and the optimization procedure was run again. The second follicle wave is not controlled by every parameter of the system, so just because one set of parameters that is returned after optimization does not display a second follicle wave does not mean every parameter is poor, just the ones that control the wave are of a concern. Since the FSH threshold was included, the parameter values for OvF_1 through Lut_4 may change, though not by much, to accommodate that threshold. Since they are not supposed to have a second wave of growth anyway, the values the optimizer gives may be better results than the originals.

Be Selective in Parameters to Optimize. This optimization procedure is repeated until two follicle waves of good height are seen and maintained. The final step of the procedure is to optimize just the auxiliary equation coefficients. The stage parameters and auxiliary equation coefficients were all optimized to this point. However, too much tinkering with the stage parameters may eliminate the wave. Once stage parameters were found that maintained both follicle waves, they were held constant and just the auxiliary equation coefficients were optimized to find the best hormone profiles based on the waves in existence. This procedure only works for the ovarian component model. In the merged model, changing auxiliary coefficients would in turn change the FSH and LH profiles which would feedback and change the stages of follicle growth regardless of whether their coefficients are held constant or not. So even though the wave looks good, the extra step in finding even better auxiliary equation coefficients is important because these ovarian component model parameter results in Table 3.1 will become the starting point for the merged model.

As can be seen in Figure 3.6, this optimization procedure resulted in curves that fit the data quite well upon inspection. Looking closer, the hardest hormone to match of the three ovarian hormones, E2 is within the data error of its peak. Note that SSEres on each graph image represents the sum squared error for each hormone for one cycle. The error results confirm that P4 is one of the easiest to match. However, leaving IHA until last in inclusion in the cost

function puts it at a disadvantage because most of the parameters for the stages will not change after E2 has been optimized. Thus, IHA has a higher error and misses many points around the peaks and troughs.

3.3.2 McLachlan Merged Model

After a set of parameters from the ovarian component model are obtained, the next step is to merge the model. Historically, the parameters obtained in the pituitary component and ovarian component models are used as a starting point for the optimization of the full merged system. However, the resulting merged parameters and curves change regardless of how accurate the individual component models are. This is due to the high accuracy of the input functions. The input functions were fixed for the component models. Now, hormones depend on one another and everything needs to find a balance. Though harder to solve for a set of optimal parameters, the parameters yield a more realistic solution than the component models both biologically and mathematically. It is more biologically realistic because it is a more authentic representation of the cycle. It is more mathematically realistic because the model is not as easily manipulated as the component models. Another concern to be aware of in the merged model is timing. The timing of the component models is always very good because the input functions are fixed. Now that the feedback loop is in effect, the cycle length may vary in the merged model.

The merged model for the five-hormone, two-wave system has all thirteen ordinary differential equations (Equations (3.9)-(3.12), (3.27)-(3.35)). The exponent a (Equation (3.9)) in some previous work on the original model was changed from eight to eleven in order to increase the sharpness of LH synthesis so changing the value for the merged follicle wave model was considered. It was tested at both eight and eleven. Eleven seemed to help promote the second follicle wave and was fixed in the model at that value. Again, e_0, p_0 and h_2 all optimized to 0 and were eliminated. The resulting parameters are included in Table 3.2 and the stages with two waves of ovarian follicle recruitment and growth are shown in Figure 3.7.

Cycle Results: Though typically the hormone profiles may not give as good of a fit to the data for a merged model as opposed to the fits for the respective component models, the overall interaction of the pituitary and the ovaries is much more accurate. The mass of the follicle stages, shapes of hormones and parameter values tend to level off to more reasonable results in the merged model because it is harder to manipulate these values by hand to have the system do what one wants. Follicle stage heights were easily manipulated by the b parameter in the ovarian component, but it is much harder to accomplish in the merged model. Thus, the expectation for the results of the merged model are for less accurate profiles, but much more knowledge of how the waves interact with the pituitary. The five-hormone, two-wave merged model for the McLachlan data accomplished just that. Both pituitary hormones have peaks

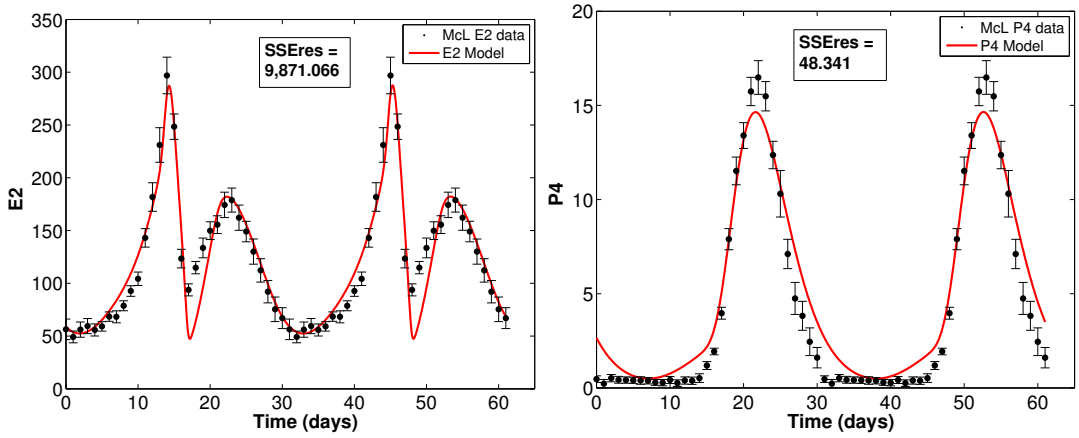

(a)

(b)

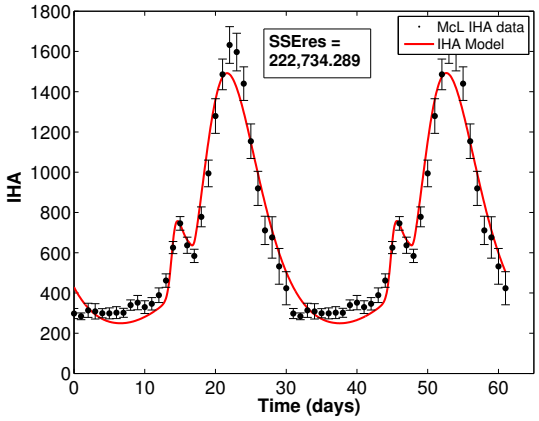

(c)

Figure 3.6 Models for **(a)** estrogen, **(b)** progesterone and **(c)** inhibin A from the ovarian component, five-hormone, two-wave model fit to the McLachlan data set. The ovarian component model results come from optimizing system parameters for the stages of follicle growth and the ovarian functions based on input functions for FSH and LH. Note here that even though a second follicle wave is present in the luteal phase, the same profiles for the ovarian hormones were achieved. SSEres is the summed squared difference between the hormone and the data for one cycle.

Table 3.2 Parameter results for the merged, five-hormone, two-wave model fitting the McLachlan data set. All of the following optimized parameters were truncated to two significant decimal digits.

Param.	Value	Units
v_{0LH}	1577.78	μg/day
v_{1LH}	25,288.06	μg/day
Km_{LH}	228.645	ng/L
$Ki_{LH,P}$	3.01	μg/L
k_{LH}	12.26	1/day
$c_{LH,P}$	0.085	L/μg
$c_{LH,E}$	9.22E-08	L/ng
d_E	0.47	days
d_P	0.80	days
v_{FSH}	5190.68	μg/day
$Ki_{FSH,IHA}$	654.11	U/L
k_{FSH}	12.83	1/day
$c_{FSH,P}$	2.46	L/μg
$c_{FSH,E}$	0.0019	$(\text{L/ng})^2$
d_{IHA}	1.66	days
α	0.31	dimensionless
β	0.022	dimensionless
γ	0.011	dimensionless
b	0.60	L/day
c_1	1.59	1/day
c_2	0.51	$(\text{L/}\mu\text{g})^{\alpha}$(1/day)
c_3	0.057	$(\text{L/}\mu\text{g})^{\beta}$(1/day)

Param.	Value	Units
c_4	0.025	(L/μg)(1/day)
c_5	0.30	$(\text{L/}\mu\text{g})^{\gamma}$(1/day)
d_1	0.70	1/day
d_2	0.59	1/day
k_1	0.66	1/day
k_2	0.63	1/day
k_3	0.60	1/day
k_4	0.80	1/day
Km_F	115.18	μg/L
p	19.80	dimensionless
atr	615.89	1/day
Ki_{atr}	4.69	μg/L
pwr_{at}	2.36	dimensionless
e_1	0.023	1/kL
e_2	0.025	1/kL
e_3	0.14	1/kL
p_1	0.0063	1/L
p_2	0.0020	1/L
h_0	208.76	U/L
h_1	0.0040	(U/L)/μg
h_3	0.66	(U/L)/μg
h_4	0.00098	(U/L)/μg

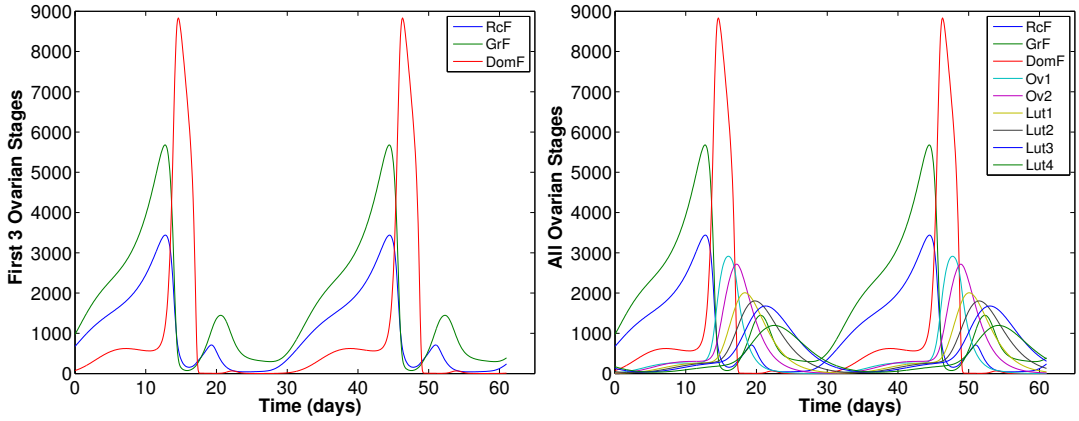

(a) **(b)**

Figure 3.7 Ovarian follicle stages of growth from the merged, five-hormone, two-wave model fit to the McLachlan data set. The model maintains both follicle waves for the recruited and growing stages of growth that were seen in the ovarian component model.

within the error for the peak data, but all three ovarian hormones miss the mark. Again, IHA is the most ill-fitting of the five hormones as it was left for last in the cost function build up. Unlike the ovarian component, IHA did not even attempt to capture its first small rise. This is not uncommon now that the system is merged. Three major areas of interest are important to discuss:

Cycle Length: The first thing to note is that the overall cycle length is just slightly longer than the 31 days of data for the McLachlan data set. This is easily seen in Figure 3.8. The first cycle for all hormones in the figure was centered to the day of the LH peak. It is clear from the panel for LH that the LH peak for the second cycle is just after the data point for the peak making the cycle slightly longer than 31 days. This is not unexpected. Changing parameters not only helps the magnitude of hormones but also changes the time length. The costs of having a better magnitude here outweigh the length of the cycle. Also interesting to note about timing is FSH. All of the hormones in Figure 3.8 had their first cycle centered around the day of the LH peak for the picture. Four of the five hormones fit their data peaks fairly well timing wise. FSH however is late. This could be due to the shortened trough width of P4 since it determines the release of FSH. The bulk of the hormones all have correct timing. This early and slow rise in P4 is directly caused by the follicle stages. This slow rise was also present in the ovarian component model.

Magnitude: IHA and P4 are shorter in height than they were in the ovarian component model but their timing is correct. The curve for LH looks quite accurate for its fit to the LH peak. This is the most important part of the curve, so the curve reaching its peak is a benefit.

Shape Oddities: There is a slight bump in the luteal phase LH that does not match the data. This is ultimately due to the second follicle wave. E2 is vital to synthesis and release of LH. E2 itself is composed of the growing (GrF), dominant ($DomF$) and fourth luteal (Lut_4) stages of growth. The two follicle waves are seen in Figure 3.7 for GrF. The stage itself looks very much like the profile for E2 so on the surface it seems like having an extra follicle wave in one of the stages needed for an auxiliary equation will not impact the hormone (note that E2 is the only hormone with an auxiliary equation that uses a stage with two waves as opposed to just one). However, GrF in combination with Lut_4 could make the second rise in E2 too large. Lut_4 cannot be downplayed or eliminated because its width is an accurate profile for the second rise in E2 while the second wave in GrF is too narrow to span the width itself. GrF in turn cannot be downplayed either because it contributes to the width and height of the first rise in E2. Thus, the result as seen in Figure 3.8 is that the second rise in E2 is higher than its data. It should be

noted that E2 does not reach its peak and its first rise is actually shorter than it was in the ovarian component model. So not only is the second rise in E2 larger, the first rise is shorter. It would be very difficult to shorten the second rise in E2 because clearly the peak height would suffer even more. So with the E2 curve as good as it can be, the larger second rise in E2 causes the extra bump in LH. Therefore the second wave in GrF causes E2 to be too large in the luteal phase and ultimately results in the extra bump in LH.

Overall, the profiles of the five hormones were maintained in the merged model after the recruited stage was changed to include the FSH threshold and a second wave of follicle growth.

Parameter Results: For the most part, the parameters in Table 3.2 for the merged model are quite similar to those in the ovarian component model as seen in Table 3.1. This should not be surprising as the results from the ovarian component were the starting point for the work on the merged model. Recall since fminsearch finds local solutions, it would be surprising if every parameter in the system changed by a lot. However, a few did change somewhat dramatically. The most surprising was the atr parameter on the atresia term for the dominant follicle. The parameter value is just shy of double its value which seems extreme on the surface. Looking closer at the results, Ki_{atr} and pwr_{at} decreased in conjunction with that change. Though the atr probably increased to maintain that no second dominant (or subsequent) wave occurs, it was balanced by these other changes and the increase is probably not as dramatic as it looks. Also, c_5, the transfer out parameter from the dominant to the first ovulatory stage decreased. Thus, the atresia term may be reducing the dominant follicle but c_5 is transferring less out and again there is some semblance of balance here. Typically, when one parameter changes in cases like this, the rest of the parameters in that term change to keep the system in balance.

It will be interesting to see if the relationship between the figures and parameters between the Welt ovarian component model and the merged model behave as similarly and as predictably as those for the McLachlan model did here.

3.3.3 Welt Ovarian Component Model

Once the two-wave model was successfully completed for the McLachlan data set, the whole process was repeated for the Welt data set beginning with the ovarian component model. Though the process and the differential equations are exactly the same as they should work for any data set, there are subtle differences between modeling to fit the Welt versus the McLachlan.

Timing: The Welt data set is three days shorter than the McLachlan. Not only is it shorter in length, the days are counted differently. The McLachlan starts counting on day zero while the Welt starts on day one. The cycle is marked by hormone events and the days they occur. By counting on day one, there is less time in the follicular phase in the Welt than there is in the McLachlan. That means certain parameters may take much longer to

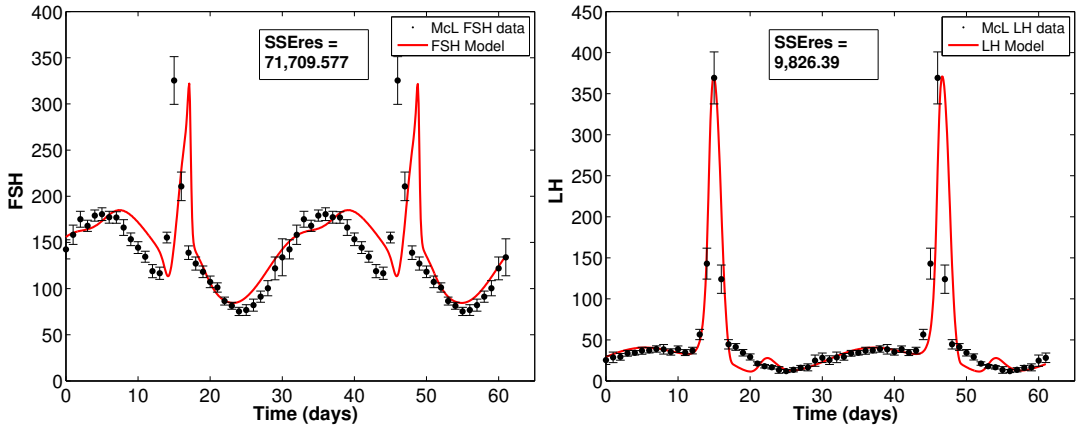

(a)

(b)

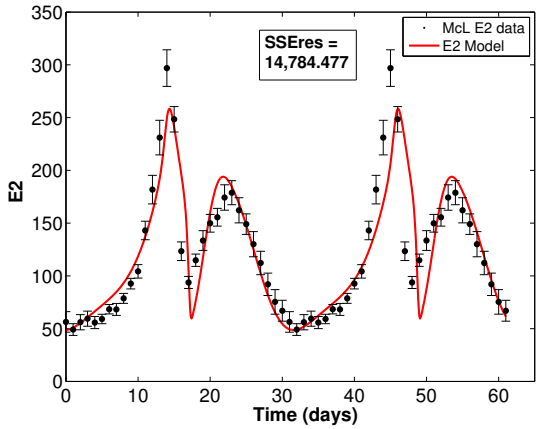

(c)

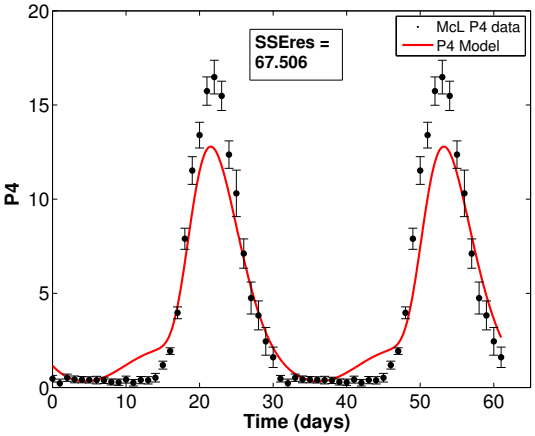

(d)

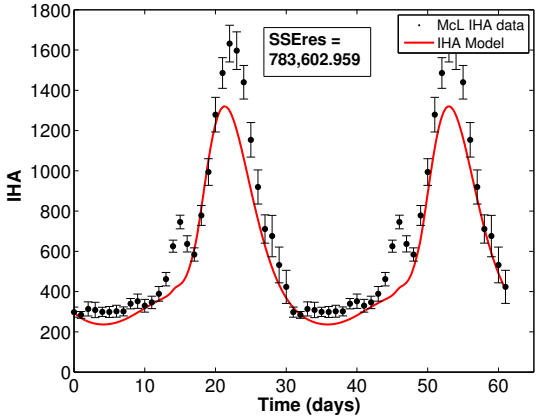

(e)

Figure 3.8 Models for **(a)** follicle-stimulating hormone, **(b)** luteinizing hormone, **(c)** estrogen, **(d)** progesterone and **(e)** inhibin A from the merged, five-hormone, two-wave model fit to the McLachlan data set. SSEres is the summed squared difference between the hormone and the data for one cycle.

identify as parameters dictate both magnitude and timing. The timing difference will be even more noticeable in the merged model when not relying on fixed input functions.

Magnitude: The magnitude of the Welt data is much less than the McLachlan based on the units used in hormone measurement. Initially using the McLachlan parameters in the Welt model may seem reasonable but the values of the parameters may lead the model astray. For instance, Km_F is the FSH concentration at half the maximum velocity. Since FSH is much shorter in numerical value based on units of measure in the Welt than the McLachlan, the parameter value found to fit for the McLachlan data is higher than the maximum FSH value in the Welt.

These differences need to be considered when transitioning from one data set to another. Here, we know the differential equations will produce a wave and we know the process that was used to find the data set works but will start from parameters that fit the one-wave system.

Input Functions: To begin the ovarian component model, we need the LH and FSH input functions that fit the Welt data set. The Welt input functions are taken directly from Pasteur [78]. They are as follows and are illustrated in Figure 3.9:

$$\text{LH} = 10 + 100e^{-\frac{(t-14)^2}{0.8}} + 12e^{-\frac{(t-13.5)^2}{50}} \tag{3.39}$$

$$\text{FSH} = 4 + 8.5e^{-\frac{(t-5)^2}{40}} + 11e^{-\frac{(t-14)^2}{1}} + 4.5e^{-\frac{(t-16.5)^2}{20}} \tag{3.40}$$

Again, in fitting the parameters the same process was followed that was used for the McLachlan data.

Adjust Parameters by Hand. The first step is to change parameters manually since the optimizer is looking for local solutions. The benefit for this model is that it has already been established as to which of these parameters will yield the second follicle wave. As before, b was increased to scale the stages, c_1 was increased above one, α was reduced by a little over half and c_2 was adjusted accordingly to maintain a stable solution. Also, since the magnitude of the McLachlan FSH is about sixteen times larger, the Km_F and p parameters on the FSH threshold were reduced as well.

Build Up Cost Function. At this point, the optimization plan was put into effect, building up the cost function until a second follicle wave and hormone profiles that upon visual inspection match the Welt data set were found. The parameters for the Welt five-hormone, two-wave ovarian component model are listed in Table 3.3.

Table 3.3 Parameter results for the five-hormone, two-wave ovarian component model fitting the Welt data set. All of the following optimized parameters were truncated to two significant decimal digits.

Parameter	**Value**	**Units**
α	0.30	dimensionless
β	0.79	dimensionless
γ	0.17	dimensionless
b	1.03	L/day
c_1	1.39	1/day
c_2	0.46	$(\text{L/IU})^{\alpha}(1/\text{day})$
c_3	0.064	$(\text{L/IU})^{\beta}(1/\text{day})$
c_4	0.049	(L/IU)(1/day)
c_5	0.58	$(\text{L/IU})^{\gamma}(1/\text{day})$
d_1	0.73	1/day
d_2	0.62	1/day
k_1	0.51	1/day
k_2	0.51	1/day
k_3	1.24	1/day
k_4	0.65	1/day
e_0	4.0052	pg/mL
e_1	0.016	(pg/mL)/IU
e_2	0.014	(pg/mL)/IU
e_3	0.0091	(pg/mL)/IU
p_0	0.00019	ng/mL
p_1	0.0020	(ng/mL)/IU
p_2	0.0015	(ng/mL)/IU
h_0	1.32	IU/mL
h_1	0.00046	1/mL
h_2	0.00069	1/mL
h_3	0.00041	1/mL
h_4	0.00021	1/mL
Km_F	6.68	IU/L
p	7.66	dimensionless
atr	86.66	1/day
Ki_{atr}	5.33	IU/L
pwr_{at}	3.14	dimensionless

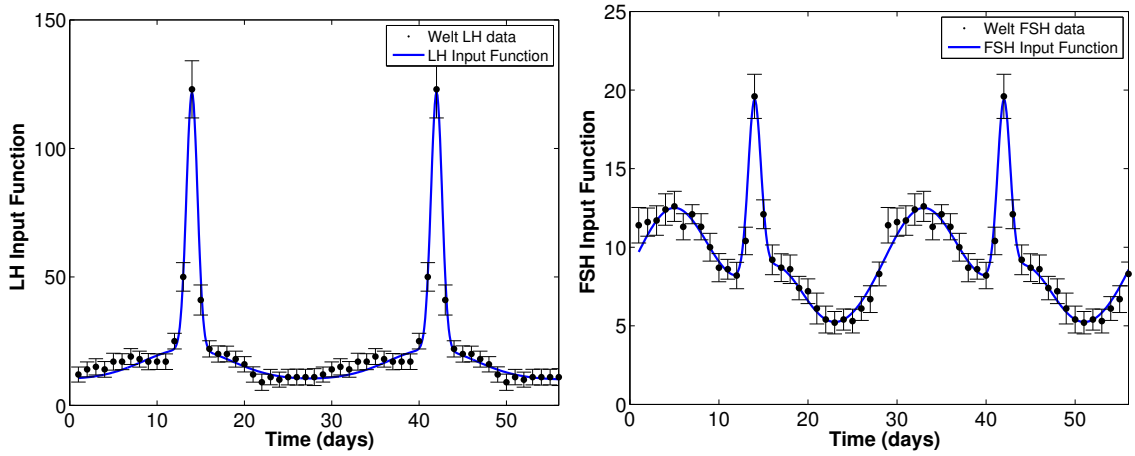

(a) (b)

Figure 3.9 Input functions that fit the Welt data set for the pituitary hormones LH and FSH. These input functions are used to solve and optimize the system of nine differential equations that model the stages of ovarian follicle growth with two follicle waves. With these stages, the auxiliary equations for the ovarian hormones can be solved.

Cycle Results: The ovarian follicle stages are included in Figure 3.10. The Welt stages look slightly different than the McLachlan. Here, the second follicle wave is much taller for the Welt data than for the McLachlan data. The proportion of height from the first wave to the second wave is much higher for this data set as is seen in Figure 3.10. However, the heights may be closer together but the second wave does not dissipate as much. The wave peaks may be as high as they are because the troughs are not nearly as low. There simply is not as much distance to grow. It will be interesting to see if this trough behavior remains after the system is merged. The ovarian hormone profiles are displayed in Figure 3.11 and appear to fit the data quite well. All three ovarian hormones reach the peak value of the data. They are all within the error of the peak data amounts as well. However, since the ovarian stages do not meet their trough, it is not surprising to see that IHA does not meet its trough either. Typically, the low levels of the hormone data have less error than the peak amounts. Not only does IHA have trouble meeting its trough, there is also very little data error in the trough compared to other parts of the cycle and IHA does not make it within the data error on the through either. However, IHA has a lower summed squared error for one cycle than it did for the McLachlan data results in the previous two sections. This could be due to the nature of the IHA data or the shape of the ovarian follicle stages.

Parameter Results: As expected, the value for Km_F is much smaller since the scale of FSH is much smaller for the Welt than the McLachlan. Similarly, atr is much smaller as well.

Overall, the parameter values in Table 3.3 are similar in most respects to the set obtained for the McLachlan as were the images. It is important to point out that e_0, p_0 and h_2 did not optimize to zero as they did in the McLachlan work.

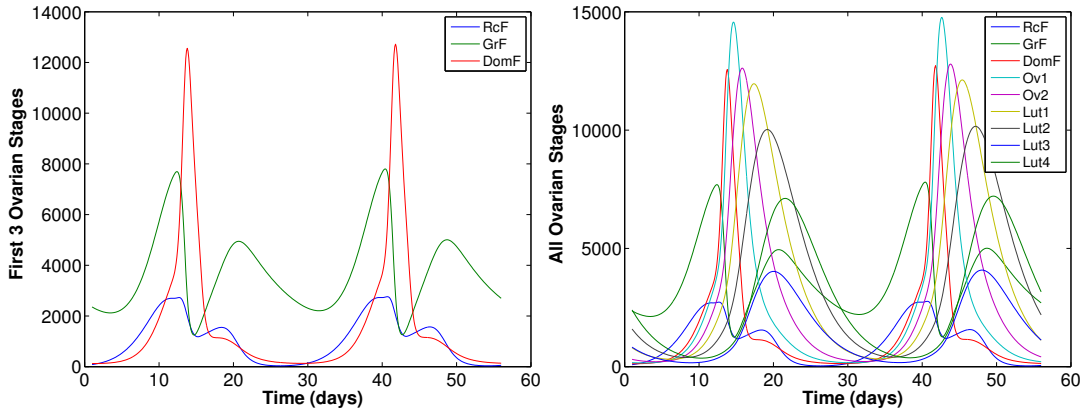

(a) **(b)**

Figure 3.10 Ovarian follicle stages of growth from the ovarian component five-hormone, two-wave model fit to the Welt data set.

3.3.4 Welt Merged Model

Finding parameters for the merged model to fit the Welt data set was approached the same as it was for the McLachlan data set.

Begin from Previous Results. The parameters obtained from the ovarian component model were used as the starting point for our new parameters for the merged model which helps put the optimizer in prime position to find an appropriate solution to the thirteen dimensional system.

Build Up Cost Function. The optimization procedure was the same except for one small change in the order hormones were added into the cost function. One by one the ovarian hormones were added, E2, then P4 then IHA before LH and finally FSH was added in. Here, the reasoning for using FSH last is because it tends to be difficult to match to data, its peak especially.

Adjust Parameters by Hand. With such a good looking luteal wave from the ovarian component model, merging this model became more of tweaking parameters by hand to fine

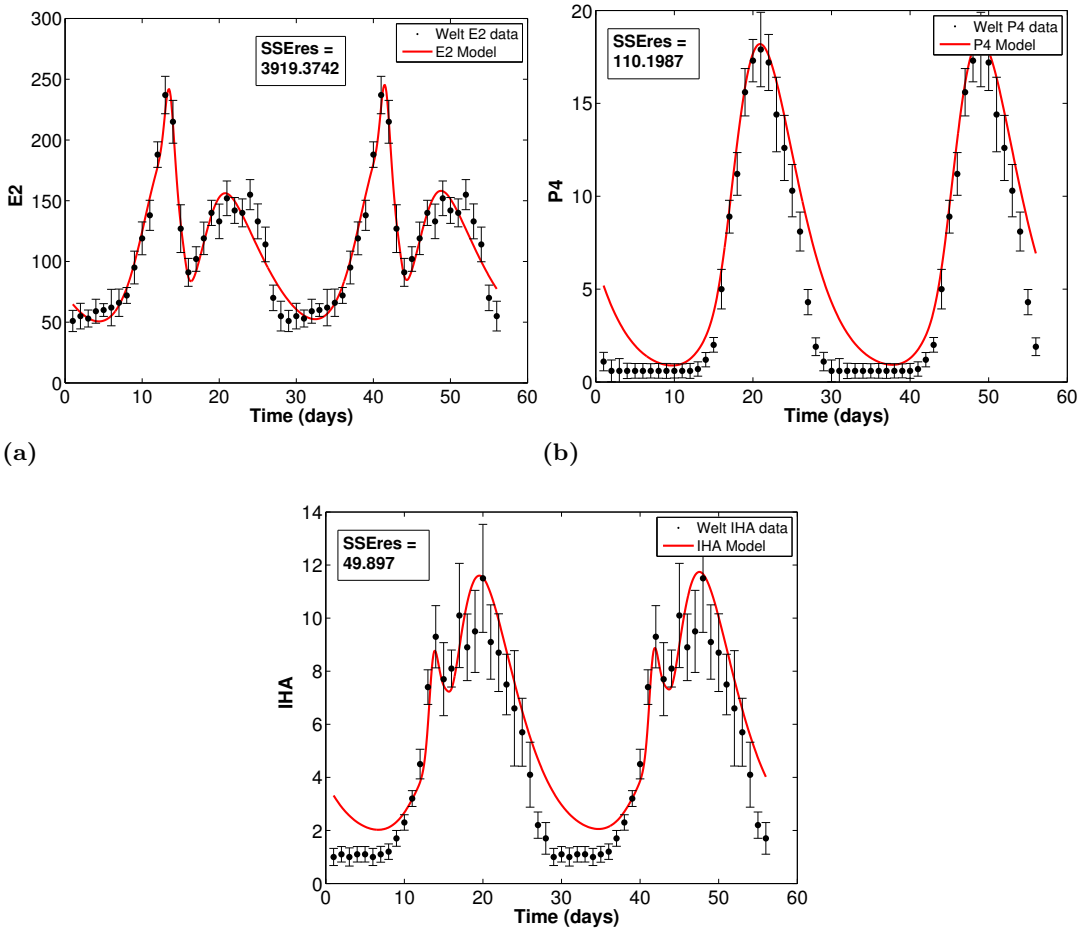

Figure 3.11 Models for **(a)** estrogen, **(b)** progesterone and **(c)** inhibin A from the ovarian component five-hormone, two-wave model fit to the Welt data set. SSEres is the summed squared difference between the hormone and the data for one cycle.

tune the model than major overhauls. Part of the tweaking was changing the parameters manually to obtain stage of growth order and higher proportion of the first and second wave height.

Change Cost Function Length of Time. Another part of the tweaking was adjusting the number of cycles given to the optimizer. Like the McLachlan merged model, the Welt seemingly had a much different cycle length than the data. Changing the optimizer to three cycles instead of two helps force a cycle length for the model closer to the Welt 28 day cycle. It is considered tweaking because it should be done after the optimization process has found a local solution that is close to approximating the data. Adding a cycle length in cost function will add to the length of time the optimization process takes, so doing so too early will be very heavy computationally.

The resulting parameters from this process are found in Table 3.4. Note that p_0 optimized to zero and was left out.

Cycle Results: As the merged model typically does, the Welt five-hormone, two-wave model balances out many of the issues that arose from the ovarian component model. The most obvious from looking at the stages in Figure 3.12 is that the trough of the luteal follicle wave is much deeper before recruitment occurs again going into the follicular phase. This figure looks more like the McLachlan merged model than the Welt ovarian component looked like the McLachlan component. The luteal follicle wave height did not suffer due to the trough change however. The proportion of the first wave to the second wave is still very good, though not as good as in the ovarian component model. The better overall shape of the waves is much more important than the reduced height of the second wave. The waves are still much larger than the McLachlan merged model. This is due to the FSH as seen in Figure 3.13. The FSH not only fits the data fairly well, it is also taller than the data in many places. The higher the FSH concentration, the more likely it surpasses the threshold allowing the follicle wave to grow larger. For FSH to be taller than the data, most of the other hormones are also taller than the data. The only one that is not (but still fits much better than the McLachlan set) is P4. Here, the ovarian hormones, in particular IHA, also reach their troughs which was an issue in the ovarian component. Very similar to the McLachlan merged model, the second rise in the merged Welt E2 is much taller than its data. Since its second rise is also narrow and pointy at the top, it is obvious that the growing stage luteal wave causes this extra rise and not the fourth luteal stage. As was seen earlier, this extra height causes a luteal phase bump in the LH profile. Also like the McLachlan merged model, the Welt merged model is slightly longer than the 28 day cycle reported in the data. The cycle is longer than the data despite using three cycle lengths of data because the manual tweaking in searching for a final parameter set alters the length of time. Though it is not exactly 28 days in length, the model length is still in the acceptable

Table 3.4 Parameter results for the merged, five-hormone two-wave model fitting the Welt data set. All of the following optimized parameters were truncated to two significant decimal digits.

Param.	**Value**	**Units**
v_{0LH}	635.68	IU/day
v_{1LH}	4000.00	IU/day
Km_{LH}	192.72	pg/mL
$Ki_{LH,P}$	6.13	ng/mL
k_{LH}	16.52	1/day
$c_{LH,P}$	3.23	mL/ng
$c_{LH,E}$	0.35	mL/pg
d_E	0.21	days
d_P	1.03	days
v_{FSH}	440.00	IU/day
$Ki_{FSH,IHA}$	4.44	IU/mL
k_{FSH}	2.97	1/day
$c_{FSH,P}$	12.34	mL/ng
$c_{FSH,E}$	0.0010	$(\text{mL/pg})^2$
d_{IHA}	1.68	days
α	0.30	dimensionless
β	0.85	dimensionless
γ	0.096	dimensionless
b	1.15	L/day
c_1	1.32	1/day
c_2	0.47	$(\text{L/IU})^{\alpha}(1/\text{day})$
c_3	0.00024	$(\text{L/IU})^{\beta}(1/\text{day})$
c_4	0.045	(L/IU)(1/day)

Param.	**Value**	**Units**
c_5	0.60	$(\text{L/IU})^{\gamma}(1/\text{day})$
d_1	0.73	1/day
d_2	0.63	1/day
k_1	0.59	1/day
k_2	0.55	1/day
k_3	0.50	1/day
k_4	0.55	1/day
e_0	12.32	pg/mL
e_1	0.022	(pg/mL)/IU
e_2	0.018	(pg/mL)/IU
e_3	0.021	(pg/mL)/IU
p_1	0.0015	(ng/mL)/IU
p_2	0.0013	(ng/mL)/IU
h_0	0.54	IU/mL
h_1	0.00090	1/mL
h_2	0.00040	1/mL
h_3	0.00082	1/mL
h_4	0.00075	1/mL
Km_F	6.90	IU/L
p	11.21	dimensionless
atr	66.48	1/day
Ki_{atr}	4.44	IU/L
pwr_{at}	3.19	dimensionless

biological range. The peak amount of pituitary hormone both exceed the data and the error associated with the data. However their summed squared error is low. That is exceptional for FSH due to the difficulty of modeling compared to the other hormones. Its fit is vital to the follicle waves.

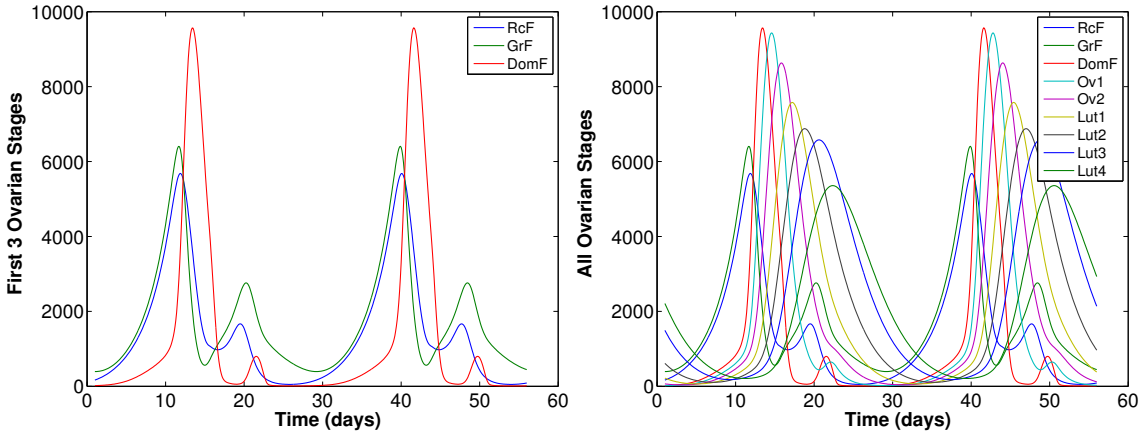

(a) (b)

Figure 3.12 Ovarian follicle stages of growth from the merged, five-hormone, two-wave model fit to the Welt data set.

Comparison of McLachlan and Welt Results:

Cycle Results: The merged models for both the McLachlan and the Welt data set look very similar despite the much more dramatic differences between their ovarian component models. Thus, merging the models tends to weed out some of the issues that arise from the component models being easily manipulated due to the fixed time dependent input functions.

- Both models have a significant sized luteal phase second follicle wave of recruitment and growth.
- In the merged model, both data sets optimized the model to an E2 profile with a second rise that is too tall because of the second follicle wave and causes an extra bump in the LH profile which was an unexpected result.
- Also, both merged models had final parameters that gave a slightly longer cycle length than their respective data sets.

Again, since fminsearch finds local solutions, these results could be different with a different cost function and procedure however, they would not be dramatically different.

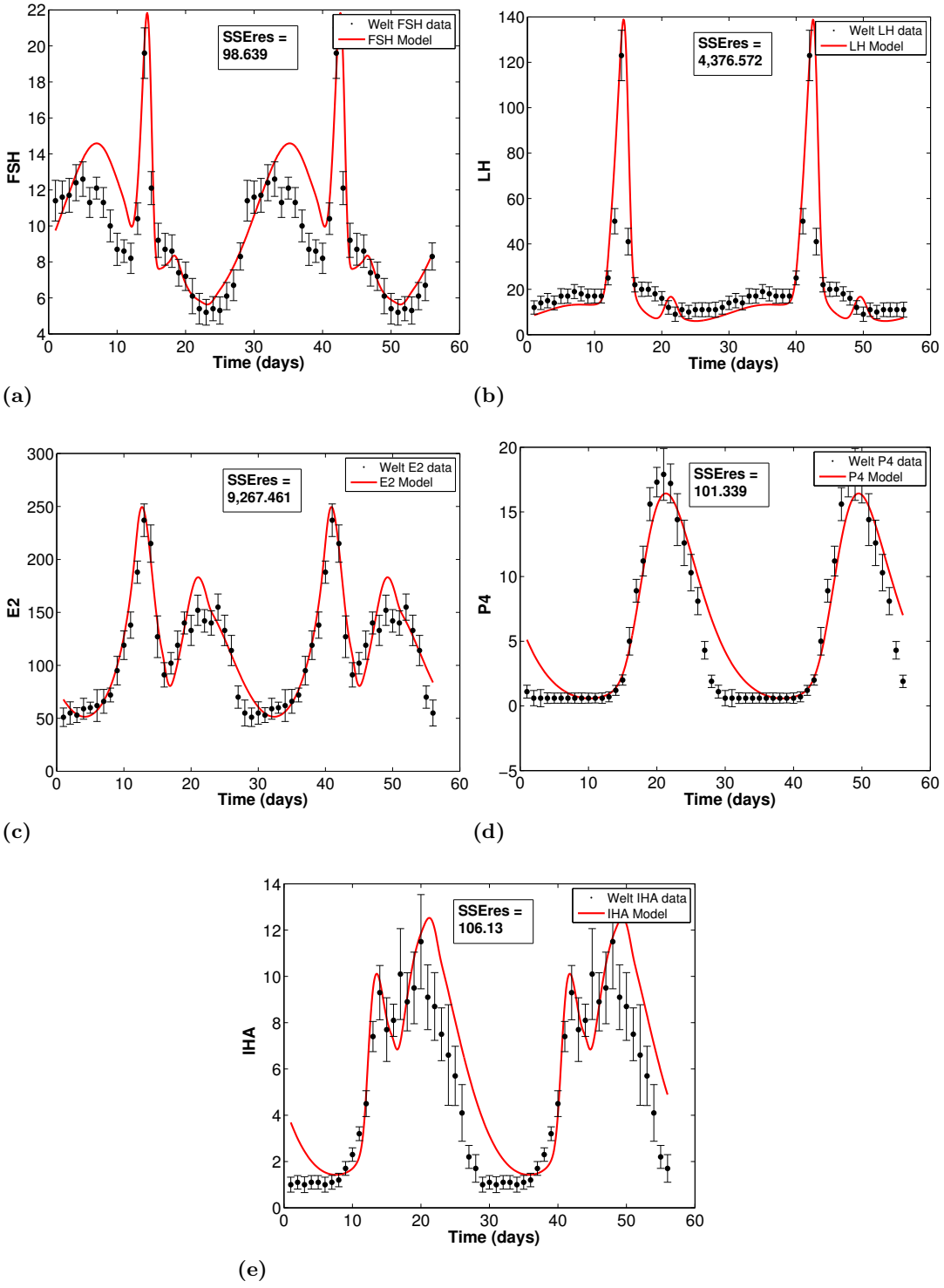

Figure 3.13 Models for **(a)** follicle-stimulating hormone, **(b)** luteinizing hormone, **(c)** estrogen, **(d)** progesterone and **(e)** inhibin A from the merged, five-hormone, two-wave model fit to the Welt data set. SSEres is the summed squared difference between the hormone and the data for one cycle.

Parameter Results: It is important to note that KmF, c_1 and p have great influence on the height of the second follicle wave as they make up the FSH threshold. If KmF was lowered by hand too much, chaotic behavior occurred. Changes to other parameters, like c_2 and α also helped regulate the second follicle wave so control of the wave is not limited to the threshold but is more widespread to the entirety of the recruited stage of growth. These parameters tend to change how the model behaves. In some cases tweaking parameters quite drastically changed the model from a stable solution. The next logical step before expanding the six-hormone model to include two waves would be to conduct sensitivity analysis on the merged five-hormone, two-wave models.

3.3.5 Sensitivity Analysis

Sensitivity analysis aids in estimating parameters and evaluating the behavior of a system. There are two immediate goals of the sensitivity analysis conducted here. The first is to confirm whether the parameters that seemed to be sensitive through all of the manual adjusting of parameters to aid with optimization really are considered sensitive. The second is to compare whether the sensitive parameters are the same across both merged models or are there differences between the Welt and the McLachlan models.

Sensitivity analysis measures how much a system changes with respect to a perturbation in parameters [103]. The purpose is to identify the parameters that have the largest impact on the system output and thus are the major contributors to the system's behavior. The parameters that greatly affect the model output when changed slightly are known as sensitive parameters while the parameters that have little effect on the model output are known as insensitive parameters [82]. In this respect, sensitivity analysis is a key component to model design and parameter estimation. Insensitive parameters can affect optimization by giving poor fits and unrealistic parameters outside the physiological realm. There are two types of analysis, local sensitivity analysis and global sensitivity analysis [103]. Local sensitivity analysis examines the effects the system undergoes when each parameter is changed one at a time. Global sensitivity analysis investigates the system after simultaneous changes to more than one parameter. For our purposes, we will be using local sensitivity analysis.

Let the vector $\mathbf{y}$ be our model output and $\mathbf{q}$ be our vector of parameters. Model output can be defined to whichever and however many states are deemed important to investigate. For instance, say there are N states for $\mathbf{y}$. Also, assume we have m parameters. The goal for local sensitivity analysis is to make changes to each parameter one at a time and to investigate our model output for subsequent changes. Let Δq_i be the perturbation to the ith parameter in $\mathbf{q}$. As vector using the standard basis vector $\mathbf{e_i}$, we can represent the change to the system parameters as $\mathbf{q} + \Delta q_i \mathbf{e_i}$. As a scalar, we can represent the change to q_i as $q_i + \Delta q_i$. Then for

each state j, we can represent y_j in a Taylor series expansion [103]. The 1st order series is given for particular time t_k is as follows:

$$y_j(\mathbf{q} + \Delta q_i \mathbf{e_i}, t_k) = y_j(\mathbf{q}, t_k) + \sum_{i=1}^{m} \frac{\partial y_j}{\partial q_i}(t_k)\Delta q_i \tag{3.41}$$

Here, the partial derivative $\dfrac{\partial y_j}{\partial q_i}(t_k)$ is known as the 1st order local concentration sensitivity coefficient. The absolute sensitivity matrix for all states and all parameters at a particular time t_k is thus given by the Jacobian:

$$\mathbf{S}(t_k) = \frac{\partial \mathbf{y}}{\partial \mathbf{q}}(t_k) = \begin{bmatrix} \dfrac{\partial y_1}{\partial q_1}(t_k) & \dfrac{\partial y_1}{\partial q_2}(t_k) & \cdots & \dfrac{\partial y_1}{\partial q_m}(t_k) \\ \dfrac{\partial y_2}{\partial q_1}(t_k) & \dfrac{\partial y_2}{\partial q_2}(t_k) & \cdots & \dfrac{\partial y_2}{\partial q_m}(t_k) \\ \vdots & \vdots & \ddots & \vdots \\ \dfrac{\partial y_N}{\partial q_1}(t_k) & \dfrac{\partial y_N}{\partial q_2}(t_k) & \cdots & \dfrac{\partial y_N}{\partial q_m}(t_k) \end{bmatrix} \tag{3.42}$$

Each column of the Jacobian recognizes the change in each state in the system due to that column's parameter perturbation and each row recognizes change in a particular state due to each parameter perturbation. To examine more than one time step, the matrices $S(t_k)$ can be stacked to form:

$$S = \begin{bmatrix} S(t_1) \\ S(t_2) \\ \vdots \end{bmatrix} \tag{3.43}$$

Thus S has all the states wished to be examined for all the time steps wished to be investigated for all parameters in one place.

Many methods have been formed to create the above Jacobian of local sensitivities. The most basic is the forward finite difference method [103]. The finite difference method is given as follows:

$$\frac{\partial y_j}{\partial q_i}(t) = \frac{y_i(\mathbf{q} + \Delta q_i \mathbf{e_i}, t) - y_i(\mathbf{q}, t)}{\Delta q_i} \tag{3.44}$$

There are three useful concepts that help make the sensitivities more relatable. The first is taking the natural logarithm of the parameters. Since all of the parameters are of different magnitudes and the goal is to compare each parameter's sensitivity to another, we can take the natural logarithm of our parameters [82]. Let $\widetilde{\mathbf{q}} = \ln(\mathbf{q})$. The second is the idea of relative sensitivities. Relative sensitivities normalize the sensitivities to allow for comparisons among a large array of magnitudes. The relative sensitivity for state j and parameter i for $y_i \neq 0$ for all

t is:

$$\frac{\partial y_j}{\partial \widetilde{q}_i}\frac{\widetilde{q}_i}{y_j} \tag{3.45}$$

The final concept is the total sensitivity. The Jacobian contains the sensitivity per parameter, per system equation and per time step. In order to compare and rank these sensitivities, we want to examine the entire body of work. To do so, we take the Euclidean norm of the jth parameter's column in the Jacobian. After all three steps, we can rank the total relative sensitivities for each parameter from largest to smallest with the largest being the most sensitive and the smallest being the least sensitive parameters.

We have seen in the previous sections' optimization results and from manually adjusting parameters that certain parameters are quite sensitive. It would be interesting to note whether they are in line with the process outlined here. Also, it would be interesting to see how sensitive the wave parameters are because they are the new parameters in the system. This knowledge will aid in creating the six-hormone model, in testing biological ideas using the model and in future work involving bifurcation analysis if desired.

Sensitivity analysis can be limited to whichever states, however many states and for whatever time periods deemed to be important. For this model, peak amounts of the hormones are critical to ovulation and the FSH curve is critical to the follicle waves. Hormone models are solved at a tenth of a day interval. Here, two scenarios are analyzed for sensitive parameters:

1. As the E2 peak controls many of the aspects of the cycle that keep it going, the time interval of two days around the peak is one scenario to be examined. Without the E2 peak, the LH surge does not occur which in turn causes ovulation. At the tenth of a day interval, we compute sensitivities using 41 time steps for the E2 peak.

2. The other scenario is the entire FSH curve for one period due to its continuous regulation of the ovarian follicle waves. For FSH we compute sensitivities for either 281 or 311 time steps for the Welt and the McLachlan respectively.

One important item to consider is that changing any parameter could change both the length of the cycle and the amount of runoff the merged model needs to find its stable solution. Thus, it is important to match the peak E2 for the original model with the peak E2 for the perturbed model. The same applies to FSH. Here, we use the natural logarithm of the parameters to keep the parameters on a narrower scale and the perturbation used is changing the parameter by 1% of its value. Because the parameters span such a wide magnitude range, comparing the sensitivities themselves will not yield as much information as the relative sensitivities so those will be computed and ranked from most sensitive to least sensitive.

The ranked sensitivities for the McLachlan and Welt five-hormone, two-wave merged models are listed in Table 3.5. The McLachlan are on the left and the Welt are on the right.

Table 3.5 The six most sensitive parameters and the eight least sensitive ranked in order from greatest to least for the five-hormone, two-wave merged model. Panel **(a)** is for the McLachlan and panel **(b)** is for the Welt. These sensitivities are ranked relative sensitivities. Relative sensitivities were used to account for the vast range of parameter magnitudes.

(a)

Rank	E2 Peak	FSH Cycle
1	v_{FSH}	v_{FSH}
2	Km_F	v_{0LH}
3	v_{0LH}	Km_F
4	α	Km_{LH}
5	$Ki_{FSH,IHA}$	α
6	Km_{LH}	$Ki_{FSH,IHA}$
37	b	b
38	β	β
39	$c_{LH,P}$	h_1
40	h_1	$c_{LH,P}$
41	h_4	d_{IHA}
42	d_{IHA}	h_4
43	d_P	$c_{LH,E}$
44	$c_{LH,E}$	d_P

(b)

Rank	E2 Peak	FSH Cycle
1	v_{0LH}	v_{FSH}
2	Km_{LH}	v_{0LH}
3	v_{FSH}	Km_{LH}
4	α	h_3
5	e_2	Km_F
6	h_3	e_1
39	d_1	k_{FSH}
40	e_1	d_E
41	k_{FSH}	d_1
42	c_3	c_3
43	b	b
44	k_2	k_2
45	d_P	d_P
46	β	β

McLachlan Sensitivity: The six most sensitive and eight least sensitive are displayed in order from greatest to least. The cutoff as to how many were chosen is arbitrary. From the table, it is easy to see that the method used, (E2 peak vs. entire FSH cycle) may change the rankings slightly but not so much that something is no longer sensitive or insensitive. The six most sensitive for the McLachlan for the E2 peak method are the same parameters for the FSH method, just in a different order. The same applies for the least sensitive McLachlan parameters. It is important to note that for the McLachlan, both Km_F and α are quite sensitive. It was hypothesized earlier that these parameters could be sensitive and testing proved that to be true. Though not included in the chart, c_2, which was also included as a possible sensitive parameter from the previous section, is in the top ten on both of the McLachlan lists. It is also interesting to see b on the list of the most insensitive parameters. In the ovarian component model, b was shown to control much of the magnitude of the ovarian follicle stages but that role diminished in the merged model because of the full feedback loop. The relative sensitivity rankings for all 44 system parameters can be seen in Figure 3.14 for the E2 peak and Figure 3.15 for the FSH cycle. These figures display from left to right the most sensitive to least sensitive parameters and their respective relative sensitivities.

Welt Sensitivity: Turning to the Welt, it is clear that there is less consistency between

the two methods. Only four of the top six most sensitive parameters are the same for both methods. Also, only one of the wave controlling parameters is in the top six for each ranking. The parameter α is sensitive for the E2 peak while KmF is sensitive for the FSH cycle. It is quite telling that the parameter on the FSH threshold, KmF is sensitive on the FSH cycle. Thus the importance of taking FSH into account for the follicle wave model. If we expand the list to the top 11, both methods for the Welt include α, KmF and c_2. The five most insensitive parameters for the Welt model are the same for both methods and seven of the bottom eight are the same for both methods. Figures 3.16 and 3.17 show the ranked relative sensitivities for the E2 peak and FSH cycle methods, respectively.

Comparing Data Sets: Comparing methods between data sets, four of the top six sensitive parameters for the E2 peak are the same for both the McLachlan and Welt models but only three of the most insensitive. For the FSH cycle, four of the top six most sensitive are the same and the top two are ranked the same for both the McLachlan and the Welt. Again only three of the bottom eight for the FSH cycle are the same for both data set models.

Two important results were discovered through this sensitivity analysis. First, the parameters that control the wave were confirmed to be sensitive as was believed from manually fitting the parameters during the optimization process. And second, using the FSH curve for sensitivity is important for examining the parameters that control the wave. These results could help in parameter identification. In the next chapter, parameters will be identified for the expanded six-hormone model.

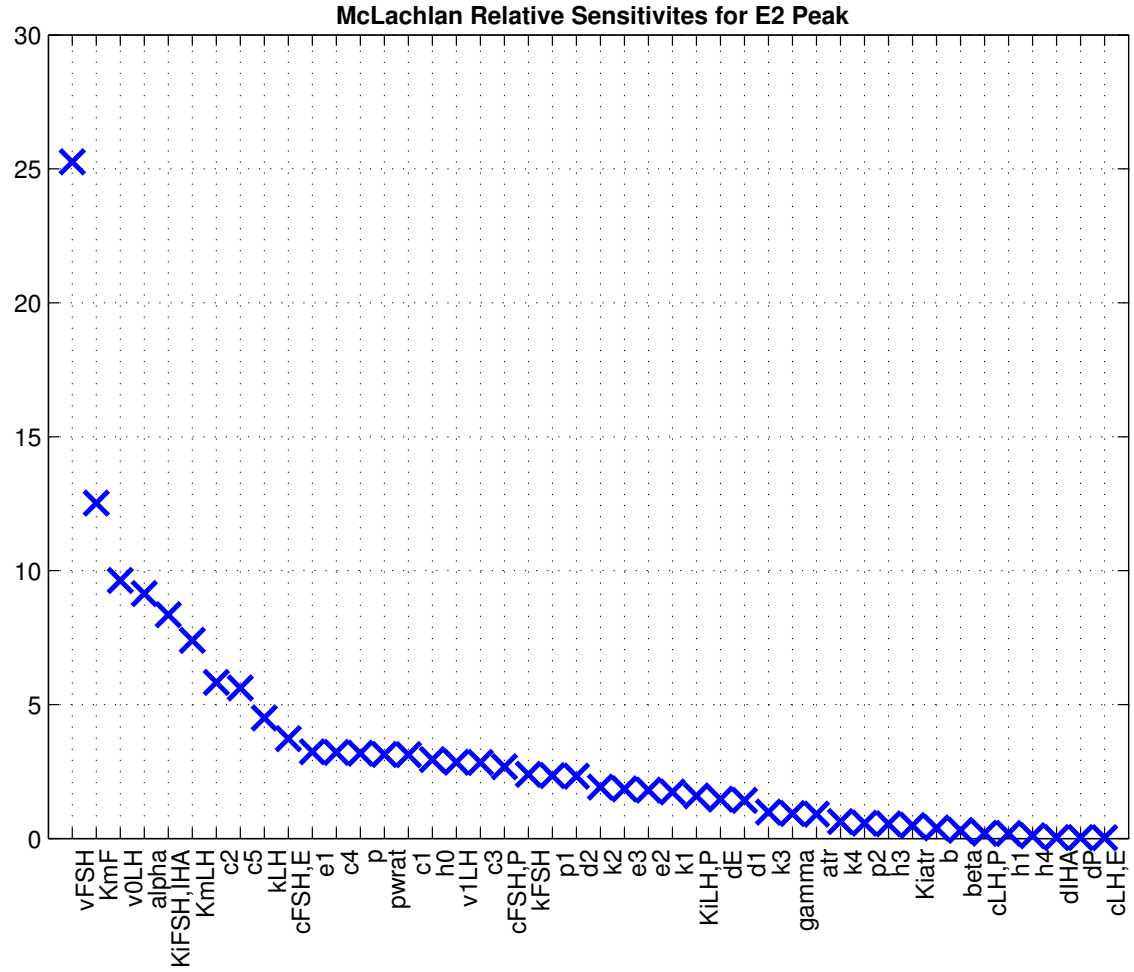

Figure 3.14 Relative sensitivities for the McLachlan five-hormone, two-wave merged model around the E2 peak ranked from most sensitive to least sensitive.

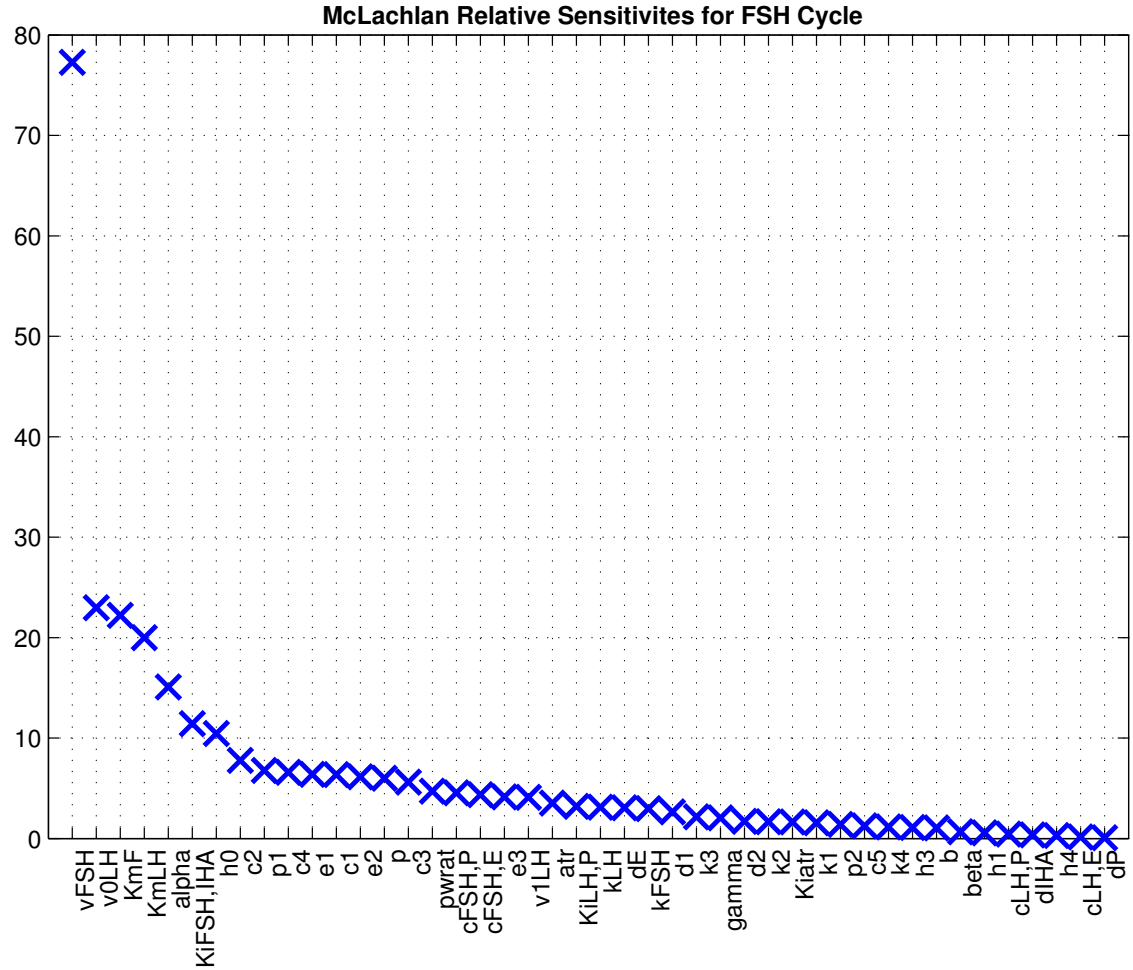

Figure 3.15 Relative sensitivities for the McLachlan five-hormone, two-wave merged model for the one FSH cycle ranked from most sensitive to least sensitive.

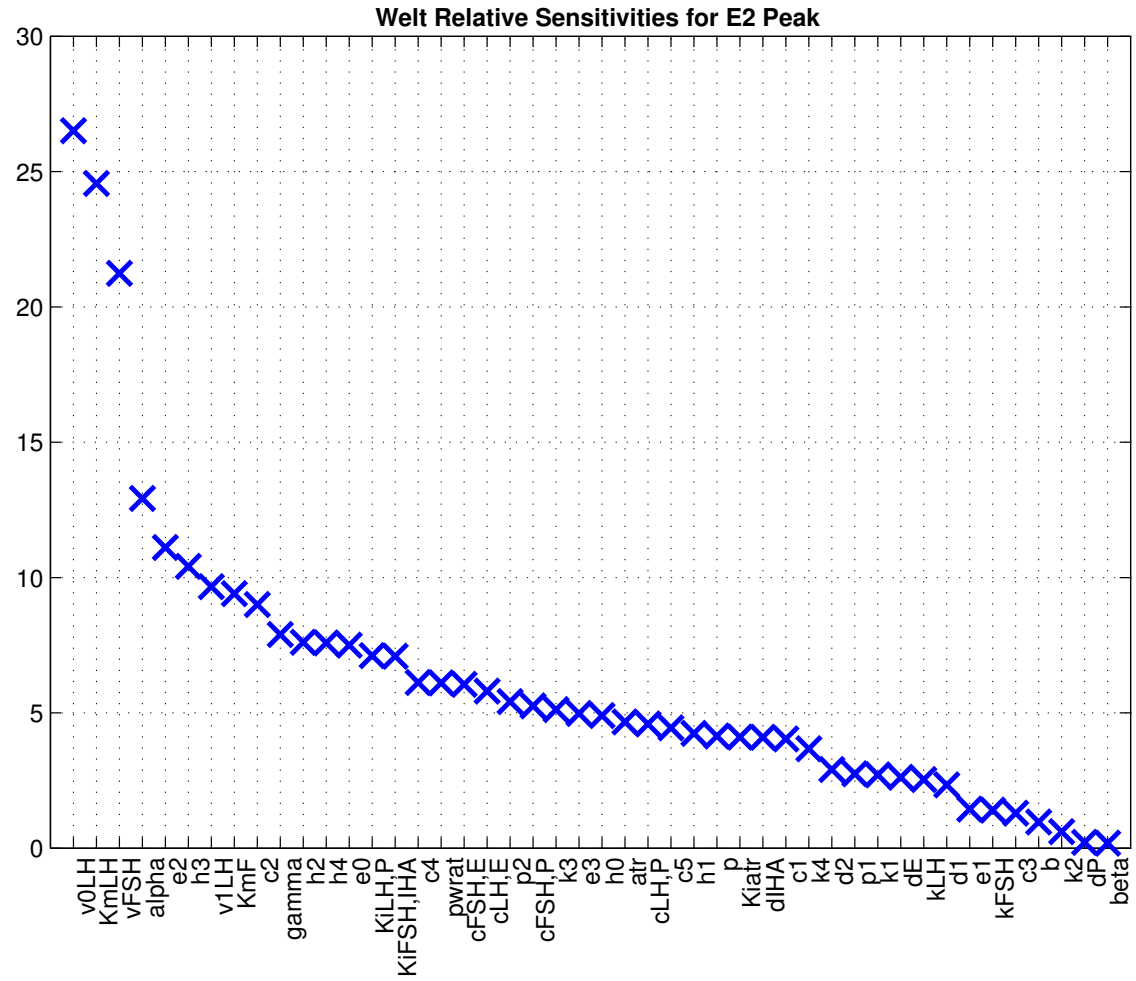

Figure 3.16 Relative sensitivities for the Welt five-hormone, two-wave merged model around the E2 peak ranked from most sensitive to least sensitive.

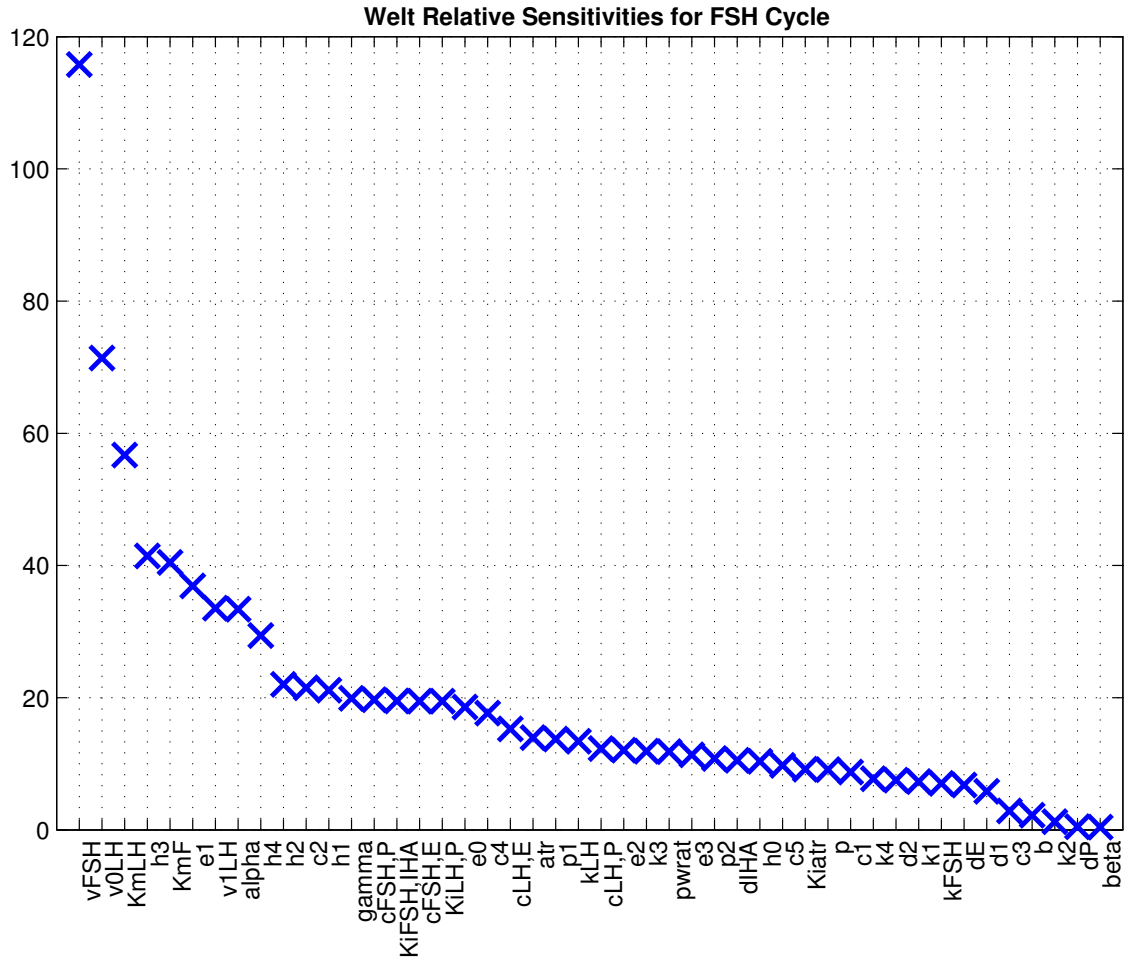

Figure 3.17 Relative sensitivities for the Welt five-hormone, two-wave merged model for the one FSH cycle ranked from most sensitive to least sensitive.

Chapter 4

Two-Wave, Six-Hormone Model

The original five-hormone model was updated to include the profile for IHB. The availability of Welt data set allowed for this model expansion. From Chapter 2, recall IHB affects the synthesis of FSH. Also, since FSH determines the number of follicle waves per cycle the logical next step in the progression of modeling ovarian follicle waves is to model them in the six-hormone system.

4.1 Original Model Development

Recall from Chapter 2, IHB is considered the follicular phase inhibin as opposed to IHA which is considered the luteal phase inhibin. Because IHB is active in the follicular phase, the ovarian follicle stages of growth were not comprehensive enough to model IHB as they were originally written in the five-hormone model. The original work transforming the five-hormone model to the six-hormone model was done by Pasteur [78] and the model was fit to the Welt data for younger women. The model was created in the same three step process of the five-hormone model, the pituitary component, the ovarian component and the final merged full feedback model.

Pituitary Component: Just like IHA, IHB is also under a time delay. Because IHB inhibits the synthesis of FSH, it is included in the pituitary reserve pool differential equation in a term similar to the one that represents IHA. IHB is included in the denominator as an inhibition agent and has its own delay d_{IHB}. The inclusion of IHB expands the number of parameters by two for the FSH differential equation. The FSH reserve pool differential equation with IHB is below and the additions to expand the five-hormone model are denoted in red:

$$\frac{d}{dt}RP_{\text{FSH}} = \frac{v_{FSH}}{1 + \frac{\text{IHA}(t - d_{IHA})}{Ki_{FSH,IHA}} + \frac{\text{IHB}(t - d_{IHB})}{Ki_{FSH,IHB}}} - \frac{k_{FSH} \cdot (1 + c_{FSH,P} \cdot P_4) \cdot RP_{\text{FSH}}}{1 + c_{FSH,E} \cdot E_2} \quad (4.1)$$

Thus, all four pituitary component differential equations are as follows:

$$\frac{d}{dt}RP_{\text{LH}} = \frac{v_{0LH} + \dfrac{v_{1LH} \cdot E_2(t-d_E)^a}{Km_{LH}^a + E_2(t-d_E)^a}}{1 + \dfrac{P_4(t-d_P)}{Ki_{LH,P}}} - \frac{k_{LH} \cdot (1 + c_{LH,P} \cdot P_4) \cdot RP_{\text{LH}}}{1 + c_{LH,E} \cdot E_2} \tag{4.2}$$

$$\frac{d}{dt}\text{LH} = \frac{1}{V} \cdot \frac{k_{LH} \cdot (1 + c_{LH,P} \cdot P_4) \cdot RP_{\text{LH}}}{1 + c_{LH,E} \cdot E_2} - a_{LH} \cdot \text{LH} \tag{4.3}$$

$$\frac{d}{dt}RP_{\text{FSH}} = \frac{v_{FSH}}{1 + \dfrac{\text{IHA}(t-d_{IHA})}{Ki_{FSH,IHA}} + \dfrac{\text{IHB}(t-d_{IHB})}{Ki_{FSH,IHB}}} - \frac{k_{FSH} \cdot (1 + c_{FSH,P} \cdot P_4) \cdot RP_{\text{FSH}}}{1 + c_{FSH,E} \cdot E_2} \tag{4.4}$$

$$\frac{d}{dt}\text{FSH} = \frac{1}{V} \cdot \frac{k_{FSH} \cdot (1 + c_{FSH,P} \cdot P_4) \cdot RP_{\text{FSH}}}{1 + c_{FSH,E} \cdot E_2} - a_{FSH} \cdot \text{FSH} \tag{4.5}$$

Ovarian Component: For the ovarian component model, input functions are needed for FSH and LH. Recall both five and six-hormone models exist for the Welt data set. Thus, the input functions used for the six-hormone ovarian component model to represent FSH and LH are the same that were used in the five-hormone model (Equations (3.39) and (3.40)) shown in Figure 3.9. The ovarian component model only needs three additional stages and an additional auxiliary equation. Two preantral stages of growth are necessary in addition to the remaining follicle stages to accurately model the follicular phase peak of the hormone profile for IHB. In addition an extra ovulatory stage was included for timing purposes of all of the ovarian hormones. Since they all peak on separate days, a new stage was needed to maintain these distinct days in their respective auxiliary equations. The system of differential equation that represents the varying stages of follicle growth has thus been expanded to twelve. The stages of ovarian follicle growth were expanded to include a prenatal ($PrAn$), small antral ($SmAn$) and an additional ovulatory stage (OvF_3). The stages of growth are as follows for the one-wave

model and the three new stages for the six-hormone model are in red:

$$\frac{d}{dt}PrAn = f_2 \cdot \frac{\left(\frac{\text{FSH}}{f_1}\right)^{\eta}}{1+\left(\frac{\text{FSH}}{f_1}\right)^{\eta}} - f_3 \cdot \text{FSH} \cdot PrAn \tag{4.6}$$

$$\frac{d}{dt}SmAn = f_3 \cdot \text{FSH} \cdot PrAn - f_4 \cdot \text{LH}^{\delta} \cdot SmAn \tag{4.7}$$

$$\frac{d}{dt}RcF = f_4 \cdot \text{LH}^{\delta} \cdot SmAn + c_1 \cdot \text{FSH} \cdot RcF - c_2 \cdot \text{LH}^{\alpha} \cdot RcF \tag{4.8}$$

$$\frac{d}{dt}GrF = c_2 \cdot \text{LH}^{\alpha} \cdot RcF + (c_3 \cdot \text{LH}^{\beta} - c_4 \cdot \text{LH}) \cdot GrF \tag{4.9}$$

$$\frac{d}{dt}DomF = c_4 \cdot \text{LH} \cdot GrF - c_5 \cdot \text{LH}^{\gamma} \cdot DomF \tag{4.10}$$

$$\frac{d}{dt}OvF_1 = c_5 \cdot \text{LH}^{\gamma} \cdot DomF - c_6 \cdot OvF_1 \tag{4.11}$$

$$\frac{d}{dt}OvF_2 = c_6 \cdot OvF_1 - d_1 \cdot OvF_2 \tag{4.12}$$

$$\frac{d}{dt}OvF_3 = d_1 \cdot OvF_2 - d_2 \cdot OvF_3 \tag{4.13}$$

$$\frac{d}{dt}Lut_1 = d_2 \cdot OvF_3 - k_1 \cdot Lut_1 \tag{4.14}$$

$$\frac{d}{dt}Lut_2 = k_1 \cdot Lut_1 - k_2 \cdot Lut_2 \tag{4.15}$$

$$\frac{d}{dt}Lut_3 = k_2 \cdot Lut_2 - k_3 \cdot Lut_3 \tag{4.16}$$

$$\frac{d}{dt}Lut_4 = k_3 \cdot Lut_3 - k_4 \cdot Lut_4 \tag{4.17}$$

One subtle yet important change in the stages listed above is in RcF. Previously, RcF was the first stage so it began with $b \cdot \text{FSH}$ and the b was important in the ovarian component model for increasing the size of the follicle stages. Here however, there is no $b \cdot \text{FSH}$ term because there is now a transfer term to start RcF. This may or may not have an impact on the work moving forward, but it is important to note. Additionally, adding in the third ovulatory stage reparameterizes the system slightly but all of the terms still look and behave as they did previously. The only previously existing stage that had a term change with regards to behavior is the recruited stage. The auxiliary equations for the three ovarian hormones E2, P4 and IHA are the same as the five-hormone model (Equations (3.22)-(3.24)). The additional stages of growth needed for the auxiliary equation for IHB were not needed to model E2, P4 or IHA. IHB utilizes the small antral stage of growth and its auxiliary equation is as follows:

$$\text{IHB} = j_0 + j_1 \cdot SmAn + j_2 \cdot DomF + j_3 \cdot OvF_1 \tag{4.18}$$

The work done by Pasteur to model the one-wave, six-hormone system was recreated as a baseline for modeling the two-wave scenario as was done in Chapter 3 for the five-hormone model. The resulting hormone profiles and follicle stages of growth are shown in Figure 4.2 and 4.1. The optimized parameters can be found in Appendix B and the initial conditions in Appendix C.

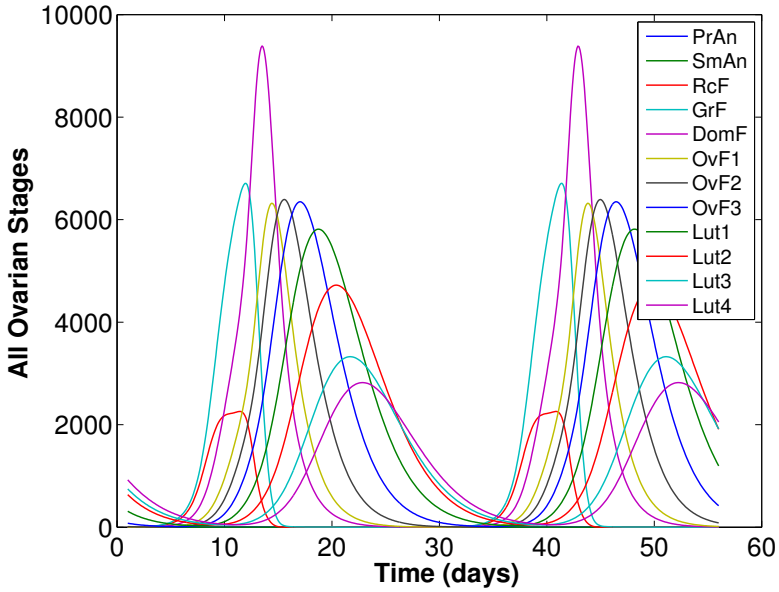

Figure 4.1 Ovarian follicle stages of growth such that the hormone profiles for the six-hormone, one-wave merged model fit the Welt data set. The original six-hormone equations from Pasteur [78] were used to find parameters to fit the Welt data and were used to model these stages. Since the original one-wave model is the starting point for the two-wave model, it made sense to recreate that model first as a baseline.

4.2 Two-Wave Model Development

The beauty of this model is that we already know from Chapter 3 what types of equations worked well to develop a second follicle wave in the recruited and growing stages and only those stages, as well as which parameters are important to controlling the wave. The most obvious concern when one considers adding a follicle wave to the six-hormone model is where the FSH threshold goes as the recruited stage is no longer the first equation in the system. Biologically, follicle waves are a recruited cohort of antral follicles.The FSH threshold goes in the recruited stage of growth just as it did in the five-hormone model, despite now having two stages prior.

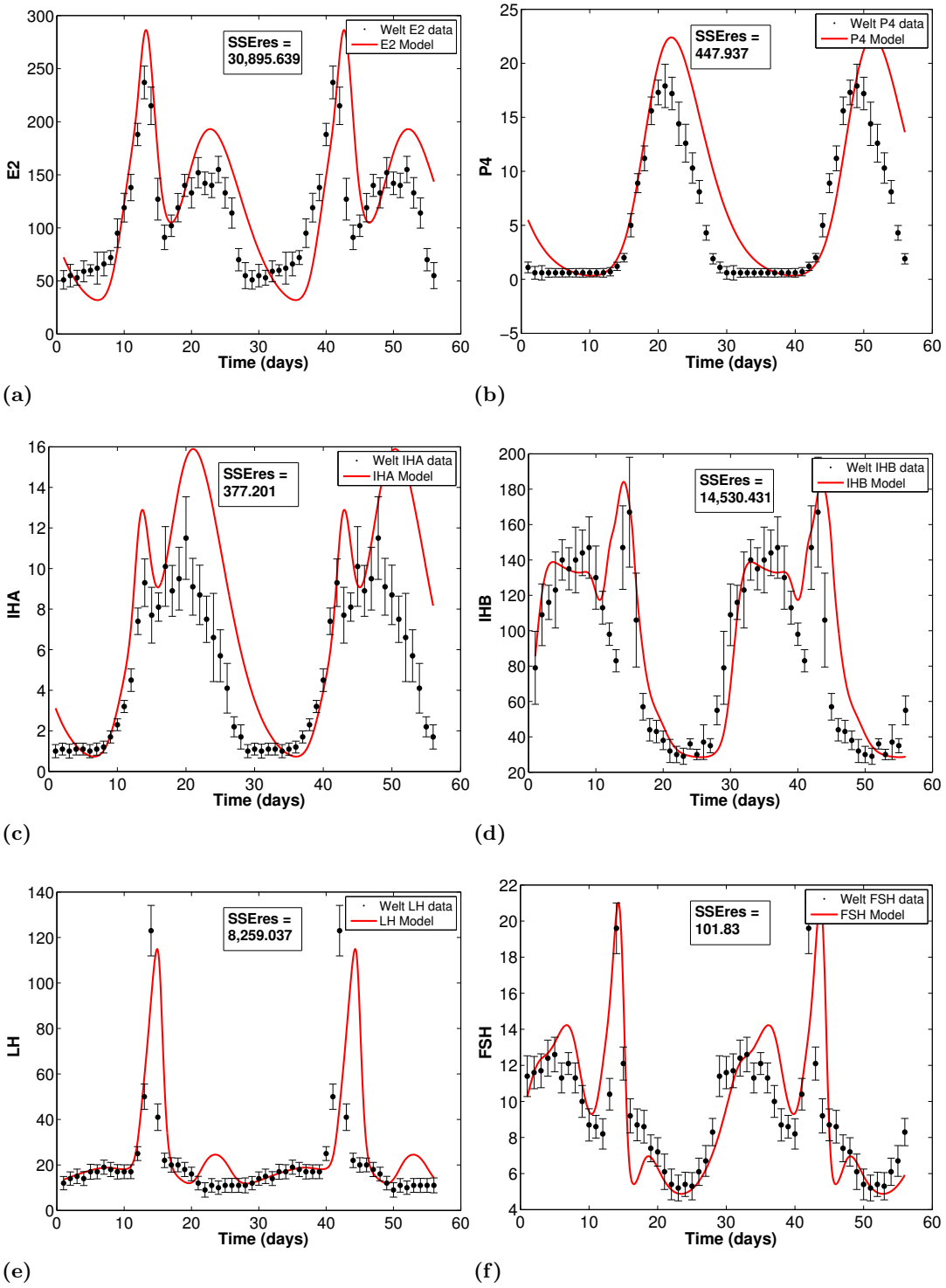

Figure 4.2 Hormone profiles for the six-hormone, one-wave merged model fit to the Welt data set using the original equations by Pasteur [78]. The parameters (Appendix B) are a starting point for the two-wave model. SSEres is the summed squared difference between the hormone and the data for one cycle.

The six-hormone model recruited stage is almost identical to its five-hormone counterpart with exception of the first term. The threshold will again go on the c_1 term as it did previously. We know the atresia term is critical to suppressing growth beyond the growing stage, so that can be immediately included in the dominant follicle stage as well. The sixteen equations for the two-wave, six-hormone model are the same four pituitary equations from the one-wave system (Equations (4.2)-(4.5)) and the following stages (with the FSH threshold and atresia terms in

red):

$$\frac{d}{dt}PrAn = f_2 \cdot \frac{\left(\frac{\text{FSH}}{f_1}\right)^{\eta}}{1+\left(\frac{\text{FSH}}{f_1}\right)^{\eta}} - f_3 \cdot \text{FSH} \cdot PrAn \tag{4.19}$$

$$\frac{d}{dt}SmAn = f_3 \cdot \text{FSH} \cdot PrAn - f_4 \cdot \text{LH}^{\delta} \cdot SmAn \tag{4.20}$$

$$\frac{d}{dt}RcF = f_4 \cdot \text{LH}^{\delta} \cdot SmAn + c_1 \cdot RcF \cdot \frac{\left(\frac{\text{FSH}}{Km_F}\right)^{p}}{1+\left(\frac{\text{FSH}}{Km_F}\right)^{p}} - c_2 \cdot \text{LH}^{\alpha} \cdot RcF \tag{4.21}$$

$$\frac{d}{dt}GrF = c_2 \cdot \text{LH}^{\alpha} \cdot RcF + (c_3 \cdot \text{LH}^{\beta} - c_4 \cdot \text{LH}) \cdot GrF \tag{4.22}$$

$$\frac{d}{dt}DomF = c_4 \cdot \text{LH} \cdot GrF - c_5 \cdot \text{LH}^{\gamma} \cdot DomF - \frac{atr \cdot DomF}{1+\left(\frac{\text{LH}}{Ki_{atr}}\right)^{pwr_{at}}} \tag{4.23}$$

$$\frac{d}{dt}OvF_1 = c_5 \cdot \text{LH}^{\gamma} \cdot DomF - c_6 \cdot OvF_1 \tag{4.24}$$

$$\frac{d}{dt}OvF_2 = c_6 \cdot OvF_1 - d_1 \cdot OvF_2 \tag{4.25}$$

$$\frac{d}{dt}OvF_3 = d_1 \cdot OvF_2 - d_2 \cdot OvF_3 \tag{4.26}$$

$$\frac{d}{dt}Lut_1 = d_2 \cdot OvF_3 - k_1 \cdot Lut_1 \tag{4.27}$$

$$\frac{d}{dt}Lut_2 = k_1 \cdot Lut_1 - k_2 \cdot Lut_2 \tag{4.28}$$

$$\frac{d}{dt}Lut_3 = k_2 \cdot Lut_2 - k_3 \cdot Lut_3 \tag{4.29}$$

$$\frac{d}{dt}Lut_4 = k_3 \cdot Lut_3 - k_4 \cdot Lut_4 \tag{4.30}$$

The optimization procedure used to find parameters for the six-hormone, two-wave model is very much the same as for the five-hormone process. One notable update to the optimization process is needed with the addition of another hormone.

Build Up Cost Function. IHB is the last hormone to be added into the cost function. There is a major reason for this choice. IHB is composed of three stages of growth that should not show any signs of a second follicle wave. It will be harder to fit E2 because both waves directly affect it which is an important reason why it remains as the first hormone in the cost function. The dominant and first ovulatory stage height should be fairly accurate after fitting E2, so few changes should occur in them as the other ovarian hormones are added to the cost function. P4 and IHA fitting will work through the ovulatory and luteal stages. With most of the stage heights established with hopefully a second follicle wave there would hopefully be little left to do to fit IHB. Since the dominant and first ovulatory stages are already fit for E2, the only stage left to consider for IHB is the small antral stage which does dictate much of the shape of IHB. However, $SmAn$ is very small in mass. That means changing $SmAn$ will not greatly impact the future stages. Here it is much more likely that the auxiliary equation coefficients for IHB will do much of the work for fitting IHB. Thus, it will be added last into the cost function.

4.3 Results

4.3.1 Welt Ovarian Component Model

As was done in the five-hormone model, we start with the ovarian component when creating the six-hormone, two-wave model for the Welt data set. The parameter set is larger so initial expectations are that solving and optimizing a new set of parameters will be a much more time consuming process. With that thought process in mind, it is important to set the model up for the best results.

Begin from Previous Results. Unlike introducing a second follicle wave into the five-hormone model from scratch, the six-hormone model has the five-hormone model to lean on for previous parameter results and sensitivities. The initial parameters used for the six-hormone, two-wave ovarian component model are from both the new parameters (in Appendix B) found to fit the equations from Pasteur that yield the results in Figures 4.2 and 4.1 for the one-wave model and the parameters from the five-hormone, two-wave ovarian component model results for the Welt data from Table 3.3. The only parameters used from Table 3.3 are the ones that control the wave, like Km_F. The rest are from the six-hormone, one-wave model.

Adjust Parameters by Hand. Parameters for the six-hormone, one-wave model have historically been harder to fit, so the expectations that many adjustments by hand and possibly restricting parameters was met for modeling two follicle waves. Fitting parameters for this

model became a battle between two scenarios. The first scenario is two beautiful follicle waves per cycle in the appropriate stages of growth but unflattering hormone profiles. The second scenario is wonderful hormone profiles fit to the data but no second follicle wave. After each step taken in the optimization process, parameters were manually tweaked to try to force the system from one of these scenarios towards the other.

Set Optimization Boundaries. Again, the ovarian component model has much more freedom in fitting parameters than the merged model due to the use of input functions. Just because c_1 (Equation (4.21)) should be larger as we saw in Chapter 3 to increase the stage mass for the entire system, does not mean it should be unrestricted. The rest of the parameters should contribute to making the stage mass larger as well. Manually decreasing c_1 and putting restrictions on the auxiliary equation parameters for IHA helped this matter. By not letting the optimizer make the coefficients for IHA too large, the optimizer needed to make the luteal stages larger to fit the data for IHA. In turn, this makes all of the stages larger overall. Once a better set of parameters is obtained, the restriction can be removed because fminseearch will not vary the solution too much from its starting point. Thus removing the restriction allows for fine tuning after a general set of parameters was found.

It should be noted that p_0 from the auxiliary equation for P4 optimized to something quite small and was assumed to be zero and removed. The final parameters for the ovarian component for the Welt six-hormone, two-wave model are shown in Table 4.1.

Parameter Results: For the most part, many of the parameters for this six-horomone system are similar to their five-hormone counterparts including Km_F, p and atr. However, one that changed to help increase the height proportion between the first and second follicle wave is α (Equation (4.21)). Recall that the starting point for α was from the one-wave six-hormone model. From the work in Chapter 3 it should not be surprising to see that this value must decrease to accommodate the wave. What is surprising is that its optimized value is a little larger than it was in the five-hormone model. This is likely due to the fact that the recruited stage now has a transfer term from the small antral stage. The small antral stage gives the recruited stage more shape than just FSH itself as in the $b \cdot FSH$ term for the five-hormone model. Thus, α probably does not need to be reduced nearly as much because it has more support in shaping the wave from the first term than it did previously. This probably also accounts for why Km_F and the other FSH threshold parameters did not change very much through the optimization process either. These parameter changes yield the hormones in Figure 4.4 and the stages in Figure 4.3.

Cycle Results: The stages in Figure 4.3 exhibit a second follicle wave of recruitment and growth. The stages here have a wideness to them like the Welt five-hormone, two-wave ovarian

Table 4.1 Parameter results for the six-hormone, two-wave ovarian component model fitting the Welt data set. All of the following optimized parameters were truncated to two significant decimal digits.

Param.	Value	Units
η	3.78	dimensionless
δ	0.15	dimensionless
α	0.37	dimensionless
β	0.027	dimensionless
γ	0.048	dimensionless
f_1	10.86	IU/L
f_2	2.17	IU/day
f_3	2.24	(L/IU)/day
f_4	0.57	$(\text{L/IU})^{\delta}(1/\text{day})$
c_1	2.06	1/day
c_2	0.58	$(\text{L/IU})^{\alpha}(1/\text{day})$
c_3	0.058	$(\text{L/IU})^{\beta}(1/\text{day})$
c_4	0.027	(L/IU)/day
c_5	0.86	$(\text{L/IU})^{\gamma}(1/\text{day})$
c_6	0.85	1/day
d_1	0.78	1/day
d_2	0.70	1/day
k_1	0.60	1/day
k_2	0.75	1/day
k_3	0.75	1/day
k_4	0.72	1/day

Param.	Value	Units
e_0	16.37	pg/mL
e_1	0.019	(pg/mL)/IU
e_2	0.029	(pg/mL)/IU
e_3	0.037	(pg/mL)/IU
p_1	0.00099	(ng/mL)/IU
p_2	0.0047	(ng/mL)/IU
h_0	0.12	IU/mL
h_1	0.0012	1/mL
h_2	0.00096	1/mL
h_3	0.0010	1/mL
h_4	0.0016	1/mL
j_0	5.31	(pg/mL)
j_1	86.65	(pg/mL)/IU
j_2	0.0032	(pg/mL)/IU
j_3	0.0022	(pg/mL)/IU
Km_F	6.13	IU/L
p	7.53	dimensionless
atr	8.77	1/day
Ki_{atr}	3.02	IU/L
pwr_{at}	2.13	dimensionless

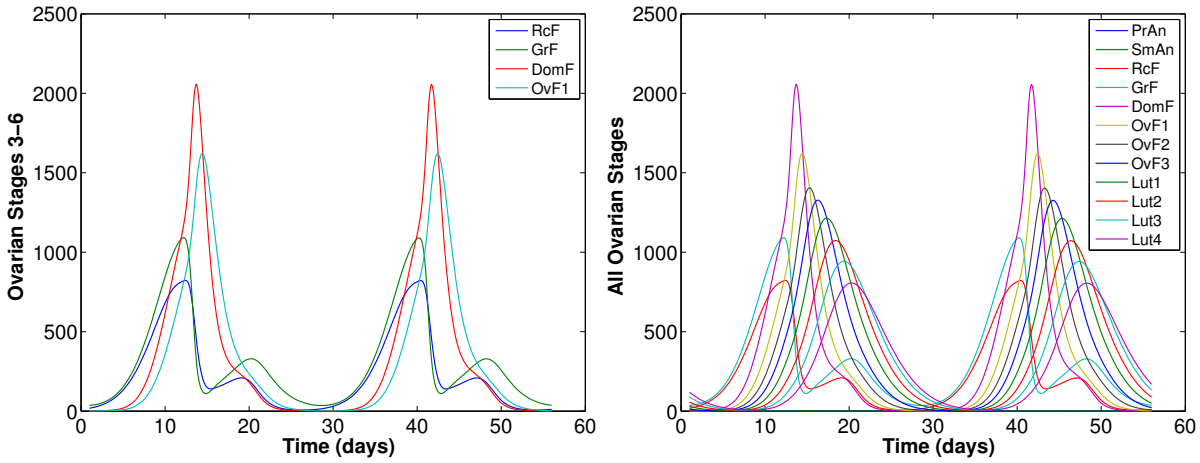

(a) **(b)**

Figure 4.3 Ovarian follicle stages of growth such that the hormone profiles for the six-hormone, two-wave ovarian component model fit the Welt data set. The panel on the left shows just the recruited, growing, dominant and first ovulatory stages while the panel on the right has all twelve stages of growth.

component model exhibited in Figure 3.10. The second follicle wave (as easily seen in panel **(a)**) almost looks wider than it is tall. When the five-hormone model was merged, that behavior vanished so the hope is that will happen with the six-hormone model as well. The waves in this figure, however, do not have the same wave proportion for the height of the first to the second as the Welt five-hormone model. The second wave in the six-hormone model is much shorter compared to the first wave than in the five-hormone model. There is little concern here however for a few reasons.

- First, the McLachlan five-hormone, two-wave model had a much smaller proportion in wave height as well.
- Second, the trough between the luteal phase wave and the subsequent follicular phase wave is much deeper than its five-hormone, two-wave Welt ovarian component counterpart.
- And third, when the model is merged, this behavior may change.

For now, the system exhibits the second wave and is a good starting point for the merged model.

We can see in Figure 4.4 that the model fits the data fairly well. Three out of four ovarian hormones reach their peak heights, IHB being the only one that does not quite reach it. However, all four do reach within the data error bars. All four actually overshoot their trough amount. One other interesting occurrence is that the timing changed slightly. Timing issues are much rarer in the ovarian component model because the input functions are rigid as opposed to the merged feedback model. Here however, the ovulatory and luteal stages are early. It is hard to pick this up just from Figure 4.3 but it is much easier to see in Figure 4.4. The E2 model meets its peak data point at the correct time. IHB also appears to fit its initial rise and final decline to the data well timing-wise. That indicates that up through the dominant or possibly first ovulatory stage the timing is correct. IHA and P4 have their initial rises and final declines earlier than the data points, which indicates the luteal stages that make up all of the auxiliary equation for P4 and most of the auxiliary equation for IHA are occurring early. Also, the second rise in E2 is early as well which again is composed of the second follicle wave from the growing stage and the luteal stage. The dominant follicle is flat at that point in time and does not contribute to the rise.

As the battle for good hormone profiles along with good second follicle wave heights continued on, the compromise between the two yielded a parameter set that caused this timing issue. As noted above, many of the parameter values are quite similar to the parameters they started from. This could be a direct result of having the preantral and small antral stages or the second follicle wave itself. This issue should be kept in mind for the merged model. There is a good possibility the merged model will have a shorter cycle length than the Welt 28 day

cycle length. The chance for a shorter cycle is even better if the wideness of the second follicle wave of growth is eliminated as is hoped causing the next cycle to start earlier.

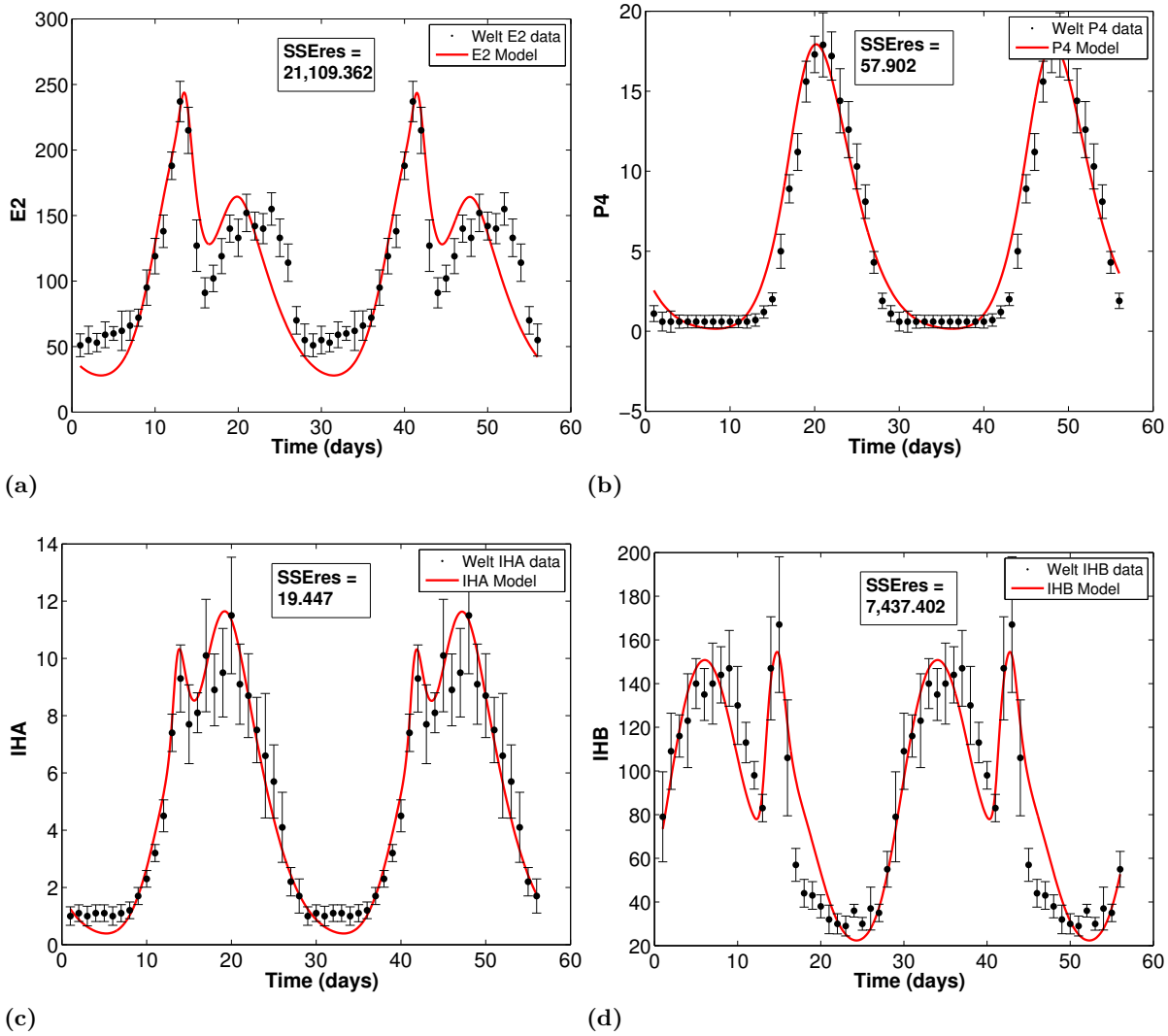

Figure 4.4 Hormone profiles for the six-hormone, two-wave ovarian component model fit to the Welt data set. SSEres is the summed squared difference between the hormone and the data for one cycle.

4.3.2 Welt Merged Model

Historically the hardest of all of the one-wave models to merge, it is finally time to merge the six-hormone, two-wave model. Like the five-hormone model, it is expected that the hormone fits will be less accurate but hopefully the behavior, especially of the second follicle wave will be more accurate as the full feedback loop is employed. It is also expected that the cycle length for a merged model will differ from the the data set that it is compared to. From the ovarian component model results, it seems likely that the merged model will have a shorter cycle than the 28 days worth of Welt data. As usual, certain steps for optimization are taken.

Begin from Previous Results. The starting point for this work are the results from the ovarian component model in the previous section and the pituitary component parameters from the new set of parameters for the merged one-wave six-hormone model that can be found in Appendix B).

Adjust Parameters by Hand.

Parameter a: The original model development, Pasteur [78] opted to increase a (Equation (4.2)) to 10 from 8. In Chapter 3, a was increased to 11 from 8 to help promote the wave. In this case it seems that from previous results an increase is required for both this model having six hormones and for having two follicle waves per cycle. Hence a in this model was set and fixed to 13 to promote wave development.

Sensitivity Results: The optimization process started slightly differently because of the number of parameters. Here, based on the five-hormone, two-wave merged Welt parameter sensitivities, two parameters were set to be constant through the initial optimization process. The two parameters that were chosen to be fixed were the delays for P4 and E2, d_P and d_E (Equation (4.2)). They were chosen because they are on the Welt insensitive list in Table 3.5 for the FSH cycle method and because those values have a direct biological significance. It does not make sense biologically for the P4 delay to be 3 days, for example. So, d_P was fixed at 1 and d_E was fixed at 0.45. Many of the other most insensitive parameters for the five-hormone model were stage transfer parameters that all change a little if one of the previous stages change. As the system is trying to adjust to find the appropriate solution, it did not make sense to fix just the ones that are least sensitive because they all work together as a team. The optimization of the remaining 57 parameters begins after those two are fixed.

Word of Caution - Maintain Biological Accuracy. As fminsearch optimizes parameters, it is important to pay attention to the values the method yields as to whether they are

biologically accurate. After all the hormones were in the cost function, the delays for IHA and IHB were both larger than two days which is quite long. The values were adjusted by hand to be below two and restrictions were put on the cost function to make sure they remained below two.

Set Optimization Boundaries. If one hormone is struggling with being fit, weighting it (or even just part of it) can make a difference. Since the curve for FSH was struggling to match the data, multiplying its term in the cost function by a constant value forces the optimizer to think FSH is contributing to more of the cost function than it did previously. Thus, when fminsearch is trying to minimize the cost function, making FSH better will help it reach that goal since it is a large contributing factor. Since the follicle wave depends greatly on FSH, the shape of that curve is vital to the system.

As the model fits the data better and as the second follicle wave is grown, alternating between manually adjusting parameters and optimizing the system continues. When the system is in the general area for an appropriate parameter set, the restrictions are taken off of the inhibin delays. The delays for E2 and P4 are also allowed to vary to see how far, if at all they stray from what they were fixed at. In the end, the balance of beautiful hormone profiles and a beautiful second follicle wave yields the parameter results in Table 4.2 from the initial conditions in Appendix C.

Parameter Results: Many of the changes in parameters from previous results to what are shown from the optimization process in Table 4.2 are not surprising. Many of the parameter values seem appropriate because they did not change drastically.

- The dominant follicle saw c_5 decrease and atr increase, so overall the mass may be the same because both decay terms adjusted in opposite directions.
- Allowing d_E and d_P to vary after the part of the optimization process when they were fixed proved worthwhile. The E2 delay did in fact change from its fixed value of 0.45 to $d_E = 0.395$.

Cycle Results: The twelve ovarian follicle stages are displayed in Figure 4.5 and resulting hormones are in Figure 4.6 . As was hoped, the wideness of the second follicle wave dissipated in the merged model giving both the first and second waves the same overall shape.

Wave Proportion: The wave proportion between the first and the second wave is not as large as it was in the five-hormone merged model for the Welt data, but is not concerning because it does resemble the proportion from the six-hormone ovarian component model.

Shape Oddities: One interesting result in the stages is the second bump in the dominant follicle. In all five of the previous results sections, the dominant follicle had an extra

Table 4.2 Parameter results for the six-hormone, two-wave merged model fitting the Welt data set. All of the following optimized parameters were truncated to two significant decimal digits.

Param.	**Value**	**Units**
v_{0LH}	747.07	IU/day
v_{1LH}	3046.49	IU/day
Km_{LH}	180.26	pg/mL
$Ki_{LH,P}$	18.18	ng/mL
k_{LH}	2.24	1/day
$c_{LH,P}$	0.31	mL/ng
$c_{LH,E}$	0.0060	mL/pg
d_E	0.39	days
d_P	1.00	days
v_{FSH}	795.60	IU/day
$Ki_{FSH,IHA}$	2.18	IU/mL
k_{FSH}	2.04	1/day
$c_{FSH,P}$	17.42	mL/ng
$c_{FSH,E}$	0.44	$(mL/pg)^2$
d_{IHA}	1.75	Days
$Ki_{FSH,IHB}$	119.83	pg/mL
d_{IHB}	1.90	Days
η	5.26	dimensionless
δ	0.076	dimensionless
α	0.36	dimensionless
β	0.055	dimensionless
γ	0.064	dimensionless
f_1	9.82	IU/L
f_2	1.79	IU/day
f_3	1.11	(L/IU)/day
f_4	0.94	$(\text{L/IU})^{\delta}(1/\text{day})$
c_1	1.94	1/day
c_2	0.57	$(\text{L/IU})^{\alpha}(1/\text{day})$
c_3	0.023	$(\text{L/IU})^{\beta}(1/\text{day})$

Param.	**Value**	**Units**
c_4	0.035	(L/IU)/day
c_5	0.74	$(\text{L/IU})^{\gamma}(1/\text{day})$
c_6	0.73	1/day
d_1	0.60	1/day
d_2	0.62	1/day
k_1	0.71	1/day
k_2	0.90	1/day
k_3	0.88	1/day
k_4	0.90	1/day
e_0	12.09	pg/mL
e_1	0.013	(pg/mL)/IU
e_2	0.019	(pg/mL)/IU
e_3	0.026	(pg/mL)/IU
p_0	0.00058	ng/mL
p_1	0.00080	(ng/mL)/IU
p_2	0.0034	(ng/mL)/IU
h_0	0.096	IU/mL
h_1	0.00098	1/mL
h_2	0.00070	1/mL
h_3	0.00092	1/mL
h_4	0.0010	1/mL
j_0	16.85	(pg/mL)
j_1	115.58	(pg/mL)/IU
j_2	3.9E-06	(pg/mL)/IU
j_3	0.0018	(pg/mL)/IU
Km_F	6.17	IU/L
p	18.03	dimensionless
atr	124.66	1/day
Ki_{atr}	4.07	IU/L
pwr_{at}	10.71	dimensionless

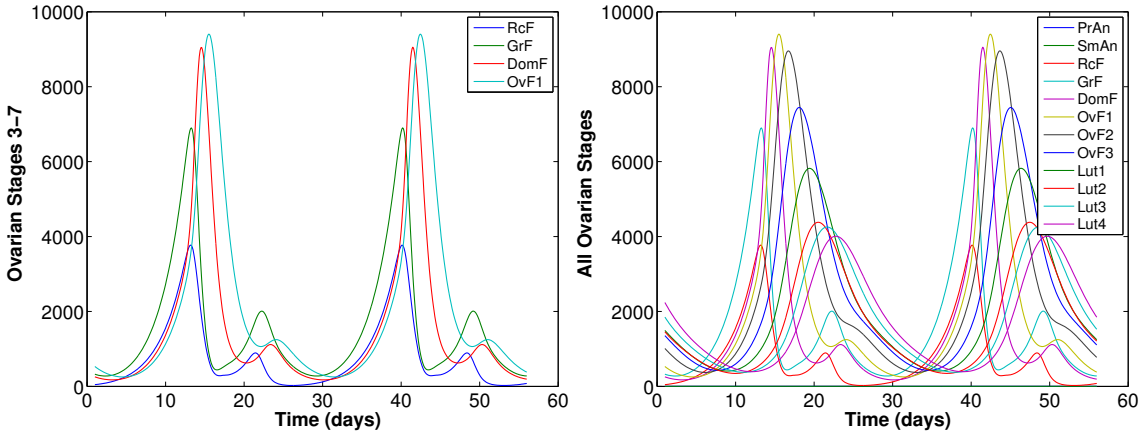

(a) **(b)**

Figure 4.5 Ovarian follicle stages of growth such that the hormone profiles for the six-hormone, two-wave merged model fit the Welt data set.

bump due to LH and the extra bump in the dominant follicle very much resembled the extra bump in LH (that was caused by the second follicle wave's resulting contribution to E2). In other words, it was very flat on either side of the bump. Here, the trough on the left between the first and second follicle waves does not decline very far let alone allow for almost complete flatness. Examination of the hormones in Figure 4.6 reveals that LH does in fact have an extra bump. It appears smaller than it is in all of the previous merged models. This shortness of the extra bump is likely due to the fact that the second rise in E2 is not greatly exceeding the data as it was in all of the previous cases. Since the profile for LH is not flat on either side of the bump, this likely contributes to that extra bump in the dominant follicle. The extra bump also carries into the first ovulatory stage, so this could also be a legitimate second follicle wave that the atresia term did not eliminate.

Cycle Timing: It is important to use the hormones with the data to examine timing. As was predicted earlier, the cycle length for this model is less than the 28 days worth of Welt data used for optimization. Because the system is so large and is quite complicated to find parameter sets to create profiles to fit these hormones, the cost function was never set to three cycles here as an attempt to force the model period due to computation time. The cycle length here is shorter but is still a reasonable length for normally cycling women.

Magnitude: The ovarian hormones have trouble meeting their troughs which was also noted in the previous Welt results, so again this is not surprising. The most interesting hormone profile in Figure 4.6 is the one for FSH. The profile for FSH has historically been the

hardest to fit, especially to its peak value. The rest of the hormone profiles and the follicle stages look quite nice, but FSH is struggling to be large enough. For the most part, the shape is quite nice, but overall the curve is too short, especially at its peak. The impressive part of this FSH profile is the size of the follicle waves it was able to produce despite the smallness of the FSH. Not reaching peaks and troughs drastically increases the error on these hormones. For example, the LH profile is within the error bars of for the data for most of the data points, but by not reaching its peak value the summed squared difference is driven up, perhaps misleadingly. Both the cycle error and the error bars examined together give an overall idea of how the curve fits.

Despite the larger system, the six-hormone, two-wave model fit to the Welt data set maintains many attributes from both the six-hormone, one-wave and five-hormone, two-wave scenarios.

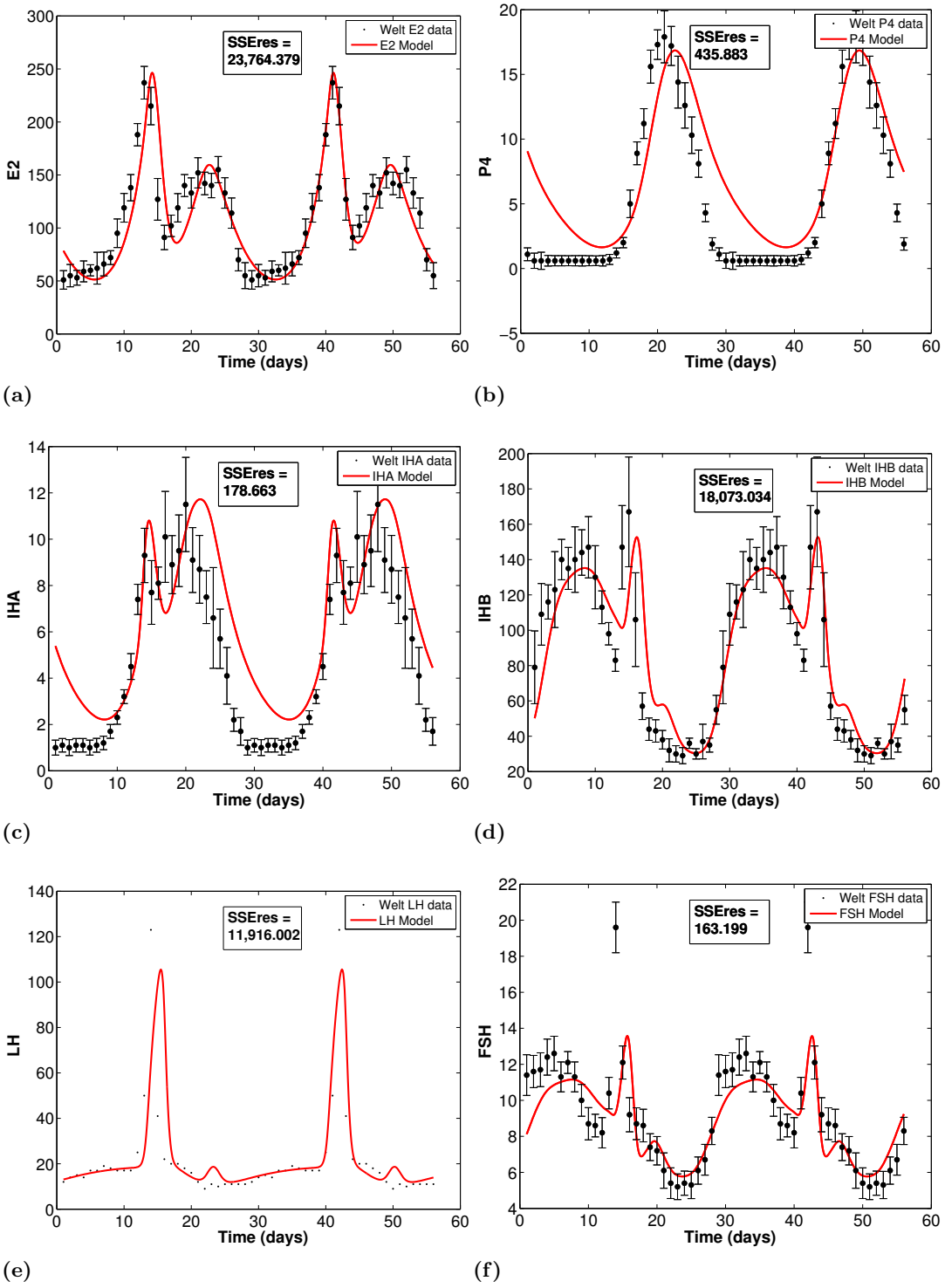

Figure 4.6 Hormone profiles for the six-hormone, two-wave merged model fit to the Welt data set. SSEres is the summed squared difference between the hormone and the data for one cycle.

Chapter 5

Consequences of Follicle Waves

Multiple follicle waves should be addressed in modeling the cycle not only to create the most accurate representation of what occurs in the body but also because there are biological consequences resulting from follicle waves. Two such issues are early menopause and the superfecundation form of dizygotic twinning.

- With the discovery of follicle waves, it seems women are using their follicles faster than was previously believed [12]. The more follicles selected for recruitment each cycle speeds up the progression towards menopause. Thus, multiple follicle waves per cycle could potentially be an indicator of early menopause in women. If that is the case, we need to know this threshold model will work for any number of follicle waves depending on the number of rises in FSH.

- Superfecundation is the fertilization of two oocytes at two different points in time during one cycle. Superfecundation results in dizygotic (fraternal) twins and could, though rare, be caused by the occurrence of follicle waves. Most cases of superfecundation only go noticed when the children have two different fathers because they look drastically different or by chance a paternity test is conducted. A recent child support case was deemed "groundbreaking" because the paternity test on a woman's twins showed that they have two different fathers and the father who was being sued only has to pay support for one of the twins [71].

Early menopause and rare cases of dizygotic twinning are both hypothesized results of having multiple follicle waves per cycle and possibly elevated levels of FSH. Modeling both of these medical concerns may shed some light on what is occurring in the body and direct future biological research. Here, we discuss how the working models in Chapters 3 and 4 can be used to predict hormone behaviors.

5.1 Early Menopause

Menopause occurs when all viable follicles have gone through recruitment or atresia. The transition to menopause lasting between four and seven years begins when a woman is in her mid 40's [95]. It is believed that as the ovarian follicle reserve decreases, FSH is able to remain at a higher level for longer periods of time than was allowed previously [33]. The observed decrease of IHB is an assumed contributing factor to this rise in FSH [55]. If this is the case, inhibin levels could be a marker for the start of the transition to menopause and the decline in ovarian follicle count [98].

Luteal out of phase (LOOP) events occur during the menopause transition when E2 rises in the mid to late luteal phase similar to its typical rise in the follicular phase from the growing and eventually ovulating follicle [49]. Because E2 is higher in the luteal phase and the levels carry over into the following follicular phase, everything including the LH surge occurs earlier causing a shorter cycle overall. Even though LOOP events occur due to atypical secretions in hormones, no concrete relationship to waves have been established. In work by Hale et al. [49], it is proposed that LOOP events are a result of a dominant follicle being selected out of phase. In other words, the typically anovulatory luteal phase wave is ovulatory and causes the LOOP event. Since FSH levels are known to be higher during the menopause transition, a follicle in the luteal phase could go on to become dominant since the likelihood of surpassing the FSH threshold is much greater. It is important to note that regardless of whether a woman has two or three waves per cycle, a LOOP event is caused by the second or luteal phase wave. These LOOP events very likely mark the start of the transition to irregular cycles and thus menopause. Potentially, the increased FSH levels may lead to exceeding the FSH recruitment threshold more often and by much higher amounts and thus could cause more than one dominant follicle to emerge. Though the resulting waves may act differently during menopause, currently there is no known information as to whether follicle wave dynamics themselves change over a woman's lifetime.

It is believed that the more follicle waves a women has per cycle, the faster she uses her ovarian follicle reserve and therefore reaches menopause earlier. Biological research is still being conducted to confirm this, but the mathematical model can be used to understand what the cycle is doing to consistently produce three waves each cycle. The ovarian component models are used to increase number of follicle waves per cycle to three and to examine the resulting hormones profiles that result.

As we saw in the previous chapters, two follicle waves are fairly typical based on normal hormone concentrations modeled in the Welt and the McLachlan data sets. We also saw that two rises in FSH resulted in two waves per cycle. The threshold function should produce any number of follicle waves depending on the number of rises in FSH. But more than two follicle waves

per cycle would be the result of more than two rises in FSH each cycle which is potentially an abnormal profile for FSH. Thus, more than two follicle waves each cycle could indicate potential medical concerns. Our goals are to test whether we are able to achieve more than two follicle waves per cycle and to explore the hormone profiles associated with such patterns.

The follicle wave model was created using a Hill function for the current levels of FSH. If FSH rises above the threshold, another wave occurs. The commonality between the McLachlan, Welt and Baerwald data are the relatively normal looking FSH profiles with two rises in FSH. For the Baerwald data, that happens to be the two-wave measurements. Recall however, the Baerwald research also has three-wave measurements that correspond to three individual rises in FSH as depicted in Figure 2.4. The results support the one-to-one concept of the number of rises in FSH to the number of follicle waves per cycle, but three rises in FSH do not occur in the FSH profile for normally cycling women. It does not necessarily indicate a medical issue, but it is a less common measurement as only approximately one-third of the women studied exhibited three waves [9].

Unfortunately, if three rises in FSH is abnormal, there is very little information on the other hormones and what they may or may not look like as a result. The Baerwald data includes two ovarian hormones, E2 and P4. No measurements for IHA or IHB were taken. Since FSH synthesis results from inhibin feedback, it is easy to hypothesize that the inhibin profiles should be different from the normal cycle results of McLachlan or Welt. The Baerwald results indicate that the extra rise in FSH occurs in the early to mid follicular phase so it stands to reason that IHB is the hormone to cause this third rise as it is high in the follicular phase.

Here we test two individual pieces in each component. First, we show that a FSH input function with three rises in FSH causes three follicle waves to emerge in the ovarian component model. Second, we show that an amended IHB input function causes FSH with three individual rises in the FSH component model. Without more concrete information on what three-wave hormone profiles should look like, we are not able to test the full merged model for the three (or more) wave occurrence.

5.1.1 McLachlan FSH with Three Rises

To determine whether an FSH curve with three separate rises produces three waves in the the recruited and growing stages of ovarian follicle growth, we use the ovarian component model. Because the McLachlan data set is much smoother for most hormones than the Welt data set, it was the logical system on which to experiment. Recall, the FSH input function used to produce the two-wave ovarian stages is as follows:

$$\text{FSH} = 75 + 110e^{-\frac{(t-4.5)^2}{46}} + 210e^{-\frac{(t-15)^2}{0.75}} + 50e^{-\frac{(t-17.5)^2}{20}} - 12e^{-\frac{(t-25)^2}{10}} \tag{5.1}$$

To test this hypothesis, a new input function needs to be created. Theoretically, the new input function itself should be able to produce three follicle waves. The ovarian component model parameters will likely need adjusting to improve the results. Since this new input function will not match any existing data sets, some liberties were taken in its creation. The spacing between rises are fairly evenly spaced and the magnitudes have been purposely exaggerated to produce more dramatic waves. Using the existing McLachlan two-rise FSH input function and the Baerwald concentrations in Figure 2.4 as examples for timing and magnitude, a new input function was created with three rises. Its equation is as follows:

$$\text{FSH} = 82.5 + 190e^{-\frac{(t-8)^2}{10}} + 180e^{-\frac{(t-0.3)^2}{0.4}} + 400e^{-\frac{(t-15.2)^2}{3}} - 20e^{-\frac{(t-24)^2}{15}} \tag{5.2}$$

Figure 5.1 depicts both the two-rise and three-rise FSH input functions.

Replacing the two-rise input function with the three rise input function dramatically decreased the size of the follicle stages. Matters needed to be taken to increase their height and to help promote the third wave. Since the goal is to predict, there is no expectation for hormone fits because there is no concrete information on what the hormones should look like. The general optimization steps used in Chapters 3 and 4, including employing fminsearch, help to settle on a stable solution with proper magnitude and timing.

Adjust Parameters by Hand. Adjusting the coefficients on the recruited stage, in particular the b multiplier (Equation (3.27)), caused the stages to grow in height. Also, because of the higher and sustained amounts of FSH from having three rises, the Km_F parameter needed to be increased as well. With these changes, three follicle waves of proper magnitude were produced.

Build Up Cost Function. Optimization was completed using just P4 for the cost function and the stage size increased more appropriately. P4 was chosen because the Baerwald concentration is very similar to the normal levels observed in both McLachlan and Welt. Next, IHA was added in the cost function simply because it is better to assume IHA looks normal in the three-wave case and use what is available to us for optimization than it is to leave it out completely. IHA is very heavily composed of luteal phase stages which should remain the same regardless of the number of follicle waves per cycle. So if any differences are involved in IHA they should be very slight which means it is more beneficial to add in IHA for optimization than it is to only use P4.

Set Optimization Boundaries. The ovarian component model is of benefit here because of the fixed input functions. This means we can use restrictions on our cost function to optimize certain parts of our system since there is no feedback loop at work. Once the

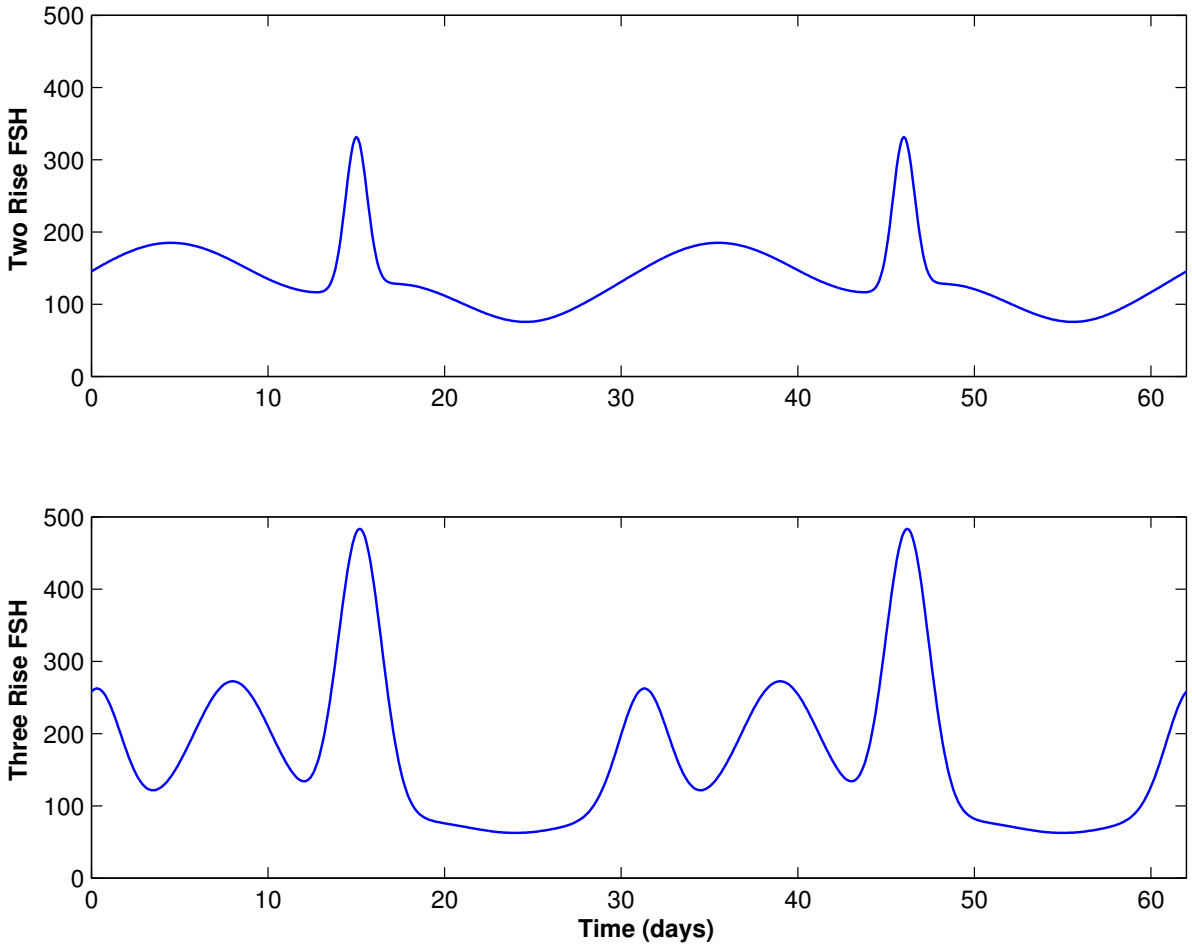

Figure 5.1 Two rise and three rise FSH input functions created for two-wave and three-wave ovarian component models. The number of follicle waves per cycle generated by the ovarian model should be a one-to-one relationship with the number of rises in FSH

stages reached an appropriate height with a definitive third wave, optimization on just the auxiliary function coefficients was completed. Doing so meant that the pituitary input functions and the follicle stages were both fixed letting the optimizer attempt to reach peaks and troughs on the hormones by adjusting only the auxiliary coefficients.

Word of Caution - Manipulating E2. The coefficients for E2 were changed by hand so that E2 model would be similar to the E2 in the McLachlan data. The E2 auxiliary equation is made up of the growing, dominant and fourth luteal stages of growth. Because the growing stage now has a third wave, the E2 function could possibly have a third rise as well. The Baerwald concentration in Figure 2.4 depicts a third rise in E2 but the third rise is in the luteal phase while the additional wave we gain is in the follicular phase which is contradictory. The coefficient on the growing stage was greatly downplayed to hide the extra follicular phase rise in E2 to match the McLachlan E2 data and the coefficient on the dominant follicle was increased to maintain the E2 peak height. Those could very much be adjusted so the third rise is present. In a merged model however, this not likely possible because changing these coefficients changes the entire system. This is why a full merged three-wave model is not possible without further knowledge about the hormone concentrations or what is causing the recorded amounts.

After adjusting the coefficients by hand one last time to maintain the height order of the stages, the final results for the stages are depicted in Figure 5.2 and for the three ovarian hormones in Figure 5.3. Error bars were included on the data and all three hormones had peaks within those error bars. No summed squared differences were given because these figures are meant to predict and not necessarily to fit data. The data is included on the graphs for reference purposes. The final parameters are included in Table 5.1. Note that though p_0 remains zero, e_0 and h_2 are no longer negligible and have results reported in Table 5.1.

Based on the information available, the hypothesis that three rises in FSH cause three follicle waves per cycle is supported through mathematical modeling. It stands to reason that any number of waves could be created with this system of equations for a particular FSH input function. The next concept that needs to be addressed is the instigator of the three rises in FSH.

5.1.2 Welt IHB with Three Rises

Now that it has been shown that three rises in FSH causes three follicle waves per cycle in the mathematical model, it is time to examine whether IHB could be causing the extra rise in FSH. Since the extra rise in FSH is in the follicular phase, it stands to reason that IHB, the follicular phase inhibin and inhibitor of the synthesis of FSH, could be the culprit. We know that normal IHB has two peaks as does FSH. There could be a one-to-one relationship between

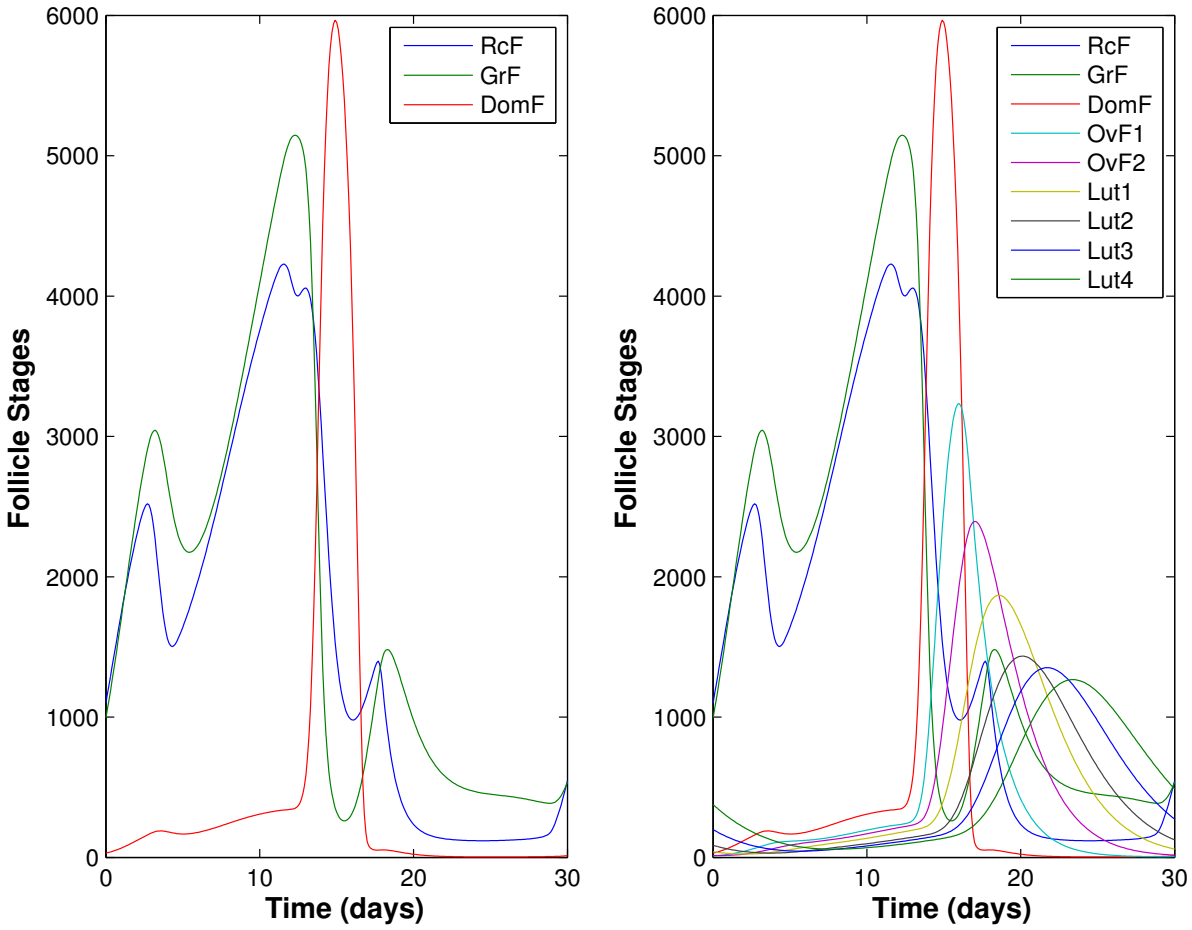

Figure 5.2 Follicle stages as a result of FSH input function with three rises in the ovarian component McLachlan model. The image on the left isolates the first three stages of follicle growth and the image on the right is the complete set of nine follicle stages. The left panel emphasizes the results showing the recruited and growing stages, RcF (-) and GrF (-), exhibit three follicle waves but the dominant stage, DomF (-) exhibits only one wave.

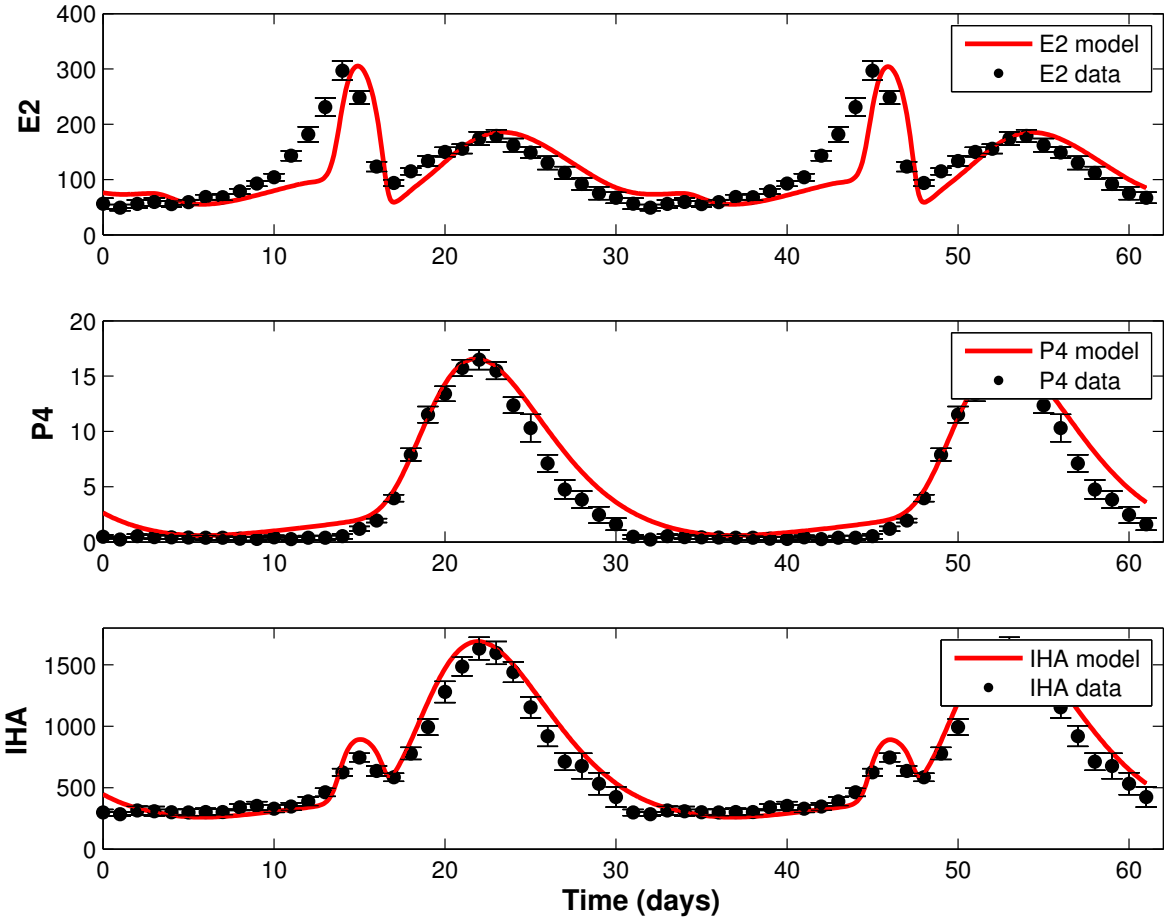

Figure 5.3 Three McLachlan ovarian hormones fit to follicle stages with three waves as a result of using the FSH input function with three rises in the ovarian component model.

Table 5.1 Parameter results for the five-hormone, three-wave ovarian component model fitting the McLachlan data set. All of the following optimized parameters were truncated to two significant decimal digits.

Parameter	**Value**	**Units**
α	0.31	dimensionless
β	0.20	dimensionless
γ	0.035	dimensionless
b	1.86	L/day
c_1	1.31	1/day
c_2	0.42	$(\text{L}/\mu\text{g})^{\alpha}(1/\text{day})$
c_3	0.14	$(\text{L}/\mu\text{g})^{\beta}(1/\text{day})$
c_4	0.035	$(\text{L}/\mu\text{g})(1/\text{day})$
c_5	0.39	$(\text{L}/\mu\text{g})^{\gamma}(1/\text{day})$
d_1	0.59	1/day
d_2	0.56	1/day
k_1	0.56	1/day
k_2	0.63	1/day
k_3	0.60	1/day
k_4	0.58	1/day
Km_F	122.10	μg/L
p	19.09	dimensionless
atr	285.45	1/day
Ki_{atr}	8.58	μg/L
pwr_{at}	1.83	dimensionless
e_0	16.00	ng/L
e_1	0.01	1/kL
e_2	0.045	1/kL
e_3	0.13	1/kL
p_1	0.011	1/L
p_2	0.001	1/L
h_0	188.05	U/L
h_1	0.087	$(\text{U/L})/(\mu\text{g})$
h_2	0.01	$(\text{U/L})/(\mu\text{g})$
h_3	0.95	$(\text{U/L})/(\mu\text{g})$
h_4	0.18	$(\text{U/L})/(\mu\text{g})$

the number of rises in IHB and FSH. Personal correspondence with Dr. Baerwald seems to confirm this idea, though her results are for perimenopausal women. Thus, the next hypothesis to test is whether IHB with three rises causes FSH with three rises on the six-hormone pituitary component model.

Up until this point, the systems needed to examine follicle waves have been the ovarian component model and the subsequent merged model. The FSH component model, half of the pituitary component model, has not been discussed because the stages of ovarian follicle growth do not directly affect the synthesis and release of FSH.

To begin, the component model has two differential equations, the FSH reserve pool and the FSH serum level that were previously seen in the merged model. The four input functions for E2, P4, IHA and IHB that fit the Welt data and when used in the pituitary component yield a FSH profile that fits the data are as follows and are shown in Figure 5.4:

$$E_2 = 55 + 135e^{-\frac{(t-13)^2}{4}} + 60e^{-\frac{(t-11)^2}{15}} + 110e^{-\frac{(t-22)^2}{15}} \tag{5.3}$$

$$P_4 = 0.4 + 17.5e^{-\frac{(t-21)^2}{21}} \tag{5.4}$$

$$\text{IHA} = 1 + 11e^{-\frac{(t-19.5)^2}{30}} \tag{5.5}$$

$$\text{IHB} = 25 + 125e^{-\frac{(t-7)^2}{40}} + 115e^{-\frac{(t-14.75)^2}{2}} \tag{5.6}$$

To create a FSH with three rises, the only change that should be made is to the IHB input function and very few changes to the parameters of the FSH differential equations. As in the previous section where the magnitude of the FSH input function was exaggerated to create a more distinct wave, the same is done with IHB in this model. Here however, the magnitude is decreased. Recall higher amounts of IHB stifle FSH so in order to test this three rise theory but not lose much of the character of FSH, the IHB curve with three rises is shorter than the original. It is as follows and is shown in Figure 5.5:

$$\text{IHB} = 25 + 100e^{-\frac{(t-9)^2}{15}} + 95e^{-\frac{(t-14.75)^2}{2}} + 75e^{-\frac{(t-2)^2}{2}} \tag{5.7}$$

Without any parameter changes from the original values obtained in Pasteur [78], the input function created a FSH profile with three distinct rises.

Adjust Parameters by Hand. Since this model only has one hormone to use in a cost function unlike the ovarian component model, there is no way to optimize this model and any parameter changes must be made by hand. In order to increase the height of the FSH

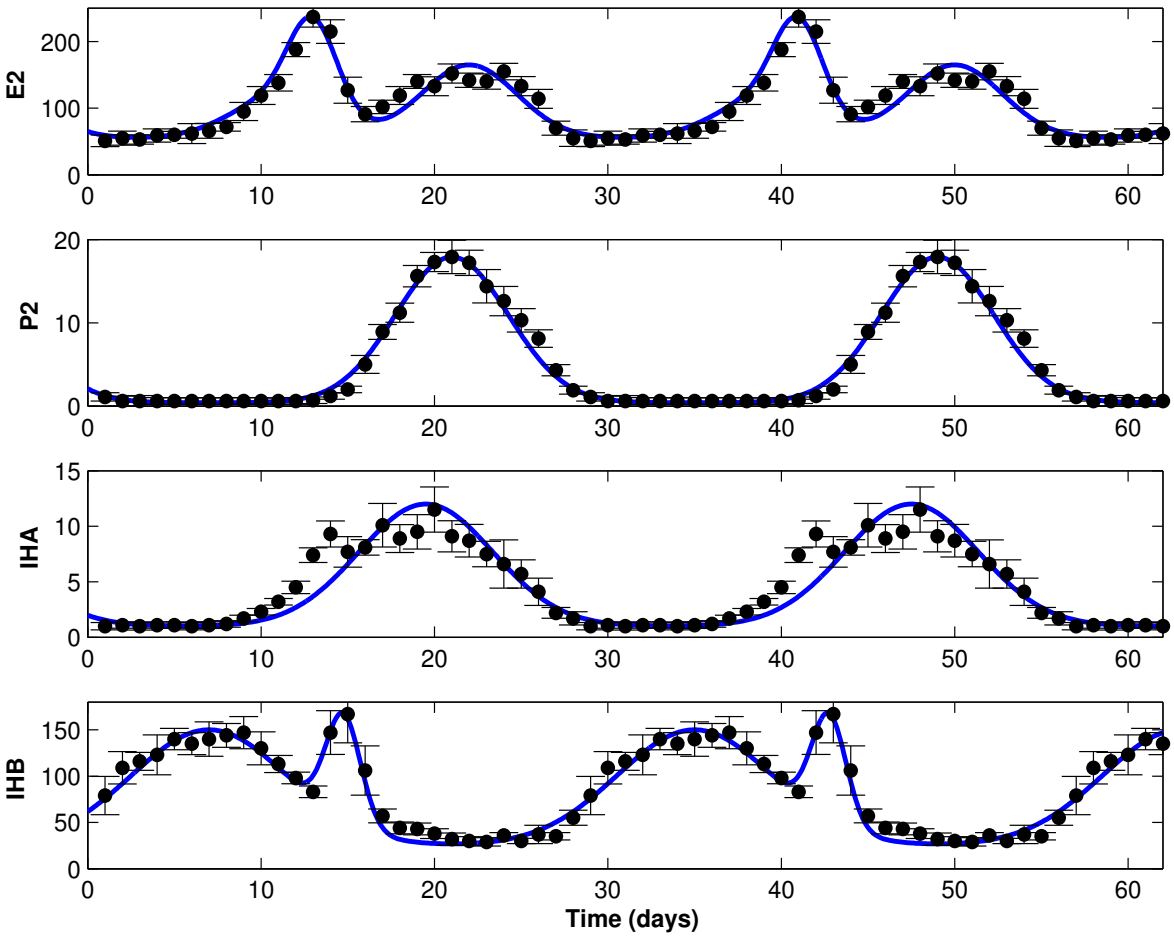

Figure 5.4 Input functions (-) for the FSH component model fit to the Welt data set (·). The input functions are for E2, P4, IHA and IHB. The FSH component model is used to show whether an IHB input function with three rises could potentially create an FSH curve with three rises. This is the original IHB curve before it is amended to accommodate three rises.

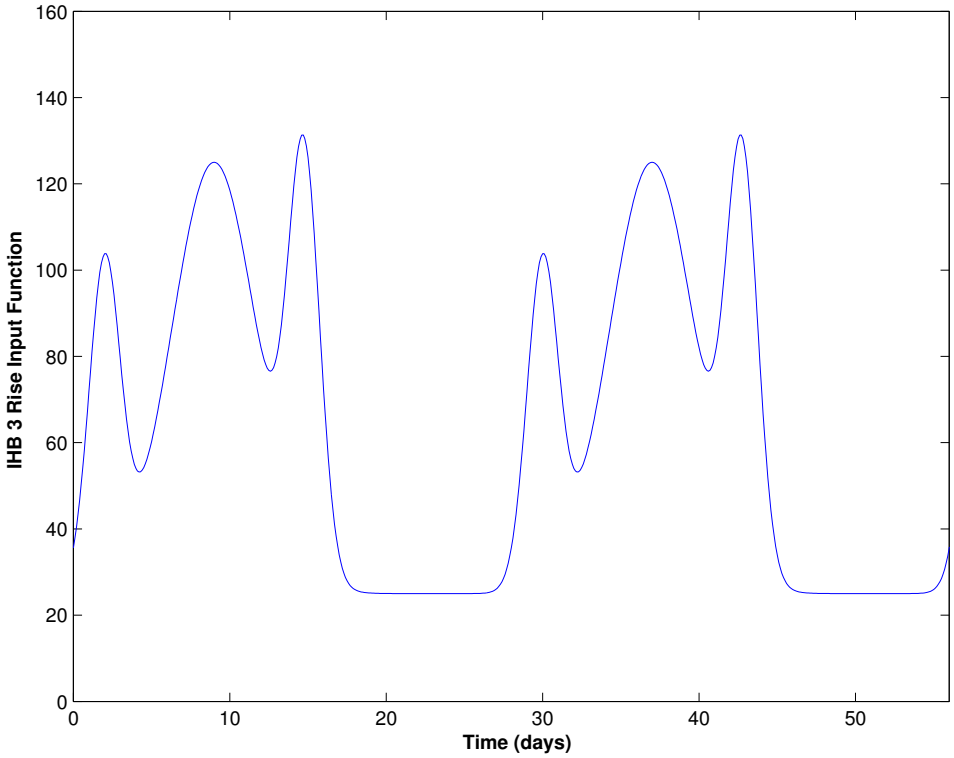

Figure 5.5 The input function for IHB has been changed from its original form based on the Welt data to have three rises. The input function is used in the FSH component model to show that the three rises in IHB will cause three rises in FSH.

Table 5.2 Parameter results for the original Welt FSH component model from Pasteur [78] and the amended parameters to make the curve taller while using the IHB input function with three rises.

Parameter	Original Value	New Value	Units
v_{FSH}	756	756	IU/day
$Ki_{FSH,IHA}$	2	2.5	IU/mL
k_{FSH}	2	1.75	1/day
$c_{FSH,P}$	38	38	mL/ng
$c_{FSH,E}$	0.35	0.35	$(mL/pg)^2$
d_{IHA}	2.5	1.5	Days
$Ki_{FSH,IHB}$	77.5	80.5	pg/mL
d_{IHB}	2.5	1.5	Days

peak amount, a handful of parameter changes were made.

The parameter values for the original values and the changed values are in Table 5.2 and Figure 5.6 shows the resulting FSH curve and the FSH data with error bars for reference as to how this is a change from the normal FSH profile.

Though the ability to put these two pieces together may not be possible right now because of a lack of hormone data, we have shown that changing the IHB profile causes three rises in FSH and that three rises in FSH cause three follicle waves per cycle.

5.1.3 Welt FSH with Three Rises

A merged model is not possible with the information available to use for optimization but an implied loop is suggested through the component models. The previous two sections almost completed that implied loop. However, the two previous steps were done for different data sets. Once the hypothesis as to IHB being the major ovarian component feeding back to the pituitary to cause three increases in FSH was supported, it was obvious that the ovarian component model would need to be recreated for the Welt data set.

The next hypothesis to test is that not only will FSH with three rises produce three follicle waves per cycle for the Welt data set but that it will also produce an IHB curve with three distinct rises as well. Again, a full merged model will not be possible so the best that can be done is to show that both the pituitary component model and the ovarian component model for the Welt data set support the dual feedback control by accurately describing the biological hypothesis.

Similar to the work done in the previous section for the McLachlan three-wave ovarian component model, the work with the Welt begins with a FSH input function with three rises.

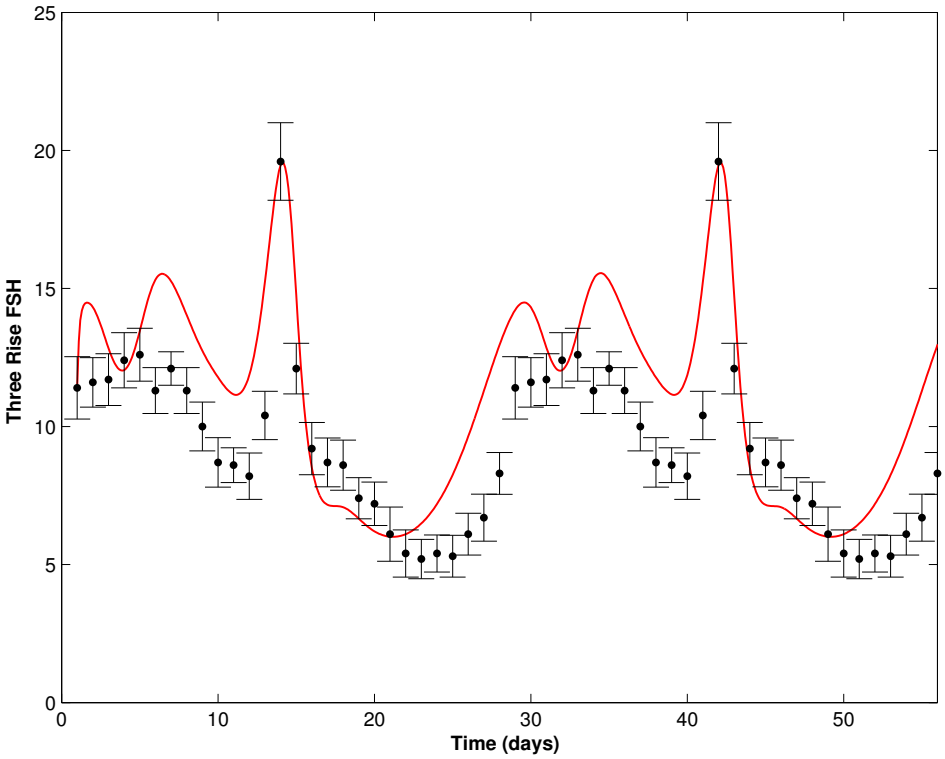

Figure 5.6 The resulting FSH curve from the IHB input function in Figure 5.5 with three rises based on the Welt data and the parameter changes in Table 5.2. Having an IHB input function with three rises does in fact create a FSH curve with three distinct rises. Though we have no data for FSH with three rises, it should be noted that this FSH model does reach the peak for the Welt data FSH with two rises. This result could be important for future work if the model is merged.

Creating the input function was a little more difficult in this case due to the timing. The Welt data is three days shorter per cycle than the McLachlan, so accommodating an extra rise into the follicular phase was going to be more challenging. The Welt data set starts counting at day one as opposed to the McLachlan at day zero, so not only is the overall cycle length shorter but the follicular phase is shorter as well. To remedy this problem, the FSH input function starts the first rise in FSH beginning in the late luteal phase as opposed to the early follicular phase. As we know from previous sections, the FSH window in addition to the threshold is just as important to consider. Starting the rise toward the first peak of FSH in the late luteal phase gives the opportunity for a decent spread on the rise as well. Again, both of the initial two rises of FSH are of similar width and height and the peak FSH amount was exaggerated for the purpose of testing whether three waves and IHB with three peaks is possible. The three-rise FSH input function used is as follows and is shown in Figure 5.7:

$$\text{FSH} = 5 + 10e^{-\frac{(t-8)^2}{}} + 8e^{-\frac{(t-1)^2}{3}} + 19e^{-\frac{(t-14)^2}{2}} + 2e^{-\frac{(t-29)^2}{9}} \tag{5.8}$$

As in the previous section, the FSH input function was used in the ovarian component model and the stages were greatly reduced in height. Following similar methods in changing parameters by hand and optimizing to P4 and IHA, the two hormones we suspect will be the same for three-wave concentrations, three follicle waves and three rises in IHB were created. The stages of growth are shown in Figure 5.8. The ovarian hormone profiles are in Figures 5.9 and 5.10 and full parameter values are in Table 5.3.

There are some items to note with this system that are specific to the Welt ovarian component model for four ovarian hormones as opposed to the three ovarian hormone model.

1. There is no b parameter (Equation (3.27)) as in the previous section to act simply as a multiplier on FSH to increase stage height. Greatly increasing f_2 (Equation (4.19)) worked well enough, but the preantral stages are larger than they have historically been. Auxiliary coefficients for IHB needed to be changed to accommodate this increase. Since the first term on the recruited stage is now a transfer term in from the previous stage as opposed to just a coefficient on FSH, there is no way to just increase the recruited stage and subsequent stages.

2. The dominant follicle in the resulting model is quite wide. In the McLachlan work in the first section of this chapter, the dominant follicle was emphasized while the growing stage was downplayed in the auxiliary equation for E2 to hide the first follicle wave that could potentially be exhibited in the E2 curve. The curve for the Welt E2 can be seen in Figure 5.9. Here, since the dominant follicle is so wide, emphasizing it takes away the trough between the first and second rise in E2. When it came to adjusting these coefficients by

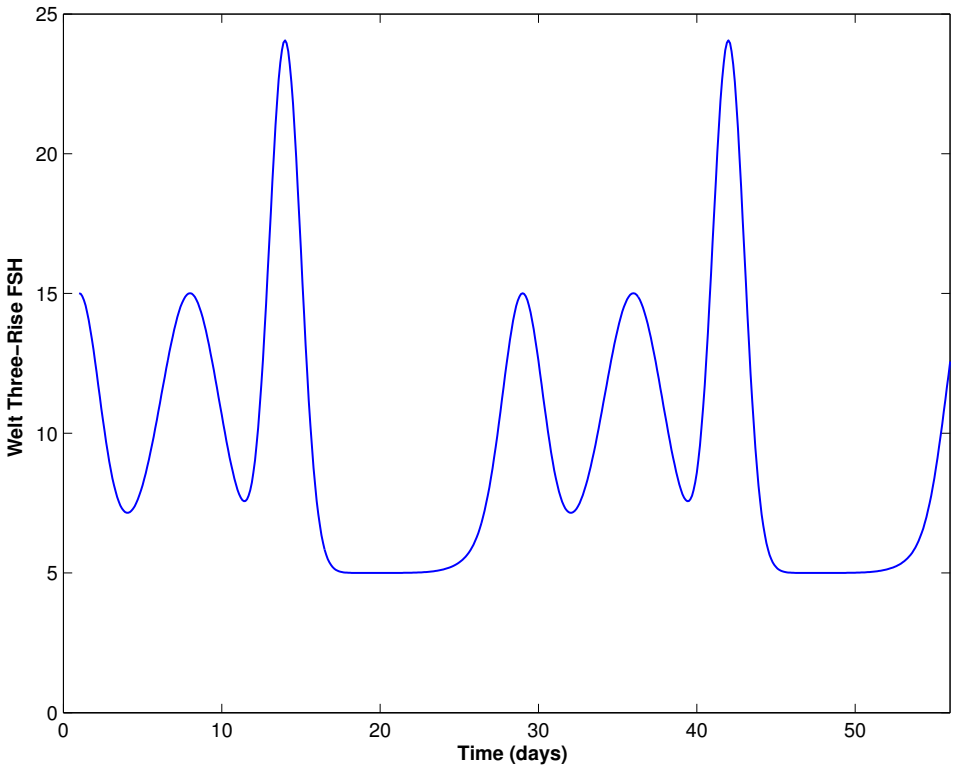

Figure 5.7 Three-rise FSH input function created for three-wave ovarian component model for the Welt data set. The number of follicle waves per cycle generated by the ovarian model should be a one-to-one relationship with the number of rises in FSH and for the Welt data set could cause three distinct rises in IHB. Unlike the McLachlan three-rise FSH because of the shorter cycle length, the Welt three-rise FSH has a first peak almost as soon as the follicular phase begins with the rise actually starting in the luteal phase.

hand (again no optimization should be done on E2) it was a better idea to let the growing stage of growth take on the burden of the peak E2 amount even if that meant a third rise in E2 is present. Thus, this Welt E2 looks different than the McLachlan E2 in the previous section, but until more biological information is gleaned, either curve could potentially represent a three-wave E2.

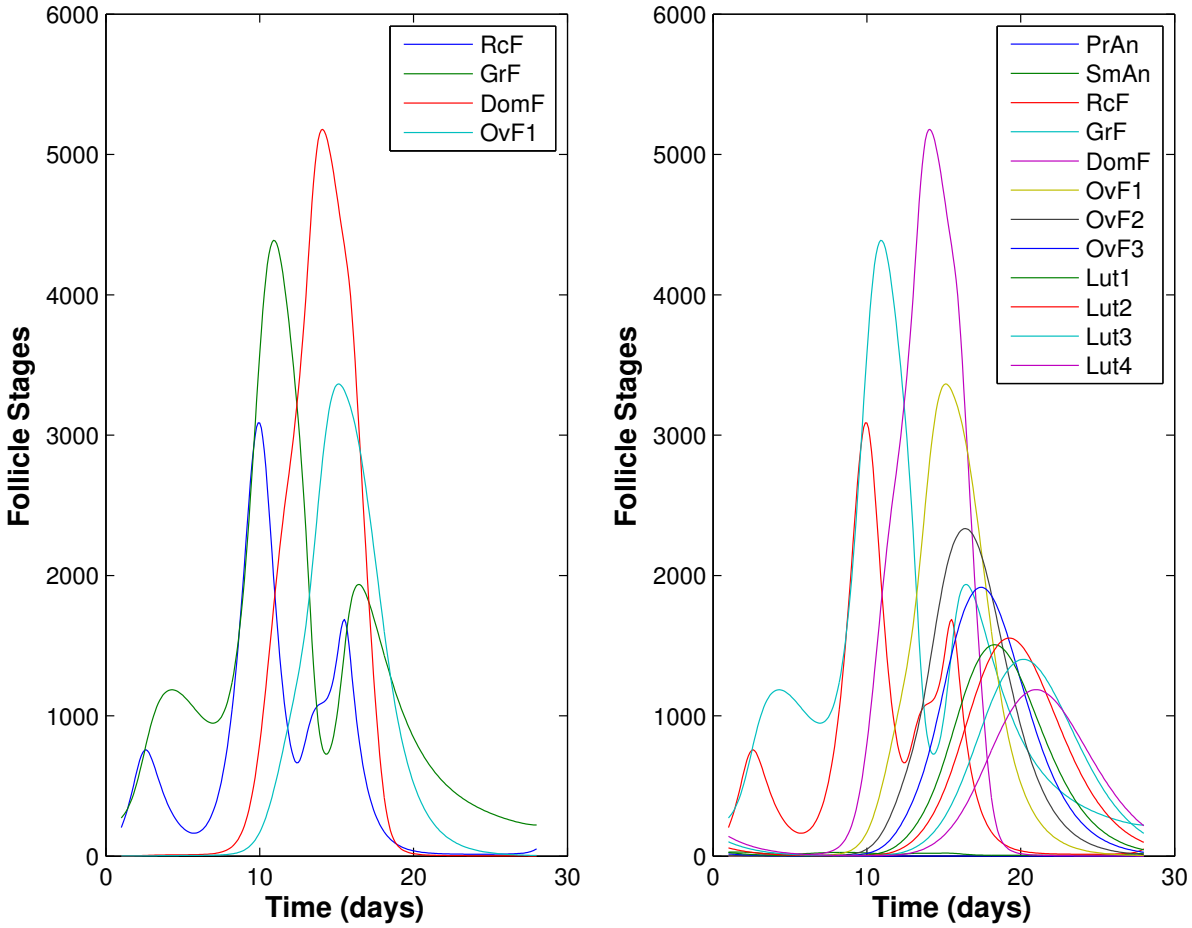

Figure 5.8 The input function for three rises in FSH shown in Figure 5.7 and the parameter values in Table 5.3 create three follicle waves per cycle in the recruited and growing stages of follicle growth for the Welt four ovarian hormone component model.

It seems that two follicle waves per cycle create hormones that fit the historical data for normal hormone profiles for women that were measured long before the existence of human ovarian follicle waves was confirmed. Three follicle waves, as was shown in the previous sections,

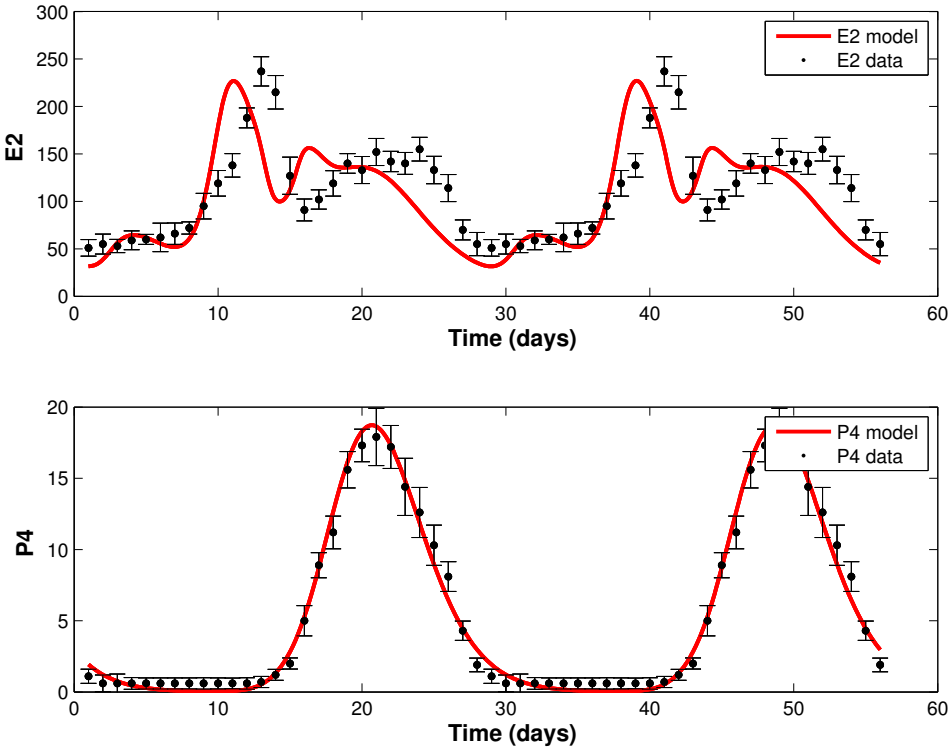

Figure 5.9 The input function for three rises in FSH shown in Figure 5.7 and the parameter values in Table 5.3 cause three follicle waves per cycle and these subsequent E2 and P4 hormone profiles. Though P4 looks normal, the E2 curve has an extra rise due to the third follicle wave. Very little is known for sure as to what the E2 curve with three follicle waves per cycle should look like, so this third rise in E2 though not fitting the Welt data set, may not be abnormal for a three-wave system.

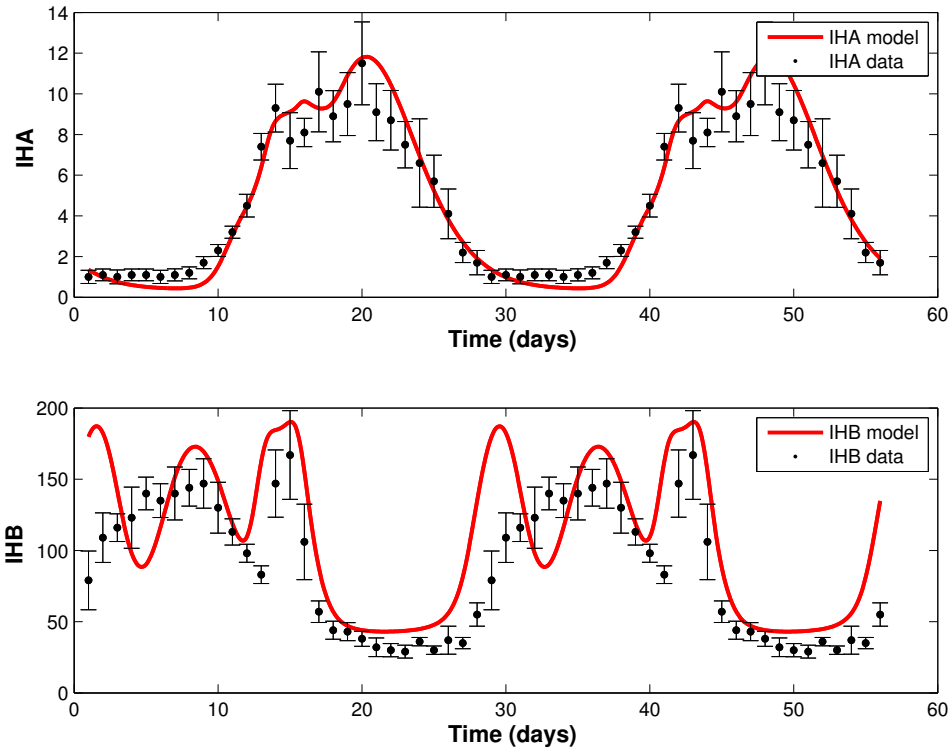

Figure 5.10 The input function for three rises in FSH shown in Figure 5.7 and the parameter values in Table 5.3 causes three follicle waves per cycle and these subsequent inhibin curves with the Welt data. IHA looks to be fairly similar to two wave case. The goal was to show that IHB would have three distinct rises if there were three follicle waves per cycle and this behavior was observed.

Table 5.3 Parameter results for the ovarian component three-wave model using the FSH input function for three rises and fitting to the Welt data set. All of the following optimized parameters were truncated to two significant decimal digits.

Param.	**Value**	**Units**
η	2.35	dimensionless
δ	0.25	dimensionless
α	0.39	dimensionless
β	0.078	dimensionless
γ	0.16	dimensionless
f_1	10.29	IU/L
f_2	70.58	IU/day
f_3	3.96	(L/IU)/day
f_4	0.90	$(\text{L/IU})^{\delta}(1/\text{day})$
c_1	2.10	1/day
c_2	0.32	$(\text{L/IU})^{\alpha}(1/\text{day})$
c_3	0.12	$(\text{L/IU})^{\beta}(1/\text{day})$
c_4	0.030	(L/IU)/day
c_5	0.25	$(\text{L/IU})^{\gamma}(1/\text{day})$
c_6	0.63	1/day
d_1	0.80	1/day
d_2	0.90	1/day
k_1	1.08	1/day
k_2	0.99	1/day
k_3	1.05	1/day
k_4	1.20	1/day

Param.	**Value**	**Units**
e_0	8.06	pg/mL
e_1	0.045	(pg/mL)/IU
e_2	0.010	(pg/mL)/IU
e_3	0.079	(pg/mL)/IU
p_0	0.00023	ng/mL
p_1	0.0050	(ng/mL)/IU
p_2	0.010	(ng/mL)/IU
h_0	0.36	IU/mL
h_1	0.0014	1/mL
h_2	0.0014	1/mL
h_3	0.0034	1/mL
h_4	0.0040	1/mL
j_0	1.98	(pg/mL)
j_1	6.33	(pg/mL)/IU
j_2	0.0062	(pg/mL)/IU
j_3	0.0069	(pg/mL)/IU
Km_F	10.99	IU/L
p	6.76	dimensionless
atr	50.00	1/day
Ki_{atr}	14.95	IU/L
pwr_{at}	14.73	dimensionless

cause hormone patterns that are slightly different than the norm. Using mathematical modeling to confirm some suspicions as to the cause of three follicle waves per cycle could benefit the long term health of women especially if more follicle waves per cycle could cause them to reach menopause sooner. Biological research on the relationship between FSH, IHB and follicle waves is important based on these model predictions.

5.2 Superfecundation

Though rare, superfecundation, a form of dizygotic twinning, can be a direct consequence of multiple follicle waves per cycle. Potentially if each wave of one cycle ovulates and if both eggs are fertilized, fraternal twins could occur due to a follicle wave event. Our goal is to use the two-wave model to examine if this scenario is possible and if so to examine what the associated hormone profiles must resemble.

By definition, dizygotic twinning occurs when ovulation occurs more than once during a menstrual cycle and two oocytes are fertilized [50]. In this case, two follicles grow to dominance during the cycle [52]. Much research has been done on dizygotic twinning in recent years due to increased likelihood of multiple births with women receiving fertility treatments and in older women [22, 99]. In both cases, higher FSH levels lead to the increase in recruitment [15, 88]. Research has actually shown that in general, many mothers of fraternal twins have elevated FSH throughout the cycle [57, 58]. Many factors such as body composition, mother's height, mother's weight, season of the year, geographic location and whether the mother smokes also contribute to the frequency of dizygotic twinning in women [7, 17, 22, 35, 37, 59, 70].

Biologically, two potential cases could result in dizygotic twins in the two-wave case. The first is that FSH greatly exceeds its threshold or the FSH window is wider than normal for first follicle wave so that two follicles grow to dominance during that wave and are fertilized at the same time [15]. The second is superfecundation which is when two ova are fertilized at different times during the same cycle [54]. The occurrence of superfecundation is usually investigated due to discordance, difference in size, of the dizygotic twins. Since there are other reasons for discordance, the easiest case of superfecundation to identify is the case of heteropaternal superfecundation where there are two different fathers of the twins. There are many specific biological cases that could result in superfecundation including the case of follicle waves. If there is enough FSH in each wave so that one dominant follicle emerges in each wave of the cycle, both could ovulate and be fertilized during that cycle. Though rare because hormones levels after a zygote has formed should prevent further ovulation, we aim to model this follicle wave case of superfecundation. Thus the main goal here is to have two dominant follicles, one per follicle wave, and two LH surges to cause ovulation from each dominant follicle.

Expectations: To demonstrate superfecundation in the model, the following hormone and

follicle stage behaviors could occur if particular changes are made in the model:

Follicle Stages: To demonstrate follicle wave superfecundation we need two fully dominant follicles and two corpus lutea, one resulting from the follicular phase wave and one resulting from the luteal phase wave. For this to happen, the atresia term needs to be removed so that the second follicle wave can occur beyond the growing stage of ovarian follicle development.

LH Surge: Also necessary for follicle wave superfecundation is a second LH surge. The LH surge in a normal cycle triggers the release of the oocyte from the dominant follicle. It is not enough to just have two dominant follicles per cycle, we also need a second, luteal-phase LH surge to cause ovulation in the second dominant follicle for the purpose of fertilization for fraternal twins. Baerwald et al. [9] proposed that P4 inhibits the luteal phase LH from rising high enough to allow for the luteal follicle wave to develop to a dominant follicle and an LH surge to allow for ovulation. In other words, if P4 decreases, a second dominant follicle and LH surge could be possible.

Timing: It as been reported that women undergoing ovarian stimulation therapy have follicles that grow faster than women with natural cycles or those using oral contraceptives [13]. Thus a shortened follicular phase would not be all that surprising for the ovarian follicle stages.

It is important to note that most women typically do not have two dominant follicles consistently during each cycle over her lifetime. More often, a double ovulation is a rare occurrence due to a perfect storm of hormone levels. The nature of the mathematical model is that whatever we are trying to demonstrate is carried out repeatedly for any number of cycles specified. We should see stable, periodic cycles with two of every stage of growth repeated over and over. With these ideas in mind, the goal is to examine whether removing the atresia term completely and adjusting parameters accordingly would yield two dominant follicles and two LH surges per cycle.

The merged two-wave model for the McLachlan data set is used for demonstration of this phenomenon. As in the early menopause case, the McLachlan data set was chosen as it is easier to fit through optimization if possible. Though data are available for the five-hormone, two-wave model for optimization, that does not mean optimization will be possible because the goal is to have two complete waves for all nine stages of ovarian follicle growth. Since all three ovarian hormone profiles are proportions of the stages themselves, it is very much expected that all the five hormone profiles change since the experiment is taking place on the merged model. The hope is for a second LH surge and a similar FSH profile to the original.

Unlike the early menopause case in which component models were used, the merged model does not allow for as much freedom with optimization or changing parameters by inspection. Changing one parameter even slightly in the merged model can completely alter the hormone profiles and follicle stages since they are all intertwined. Thus, if superfecundation can be shown, the hormone profiles may not be as accurate as they would be in the component model. However, the merged model would be a more accurate representation of the cycle because it is the full feedback loop and the parameters cannot be manipulated beyond a reasonable estimate to obtain a desirable profile as is the case in the component model.

Cycle Results: The model performed very much to the expectations laid out above.

Follicle Stages: The model for follicle wave superfecundation does produce a second complete wave from recruitment through luteinization with the removal of the atresia term and alteration of parameters. As can be seen in Figure 5.11, a second dominant follicle, second ovulatory follicles and second corpus luteum are present in the amended model. Figure 5.12 indicates that the second corpus luteum is apparent in both P4 and IHA as well. These hormones exhibit two rises since every stage of growth now has two rises.

Timing: As expected, the cycle length is shorter than the 31 days of McLachlan data for one cycle as is easily seen in Figure 5.12 and Figure 5.13.

LH Surge: Figure 5.13 shows that two LH surges were also created. It stands to reason that this LH surge is made possible by E2. We can see in Figure 5.12 that E2 has a much higher and much sharper second rise than it did originally due to the second dominant follicle wave (recall E2 is a proportional sum of the growing, dominant and fourth luteal stage). Since E2 promotes the synthesis and release of LH, this large amount of E2 in the second rise most likely promotes the LH surge. This also explains why the second follicle wave is much higher than the first. Also as per the idea from Baerwald et al. [9] as to the lowering of P4 and its relation to the LH surge, as the coefficients p_1 and p_2 were lowered by hand, the second LH surge did in fact increase.

FSH: FSH is also quite interesting looking. FSH still reaches its peak despite all of the other changes due to the fact that IHA is much shorter than its corresponding data. Historically, the FSH peak is one of the hardest points of the model to reach and this merged model does just fine. However, the rest of the FSH curve is much shorter and there is an extra rise in FSH after the FSH peak. Since FSH synthesis and release is controlled by all three ovarian hormones, it is likely that the extra rises and especially the dramatic changes in E2 cause these issues.

Like the previous work on early menopause, here parameters were both optimized and changed by hand.

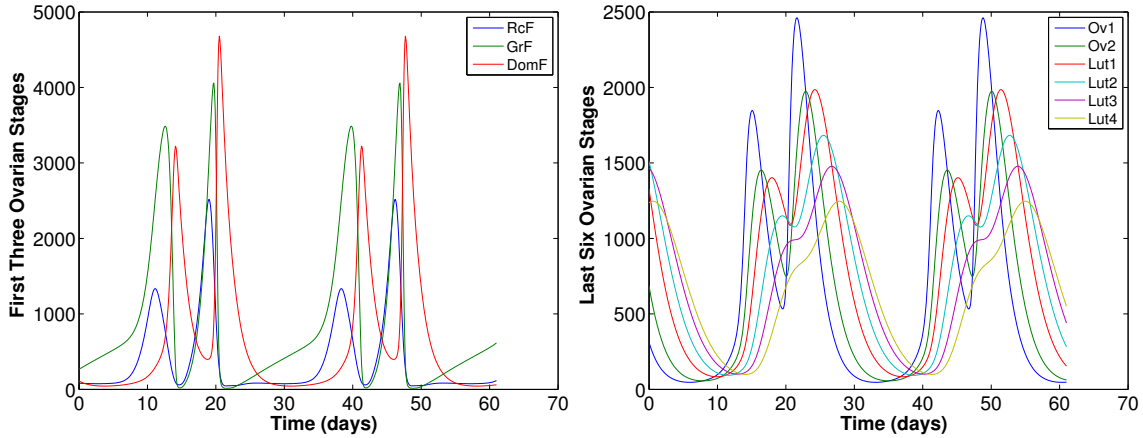

(a) **(b)**

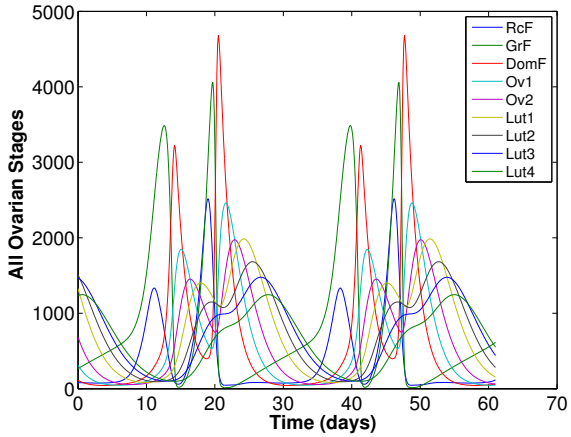

(c)

Figure 5.11 Models for **(a)** the first three growth stages, **(b)** the last six stages of growth and **(c)** all nine stages from the merged, five-hormone model representing superfecundation compared to the McLachlan data. Follicle wave superfecundation requires each wave of follicle growth to encounter every stage. Here, we can see that the model was successful after removal of the atresia term and alteration of the original two-wave parameters from Chapter 3.

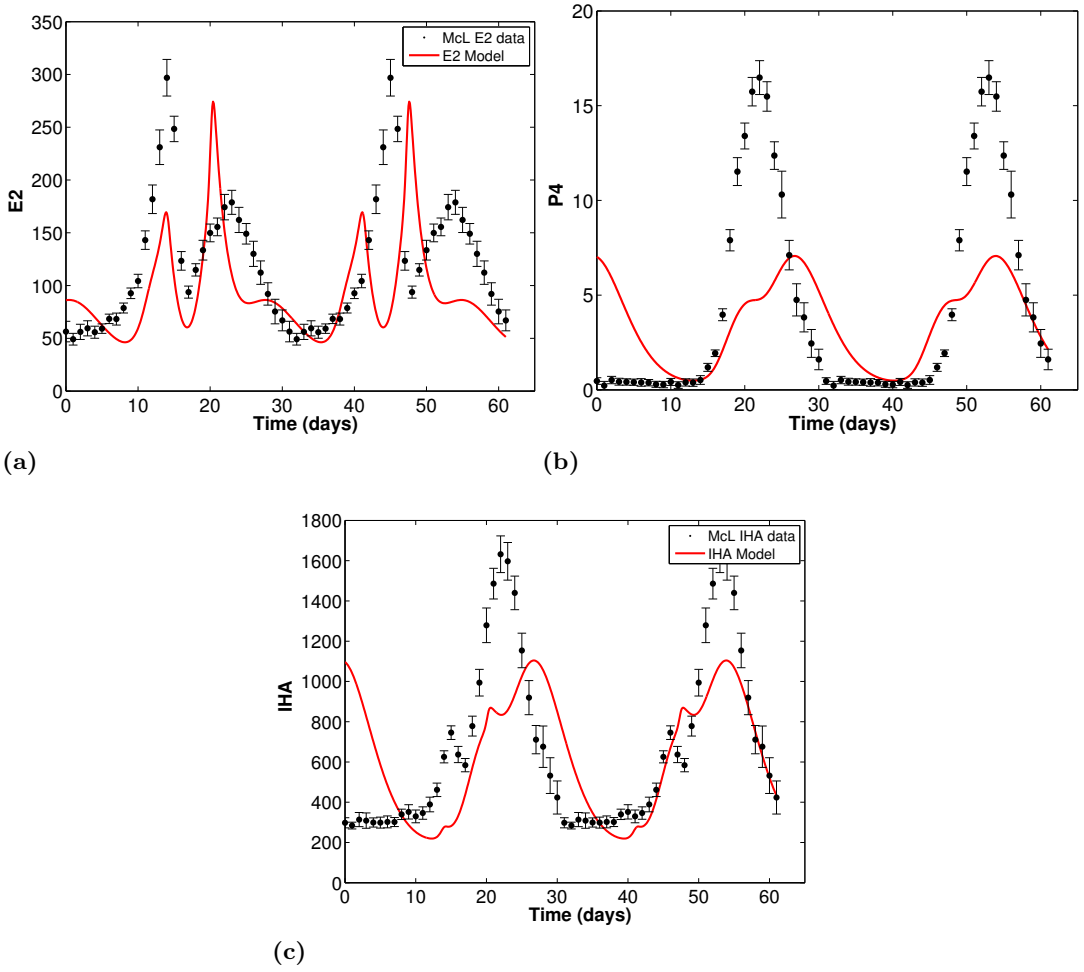

Figure 5.12 Models for **(a)** estrogen, **(b)** progesterone and **(c)** inhibin A from the merged, five-hormone model representing follicle wave superfecundation compared to the McLachlan data. P4 is much shorter in order to accommodate a second LH surge while IHA is much shorter so FSH can surpass its threshold enough to cause two dominant follicles, one in each wave. The sharp dip and narrow second rise in E2 is due to the second dominant follicle in the luteal phase wave.

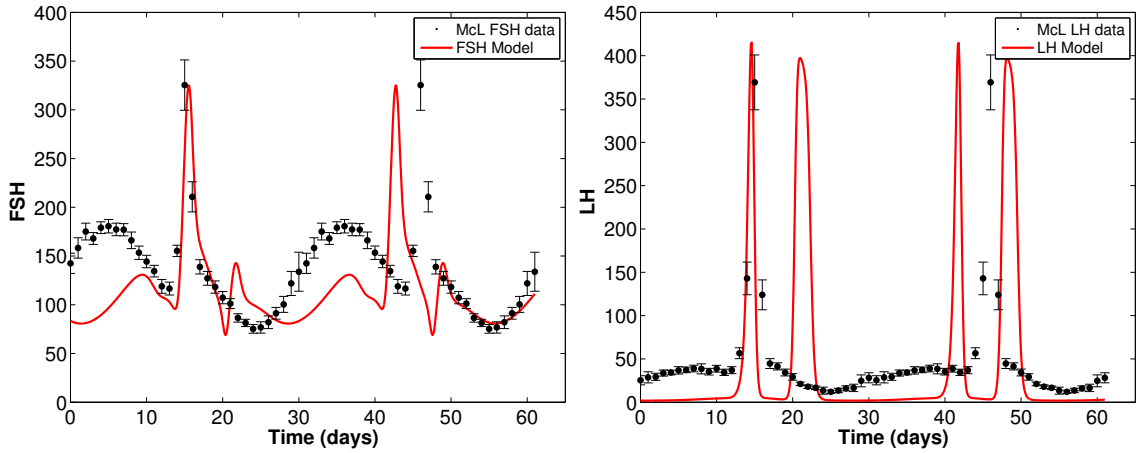

(a) **(b)**

Figure 5.13 Models for **(a)** FSH and **(b)** LH from the merged, five-hormone model representing follicle wave superfecundation compared to the McLachlan data. A second LH surge is present due to the rising E2 levels from having a second dominant follicle. A second LH surge allows for ovulation of the second dominant follicle for potential fertilization resulting in superfecundation.

Adjust Parameters by Hand.

- Obviously, the first step was to remove the atresia term but the immediate second step was somewhat unexpected. Since the atresia term changed the weighting of the dominant follicle as a decay, the transfer term out of the dominant follicle and into the first ovulatory follicle needed increased to balance out this change. So c_5 (Equation (4.23)) needed increased to keep the mass of the dominant follicle at a realistic level compared to the other stages around it.
- Also upon removing the atresia, v_{0LH} (Equation (4.2)) needed to be reduced as well. The parameter was lowered by hand slightly toward the beginning of the optimization process and the optimizer lowered it even more. It is not unexpected that RP_{LH} and LH parameters should change drastically as the goal is to obtain a very different LH profile. Here a reduction in v_{0LH} helps the second LH surge to be larger. This significant drop is likely due to the lower levels of P4. Recall P4 occurs in the denominator of the same term with v_{0LH} so it could be quite possible that the parameter is so much smaller to balance out some of the changes to the ovarian hormones. Also, with all other parameters held at their value in Table 5.4, lowering v_{0LH} below its optimized value of 212.68 makes both LH surges much larger. Raising it a little makes the second LH surge decrease in size. Raising it to a value substantially higher than 212.68 actually eliminates the second LH surge. Raising it even higher eliminates the

second follicle wave entirely from the dominant stage and beyond.

- Another parameter of note that was changed is v_{1LH} (Equation (4.2)). Increasing it allowed the LH levels to remain high to its peak amount. Other hormone changes were made by hand before any optimization took place to get the system to a place where the optimizer would find an appropriate solution.

Build Up Cost Function. Also similar to the last section, it made little sense to use certain hormones in the cost function for the optimizer. In this case, LH was obviously never used in the cost function because the goal was for it to look drastically different from the data set. The final cost function was a sum of FSH, E2 and IHA. Again, follicle wave superfecundation is rare with no known data on hormone levels so we must assume that the hormones besides LH are normal. P4 was intentionally left out of the cost function. As was stated above, lowering the auxiliary coefficients on P4 increased the second LH surge height. Putting P4 into the cost function would be counterproductive to these changes. P4 is one of the easiest functions to optimize because it is so simple. If the optimizer matches luteal stages and auxiliary coefficients to P4, we would likely lose the height of the second LH surge if not lose it entirely.

The final parameters for this simulation can be found in Table 5.4.

Though hormone data and biological studies may be lacking, mathematical modeling supports hypotheses about the relationship of follicle waves and the hormones that result from them.

- No one knows for certain if more than two follicle waves per cycle leads to early menopause in women, but we have shown that three rises in FSH cause three follicle waves per cycle and in turn causes three rises in IHB that feeds back on FSH. Thus, the relationship between FSH and IHB could be an important place to start an investigation as to answering the question on early menopause.

- Superfecundation from ovulating follicles in different follicle waves of the same cycle is possible as was shown in mathematical modeling. Superfecundation is hard to identify biologically and occurs in rare situations. Though the model produces two dominant follicles and two LH surges per cycle repeatedly which is unlikely in real life, it does show that a second dominant follicle could manipulate the ovarian hormones enough to cause a second ovulation and subsequent corpus luteum.

Table 5.4 Superfecundation parameter results for the merged, two-wave model fitting the McLachlan data set. All of the following optimized parameters were truncated to two significant decimal digits.

Param.	**Value**	**Units**
v_{0LH}	212.68	μg/day
v_{1LH}	35,656.90	μg/day
Km_{LH}	170.00	ng/L
$Ki_{LH,P}$	2.81	μg/L
k_{LH}	11.41	1/day
$c_{LH,P}$	0.084	L/μg
$c_{LH,E}$	0.0020	L/ng
d_E	0.50	days
d_P	1.00	days
v_{FSH}	4500.00	μg/day
$Ki_{FSH,IHA}$	646.30	U/L
k_{FSH}	11.55	1/day
$c_{FSH,P}$	3.16	L/μg
$c_{FSH,E}$	0.0023	$(\text{L/ng})^2$
d_{IHA}	1.74	days
α	0.30	dimensionless
β	0.020	dimensionless
γ	0.010	dimensionless
b	0.60	L/day
c_1	1.56	1/day

Param.	**Value**	**Units**
c_2	0.55	$(\text{L/}\mu\text{g})^{\alpha}(1/\text{day})$
c_3	0.051	$(\text{L/}\mu\text{g})^{\beta}(1/\text{day})$
c_4	0.027	$(\text{L/}\mu\text{g})(1/\text{day})$
c_5	0.60	$(\text{L/}\mu\text{g})^{\gamma}(1/\text{day})$
d_1	0.70	1/day
d_2	0.70	1/day
k_1	0.60	1/day
k_2	0.65	1/day
k_3	0.70	1/day
k_4	0.80	1/day
Km_F	115.00	μg/L
p	15.00	dimensionless
e_1	0.025	1/kL
e_2	0.047	1/kL
e_3	0.060	1/kL
p_1	0.0047	1/L
p_2	0.00016	1/L
h_0	140.00	U/L
h_1	0.020	$(\text{U/L})/\mu g$
h_2	0.63	$(\text{U/L})/\mu g$
h_3	0.020	$(\text{U/L})/\mu g$

Chapter 6

Conclusions

6.1 Concluding Remarks

For many years, only basic knowledge of how the human menstrual cycle works was known. Until technology developed enough to gather more information as to the mechanisms and actions taking place, it was believed that the recruitment leading to ovulation was all that took place each cycle. Though the basic ideas of ovulation and reproduction were maintained, current research gives a more complete picture of what truly happens during a woman's cycle. Follicle waves are one such area of research that has very much changed the way the cycle is viewed.

Further research on waves can only expand that view. For many women, a second follicle wave each cycle may not mean anything to their long term well-being or health. But for others, a second follicle wave could lead to dizygotic twins due to a superfecundation event or a LOOP event indicating the transition to menopause. And for some, their cycles may have more than two waves per cycle which could potentially propel them to menopause sooner than if they only had two waves per cycle. On the surface, follicle waves may seem like something extra and unimportant happening during the cycle because ovulation and fertilization is the purpose of the reproductive cycle but follicle waves can lend much information to health and wellness studies. Thus, including them in the mathematical model of the menstrual cycle is essential for a precise picture of what is happening between the hypothalamus-pituitary and the ovaries.

With an abundance of data for normally cycling women available, many scenarios for modeling follicle waves were successfully approached. The five-hormone, two-wave model was constructed for two data sets. Though the parameters are different to accommodate different units of measure, the Hill function for the FSH threshold and the atresia term construct a working model yielding two follicle waves in the recruited and growing stages of growth and only one dominant follicle ovulation and resulting corpus luteum per cycle. This model outlined in Chapter 3 works for not only the ovarian component model that uses pituitary hormones as

input functions but also works for the full merged feedback model. This model accurately represents the follicular phase wave going through recruitment, ovulation and luteinization and the luteal phase wave just going through recruitment. The concentrations for two-wave cycles per Baerwald et al. [9] very much mirror the profiles of the McLachlan and Welt data for normally cycling women so not only did the model succeed in producing two follicle waves per cycle it also maintained the hormone profiles for the data sets it modeled. It was also confirmed through sensitivity analysis that some of the parameters that were believed intuitively to be sensitive actually are, including some that control the follicle waves.

Chapter 4 expanded the two-wave model to include all six hormones outlined in the Welt data set. The same FSH threshold function and atresia term were used, but the FSH threshold was incorporated slightly differently because the recruited stage of growth is no longer the first stage in the six-hormone model. Again, success was found in both the six-hormone ovarian component model as well as the merged model. Two follicle waves of recruitment and growth were produced while only one went on to dominance and luteinization. The model also accurately produced profiles for the two pituitary hormones and four ovarian hormones of the Welt data set.

A benefit of the mathematical modeling of biological systems is using the model to test what we cannot, should not, or prefer not to test on human beings. There is much that has not been confirmed about the role follicle waves play in the lives of women, but with an accurate model of the cycle some theories have been tested. In Chapter 5, hypothesis testing as to what causes three follicle waves per cycle and if follicle waves could cause superfecundation was completed. Though the biological significance of more than two follicle waves per cycle is still unclear, the suggestion that it could be an indicator of an earlier onset of menopause is a reason to investigate. The FSH threshold Hill function works on a one-to-one relationship between the number of rises of FSH and the number of follicle waves being produced. Though the Baerwald et al. [9] concentrations do not include profiles for the inhibins, IHB is a logical choice for the cause of the follicular phase differences between the two-wave and three-wave profiles. This theory was tested using the mathematical model. Success was found by first showing that using an FSH input function with three rises in the five-hormone ovarian component model produces three follicle waves per cycle. Thus, the follicle wave model should produce any number of follicle waves desired by altering the FSH inputed into the system. It was also shown that an IHB input function with three rises used in the pituitary component model produces an FSH profile with three rises. Finally circling back to the ovarian component model with the three-rise FSH input function, it was retested on the six-hormone system to confirm that three-waves are produced but also to show that the IHB profile has three rises as a result. The three-wave results from mathematical modeling of follicle waves indicate that IHB should be an important candidate for further investigation of more than two follicle waves per cycle.

Chapter 5 also focused on the hypothesis testing of superfecundation, the fertilization of two oocytes on two separate occasions during the same cycle. Though there are different possible combinations of when the two oocytes are released and when they are fertilized, follicle waves are one such possibility. On rare occasions, a follicle could grow to be dominant and release an oocyte in each wave of follicle growth during a cycle and be fertilized. The two-wave, five-hormone merged model was successfully changed to demonstrate this case by removal of the atresia term from the dominant follicle. The removal of that term caused two waves for all nine stages of follicle growth. Thus, each wave went through recruitment, growth, ovulation and luteinization. An LH surge was produced for each wave as well as would be needed to trigger ovulation. Even though most women do not typically have two ovulating follicles during one cycle and most definitely do not have two ovulating follicles per cycle repeatedly each month, the model does show that superfecundation could result from ovarian follicle waves.

6.2 Future Work

Much work is still possible for modeling follicle waves. The most prominent as mentioned previously is a full merged model for three follicle waves per cycle. Unfortunately, the Baerwald et al. [9] data only accounted for four of the six hormones that would need to be examined. Not only does that mean that there are two hormones that are unavailable for optimization purposes, but we are not sure what the hormones should look like either. We speculated in Chapter 5 as to what type of curve should represent IHB in general but variations are possible. Also, we have no indication as to whether the curve for the average concentration of IHA should change or not. For the most part, P4 looks normal but the E2 curve has an additional and unaccounted for luteal rise. At this point in time, there is not enough information as to what the hormone concentrations are for IHA and IHB or as to why the other three-wave hormones look the way they do to merge the model. As more information becomes available, this would be the next logical step for the follicle wave model in showing that the two components in Chapter 5 can be merged and the full feedback cycle holds.

Also in Chapter 5, the five-hormone model was used to represent the dual ovulation for follicle wave superfecundation. All of the hormone profiles that were a result of that model were slightly different from the normal data, most especially the LH with two surges. It would be interesting to test follicle wave superfecundation on the six-hormone model to see what changes occur in IHB, if any. The major change in the follicle stages was that two dominant follicles, two ovulatory follicles and two corpus lutea were produced. Since IHB is active in the follicular phase, little change would be expected in its hormone profile. Testing would confirm that suspicion.

The six-hormones outlined in the McLachlan and Welt data sets are not the only things

believed to be influencing the development of follicle waves. In Hale et al. [49] it was suggested that AMH may play a part in triggering a follicle wave. Including AMH in the model could be another possibility in the future. At this time, there does not seem to be any concrete evidence that it does affect the development of follicle waves which means there is no information on how it could trigger them. The inclusion of AMH in the follicle wave model could influence the waves in the existing model.

Also in the work by Hale et al. [49], the concept of LOOP events is believed to be caused by follicle waves. LOOP events could potentially be modeled as well. To model a LOOP event, the model would need to trigger the luteal wave to become dominant instead of the follicular phase wave. It seems a LOOP event is a one time occurrence that has a domino affect on the cycle so it remains in flux until the end of the menopause transition when cycling ends entirely. Like follicle wave superfecundation, modeling a LOOP event would likely first start as attempting a non-ovulatory follicular phase wave and an ovulatory luteal phase wave that is repeated each cycle. Then it can be investigated as to whether the E2 levels that result correspond to the results that have been found biologically. Demonstrating LOOP events would be a likely candidate for the ovarian component model, at least to start. Reversing which wave is ovulatory may prove quite difficult for the merged model so starting with the ovarian component model may give insight into some factors that could cause this LOOP event.

While very little is known as to how follicle wave dynamics change over the course of a woman's lifetime, a lifelong model of follicle waves would be a worthwhile endeavor. As the levels of FSH rise through the menopause transition, not only could LOOP events occur, the number of follicle waves per cycle may change as well. Personal correspondence with Dr. Baerwald indicates that research has been conducted on follicle waves and older women, so more information might be available in the near future. We have seen that as the levels of FSH and IHB change, more follicle waves per cycle are possible. It has also been shown biologically that FSH levels are higher and IHB levels are lower through the transition to menopause. As a woman ages, do more follicle waves per cycle occur? Incorporating follicle waves into a life-long model similar to the one developed by Margolskee and Selgrade [61] could answer that question.

Finally, as seen in Chapter 3, there are many sensitive parameters in this model. The results of the sensitivity analysis reported in Chapter 3 can be used in bifurcation analysis. The original one-wave models have been analyzed for bifurcations, so examining this model is important to see how the parameters affect the dynamical behavior of the model. The more sensitive parameters are the most likely candidates for causing bifurcations, so the results from Chapter 3 can easily be put to use with the MATLAB DDE-BIFTOOL. The parameters from the recruited stage, especially on the FSH threshold are of extreme interest.

There is much still to learn about human ovarian follicle waves. While most of that learning will be done in a research lab through blood testing and ultrasounds, some can be done

through mathematical modeling. Through creating a more biologically accurate model of the cycle by including ovarian follicle waves, many suspicions have been confirmed and directions as to further mathematical and biological research have been found. Updating the original mathematical model for endocrine control of the human female reproductive system to include two follicle waves each cycle for both the five-hormone and six-hormone models still produces the same hormone profiles as it did before the changes were made. Thus, a two-wave cycle produces normal hormone profiles and should be considered commonplace for all women. Modeling three follicle waves per cycle indicates that IHB should be investigated as to how more than two follicle waves per cycle affects women and if it is a potential problem. Showing that ovulation in each follicle wave is possible in the model sheds more light on the possible reasons why superfecundation occurs. As more biological research becomes available, more questions can be answered and more precision can be added to the model. Mathematical modeling of follicle waves is a cost-effective, ethical and safe way to test hypotheses as to what biological steps could be taken next. Though follicle waves are a very young topic in reproductive health with respect to other aspects of the cycle, mathematical modeling has shown that it is vital that they are investigated further.

REFERENCES

[1] 113th Congress. *House Resolution 1851- Family Act of 2013*. www.congress.gov/bill/113th-congress/house-bill/1851. 2013-2014 (accessed May 25, 2015).

[2] G. P. Adams. Control of ovarian follicular wave dynamics in cattle: Implications for synchronization and superstimulation. *Theriogenology*, 41(1):19–24, 1994.

[3] G. P. Adams. Comparative patterns of follicle development and selection in ruminants. *Journal of Reproduction and Fertility*, Supplement(54):17–32, 1999.

[4] G. P. Adams, R. L. Matteri, J. P. Kastelic, J. C. H. Ko, and O. J. Ginther. Association between surges of follicle-stimulating hormone and the emergence of follicular waves in heifers. *Journal of Reproduction and Fertility*, 94(1):177–188, 1992.

[5] G. Adams and R. Pierson. Bovine model for study of ovarian follicular dynamics in humans. *Theriogenology*, 43(1):113–120, 1995.

[6] G. Adams, R. Jaiswal, J. Singh, and P. Malhi. Progress in understanding ovarian follicular dynamics in cattle. *Theriogenology*, 69(1):72–80, 2008.

[7] D. J. Anderson. On the Evolution of Human Brood Size. *Evolution*, 44(2):438–440, 1990.

[8] S. E. Aydos, A. H. Elhan, and A. Tükün. Is telomere length one of the determinants of reproductive life span? *Archives of Gynecology and Obstetrics*, 272(2):113–116, 2005.

[9] A. R. Baerwald, G. P. Adams, and R. A. Pierson. A new model for ovarian follicular development during the human menstrual cycle. *Fertility and Sterility*, 80(1):116–122, 2003.

[10] A. R. Baerwald, G. P. Adams, and R. A. Pierson. Characterization of ovarian follicular wave dynamics in women. *Biology of Reproduction*, 69(3):1023–1031, 2003.

[11] A. R. Baerwald, G. P. Adams, and R. A. Pierson. Form and function of the corpus luteum during the human menstrual cycle. *Ultrasound in Obstetrics and Gynecology*, 25(5):498–507, 2005.

[12] A. R. Baerwald, G. P. Adams, and R. A. Pierson. Ovarian antral folliculogenesis during the human menstrual cycle: a review. *Human Reproduction Update*, 18(1):73–91, 2012.

[13] A. R. Baerwald, R. A. Walker, and R. A. Pierson. Growth rates of ovarian follicles during natural menstrual cycles, oral contraception cycles, and ovarian stimulation cycles. *Fertility and Sterility*, 91(2):440–449, 2009.

[14] A. Baerwald, P. Anderson, A. Yuzpe, A. Case, and M. Fluker. Synchronization of ovarian stimulation with follicle wave emergence in patients undergoing in vitro fertilization

with a prior suboptimal response: a randomized, controlled trial. *Fertility and Sterility*, 98(4):881–887, 2012.

[15] D. T. Baird. A model for follicular selection and ovulation: Lessons from superovulation. *Journal of Steroid Biochemistry*, 27(1):15–23, 1987.

[16] T. G. Baker. A Quantitative and Cytological Study of Germ Cells in Human Ovaries. *Proceedings of the Royal Society of London B: Biological Sciences*, 158(972):417–433, 1963.

[17] O. Basso, E. A. Nohr, and K. Christensen. Risk of Twinning as a Function of Maternal Height and Body Mass Index. *JAMA*, 291(13):1564–1566, 2004.

[18] G. A. Bó, P. S. Baruselli, and M. F. Martínez. Pattern and manipulation of follicular development in Bos indicus cattle. *Animal Reproduction Science*, 78(3):307–326, 2003.

[19] H. M. T. Boer, S. Röblitz, C. Stötzel, R. F. Veerkamp, B. Kemp, and H. Woelders. Mechanisms regulating follicle wave patterns in the bovine estrous cycle investigated with a mathematical model. *Journal of Dairy Science*, 94(12):5987–6000, 2011.

[20] R. J. Bogumil, M. Ferin, and R. L. Vande Wiele. Mathematical studies of the human menstrual cycle. II. Simulation performance of a model of the human menstrual cycle. *The Journal of Clinical Endocrinology and Metabolism*, 35(1):144–156, 1972.

[21] R. J. Bogumil, M. Ferin, J. Rootenberg, L. Speroff, and R. L. Vande Wiele. Mathematical studies of the human menstrual cycle. I. Formulation of a mathematical model. *The Journal of Clinical Endocrinology and Metabolism*, 35(1):126–143, 1972.

[22] R. Bortolus, F. Parazzini, L. Chatenoud, G. Benzi, M. M. Bianchi, and A. Marini. The epidemiology of multiple births. *Human Reproduction Update*, 5(2):179–187, 1999.

[23] R. W. Bretveld, P. T. J. Scheepers, N. Roeleveld, C. M. G. Thomas, and G. A. Zielhuis. Pesticide exposure: the hormonal function of the female reproductive system disrupted? *Reproductive Biology and Endocrinology*, 4:30, 2006.

[24] J. B. Brown. Pituitary Control of Ovarian Function-Concepts Derived from Gonadotrophin Therapy. *Australian and New Zealand Journal of Obstetrics and Gynaecology*, 18(1):47–54, 1978.

[25] G. M. Chambers, E. A. Sullivan, O. Ishihara, M. G. Chapman, and G. D. Adamson. The economic impact of assisted reproductive technology: a review of selected developed countries. *Fertility and Sterility*, 91(6):2281–2294, 2009.

[26] A. Chandra, C. E. Copen, and E. H. Stephen. Infertility and impaired fecundity in the United States, 1982-2010: data from the National Survey of Family Growth. *National Health Statistics Reports*, (67):1–18, 2013.

[27] A. Chandra, C. E. Copen, and E. H. Stephen. Infertility service use in the United States: data from the National Survey of Family Growth, 1982-2010. *National Health Statistics Reports*, (73):1–21, 2014.

[28] J. E. Chavarro, W. C. Willet, and P. J. Skerrett. Fat, Carbs and the Science of Conception. *Newsweek*, 150(24):54–62, 2007.

[29] S. M. Choi, S. D. Yoo, and B. M. Lee. Toxicological Characteristics of Endocrine-Disrupting Chemicals: Developmental Toxicity, Carcinogenicity, and Mutagenicity. *Journal of Toxicology and Environmental Health, Part B: Critical Reviews*, 7(1). 2004.

[30] L. H. Clark, P. M. Schlosser, and J. F. Selgrade. Multiple stable periodic solutions in a model for hormonal control of the menstrual cycle. *Bulletin of Mathematical Biology*, 65(1):157–173, 2003.

[31] M. P. Connolly, S. Hoorens, and G. M. Chambers. The costs and consequences of assisted reproductive technology: an economic perspective. *Human Reproduction Update*, 16(6):603–613, 2010.

[32] D. A. Crain, J. Schwartz, N. Skakkebaek, A. M. Soto, S. Swan, C. Walker, T. J. Woodruff, T. K. Woodruff, L. C. Giudice, L. J. Guillette, S. J. Janssen, T. M. Edwards, J. Heindel, S.-m. Ho, P. Hunt, T. Iguchi, A. Juul, and J. A. McLachlan. Female reproductive disorders: the roles of endocrine-disrupting compounds and developmental timing. *Fertility and Sterility*, 90(4):911–940, 2008.

[33] C. de Koning, J. McDonnell, A. Themmen, F. de Jong, R Homburg, and C. Lambalk. The endocrine and follicular growth dynamics throughout the menstrual cycle in women with consistently or variably elevated early follicular phase FSH compared with controls. *Human Reproduction*, 23(6):1416–1423, 2008.

[34] I. Dervain. Ultrasound study of the growth of the normal ovarian follicle and detection of ovulation. PhD thesis. Universite Louis Pasteur, 1980.

[35] C. E. Dionne, M. Söderström, and S. M. Schwartz. Seasonal variation of twin births in Washington State. *Acta Geneticae Medicae et Gemellologiae*, 42(2):141–149, 1993.

[36] R. Ecochard and A. Gougeon. Side of ovulation and cycle characteristics in normally fertile women. *Human Reproduction*, 15(4):752–755, 2000.

[37] A. W. Eriksson and J. Fellman. Seasonal variation of livebirths, stillbirths, extramarital births and twin maternities in Switzerland. *Twin Research*, 3(4):189–201, 2000.

[38] H. Fevold, F. Hisaw, and S. Leonard. The gonad stimulating and the luteinizing hormones of the anterior lobe of the hypophesis. *American Journal of Physiology-Legacy Content*, 97(2):291–301, 1931.

[39] J. E. Fortune. Ovarian follicular growth and development in mammals. *Biology of Reproduction*, 50(2):225–232, 1994.

[40] M. A. F. Fritz and L. Speroff. *Clinical Gynecologic Endocrinology and Infertility*. 8th. Lippincott Williams and Wilkins, 2010.

[41] O. J. Ginther, J. P. Kastelic, and L. Knopf. Intraovarian relationships among dominant and subordinate follicles and the corpus luteum in heifers. *Theriogenology*, 32(5):787–795, 1989.

[42] O. J. Ginther, M. A. Beg, E. L. Gastal, M. O. Gastal, A. R. Baerwald, and R. A. Pierson. Systemic concentrations of hormones during the development of follicular waves in mares and women: a comparative study. *Reproduction*, 130(3):379–388, 2005.

[43] O. Ginther, E. Gastal, M. Gastal, D. Bergfelt, A. Baerwald, and R. Pierson. Comparative Study of the Dynamics of Follicular Waves in Mares and Women. *Biology of Reproduction*, 71(4):1195–1201, 2004.

[44] O. Ginther, M. Beg, M. Gastal, and E. Gastal. Follicle dynamics and selection in mares. *Animal Reproduction*, 1(1):45–63, 2004.

[45] A. Gougeon. Regulation of ovarian follicular development in primates: facts and hypotheses. *Endocrine Reviews*, 17(2):121–155, 1996.

[46] A. Gougeon. Chapter 2-Dynamics of Human Follicular Growth: Morphologic, Dynamic, and Functional Aspects. *The Ovary (Second Edition)*. Ed. by P. C. Leung and E. Y. Adashi. Second Edition. San Diego: Academic Press, 2003, 25–43, III–IV.

[47] B. J. Hackelöer, R. Fleming, H. P. Robinson, A. H. Adam, and J. R. Coutts. Correlation of ultrasonic and endocrinologic assessment of human follicular development. *American Journal of Obstetrics and Gynecology*, 135(1):122–128, 1979.

[48] G. E. Hale, D. M. Robertson, and H. G. Burger. The perimenopausal woman: endocrinology and management. *The Journal of Steroid Biochemistry and Molecular Biology*, 142:121–131, 2014.

[49] G. E. Hale, C. L. Hughes, H. G. Burger, D. M. Robertson, and I. S. Fraser. Atypical estradiol secretion and ovulation patterns caused by luteal out-of-phase (LOOP) events underlying irregular ovulatory menstrual cycles in the menopausal transition. *Menopause*, 16(1):50–59, 2009.

[50] J. G. Hall. Twinning. *The Lancet*, 362(9385):735–743, 2003.

[51] S. M. Hawkins and M. M. Matzuk. The Menstrual Cycle. *Annals of the New York Academy of Sciences*, 1135(1):10–18, 2008.

[52] C. Hoekstra, Z. Z. Zhao, C. B. Lambalk, G. Willemsen, N. G. Martin, D. I. Boomsma, and G. W. Montgomery. Dizygotic twinning. *Human Reproduction Update*, 14(1):37–47, 2008.

[53] R. S. Jaiswal, J. Singh, L. Marshall, and G. P. Repeatability of 2-wave and 3-wave patterns of ovarian follicular development during the bovine estrous cycle. *Theriogenology*, 72(1):81–90, 2009.

[54] W. H. James. Gestational age in twins. *Archives of Disease in Childhood*, 55(4):281–284, 1980.

[55] N. A. Klein, B. S. Houmard, K. R. Hansen, T. K. Woodruff, P. M. Sluss, W. J. Bremner, and M. R. Soules. Age-Related Analysis of Inhibin A, Inhibin B, and Activin A Relative to the Intercycle Monotropic Follicle-Stimulating Hormone Rise in Normal Ovulatory Women. *The Journal of Clinical Endocrinology and Metabolism*, 89(6):2977–2981, 2004.

[56] D. M. de Kretser and D. M. Robertson. The isolation and physiology of inhibin and related proteins. *Biology of Reproduction*, 40(1):33–47, 1989.

[57] C. B. Lambalk, C. H. D. Koning, and D. D. M. Braat. The endocrinology of dizygotic twinning in the human. *Molecular and Cellular Endocrinology*, 145(1):97–102, 1998.

[58] C. B. Lambalk, D. I. Boomsma, L. D. Boer, C. H. D. Koning, E. Schoute, C. Popp-Snijders, and J. Schoemaker. Increased levels and pulsatility of follicle-stimulating hormone in mothers of hereditary dizygotic twins. *The Journal of Clinical Endocrinology and Metabolism*, 83(2):481–486, 1998.

[59] V. Lummaa, E. Haukioja, R. Lemmetyinen, and M. Pikkola. Natural selection on human twinning. *Nature*, 394(6693):533–534, 1998.

[60] T. Lundy, P. Smith, A. O'Connell, N. L. Hudson, and K. P. McNatty. Populations of granulosa cells in small follicles of the sheep ovary. *Journal of Reproduction and Fertility*, 115(2):251–262, 1999.

[61] A. Margolskee and J. F. Selgrade. A lifelong model for the female reproductive cycle with an antimüllerian hormone treatment to delay menopause. *Journal of Theoretical Biology*, 326:21–35, 2013.

[62] A. J. Margolskee. A Whole Life Model of the Human Menstrual Cycle. PhD thesis. North Carolina State University, 2013.

[63] M. M. Matzuk and D. J. Lamb. Genetic dissection of mammalian fertility pathways. *Nature Cell Biology*, 4(Supplement):s41–49, 2002.

[64] E. A. McGee and A. J. W. Hsueh. Initial and Cyclic Recruitment of Ovarian Follicles. *Endocrine Reviews*, 21(2):200–214, 2000.

[65] J. A. McLachlan and S. F. Arnold. Environmental Estrogens. *American Scientist*, 84(5):452–461, 1996.

[66] R. I. McLachlan, N. L. Cohen, K. D. Dahl, W. J. Bremner, and M. R. Soules. Serum inhibin levels during the periovulatory interval in normal women: relationships with sex steroid and gonadotrophin levels. *Clinical Endocrinology*, 32(1):39–48, 1990.

[67] M. S. Medan, T. Takedom, Y. Aoyagi, M. Konishi, S. Yazawa, G. Watanabe, and K. Taya. The effect of active immunization against inhibin on gonadotropin secretions and follicular dynamics during the estrous cycle in cows. *The Journal of Reproduction and Development*, 52(1):107–113, 2006.

[68] M. Mihm, S. Gangooly, and S. Muttukrishna. The normal menstrual cycle in women. *Animal Reproduction Science*, 124(3):229–236, 2011.

[69] F. Miro. The onset of the initial rise in follicle-stimulating hormone during the human menstrual cycle. *Human Reproduction*, 20(1):96–100, 2004.

[70] M. M. Morales-Suárez-Varela, B. H. Bech, K. Christensen, and J. Olsen. Coffee and smoking as risk factors of twin pregnancies: the Danish National Birth Cohort. *Twin Research and Human Genetics*, 10(4):597–603, 2007.

[71] B. Mueller. Paternity Case for a New Jersey Mother of Twins Bears Unexpected Results: Two Fathers: Metropolitan Desk. *New York Times*:A.20, 2015.

[72] S. Muttukrishna, P. Fowler, N. Groome, G. Mitchell, W. Robertson, and P. Knight. Endocrinology: Serum concentrations of dimeric inhibin during the spontaneous human menstrual cycle and after treatment with exogenous gonadotrophin. *Human Reproduction*, 9(9):1634–1642, 1994.

[73] T. B. Nippoldt, N. E. Reame, R. P. Kelch, and J. C. Marshall. The Roles of Estradiol and Progesterone in Decreasing Luteinizing Hormone Pulse Frequency in the Luteal Phase of the Menstrual Cycle. *The Journal of Clinical Endocrinology and Metabolism*, 69(1):67–76, 1989.

[74] R. Palermo. Differential actions of FSH and LH during folliculogenesis. *Reproductive Biomedicine Online*, 15(3):326–337, 2007.

[75] S. J. Park, L. T. Goldsmith, and G. Weiss. Age-Related Changes in the Regulation of Luteinizing Hormone Secretion by Estrogen in Women. *Experimental Biology and Medicine*, 227(7):455–464, 2002.

[76] K. Parker, D. Robertson, N. Groome, and K. Macmillan. Plasma Concentrations of Inhibin A and Follicle-Stimulating Hormone Differ Between Cows with Two or Three Waves of Ovarian Follicular Development in a Single Estrous Cycle. *Biology of Reproduction*, 68(3):822–828, 2003.

[77] R. D. Pasteur and J. F. Selgrade. A deterministic, mathematical model for hormonal control of the menstrual cycle. *Understanding the Dynamics of Biological Systems*. Springer, 2011, 39–58.

[78] R. D. Pasteur II. A Multiple Inhibin Model of the Human Menstrual Cycle. PhD thesis. North Carolina State University, 2008.

[79] H. Peters. *The ovary : a correlation of structure and function in mammals*. Berkeley: University of California Press, 1980.

[80] R. A. Pierson and O. J. Ginther. Ultrasonography of the bovine ovary. *Theriogenology*, 21(3):495–504, 1984.

[81] L. Plouffe and S. N. Luxenberg. Biological modeling on a microcomputer using standard spreadsheet and equation solver programs: The hypothalamic-pituitary-ovarian axis as an example. *Computers and Biomedical Research*, 25(2):117–130, 1992.

[82] S. R. Pope, L. M. Ellwein, C. L. Zapata, V. Novak, C. T. Kelley, and M. S. Olufsen. Estimation and identification of parameters in a lumped cerebrovascular model. *Mathematical Biosciences and Engineering*, 6(1):93–115, 2009.

[83] C. A. Price and P. D. Carriére. Alternate two- and three-follicle wave interovulatory intervals in Holstein heifers monitored for two consecutive estrous cycles. *Canadian Journal of Animal Science*, 84(1):145–147, 2004.

[84] E. Rajakoski. The ovarian follicular system in sexually mature heifers with special reference to seasonal, cyclical, end left-right variations. *Acta endocrinologica*, 34(Supplementum 52):1–68, 1960.

[85] F. M. Rhodes, G. De'ath, and K. W. Entwistle. Animal and temporal effects on ovarian follicular dynamics in Brahman heifers. *Animal Reproduction Science*, 38(4):265–277, 1995.

[86] I. Schipper, W. C. Hop, and B. C. Fauser. The Follicle-Stimulating Hormone (FSH) Threshold/Window Concept Examined by Different Interventions with Exogenous FSH during the Follicular Phase of the Normal Menstrual Cycle: Duration, Rather Than Magnitude, of FSH Increase Affects Follicle Development. *The Journal of Clinical Endocrinology and Metabolism*, 83(4):1292–1298, 1998.

[87] P. M. Schlosser and J. F. Selgrade. A model of gonadotropin regulation during the menstrual cycle in women: Qualitative features. *Environmental Health Perspectives*, 108(supplement 5):873–881, 2000.

[88] J. Schoemaker, M. V. Weissenbruch, F. Scheele, and M. V. D. Meer. The FSH threshold concept in clinical ovulation induction. *Bailliére's Clinical Obstetrics and Gynaecology*, 7(2):297–308, 1993.

[89] N. B. Schwartz. Cybernetics of Mammalian Reproduction. *Mammalian Reproduction*. Ed. by H. Gibian and E. J. Plotz. Vol. 21. Colloquium der Gesellschaft für Biologische Chemie in 9.11. April 1970 in Mosbach/Baden. Springer Berlin Heidelberg, 1970.

[90] J. F. Selgrade and P. M. Schlosser. A model for the production of ovarian hormones during the menstrual cycle. *Differential Equations with Applications to Biology*. Vol. 21. American Mathematical Society, Fields Institute Communications, 1999, 429–446.

[91] J. F. Selgrade. Modeling hormonal control of the menstrual cycle. *Comments on Theoretical Biology*, 6(1):79–101, 2001.

[92] J. Singh, G. P. Adams, and R. A. Pierson. Promise of new imaging technologies for assessing ovarian function. *Animal Reproduction Science*, 78(3):371–399, 2003.

[93] S. Sunderam, D. M. Kissin, S. B. Crawford, S. G. Folger, D. J. Jamieson, W. D. Barfield, and Centers for Disease Control and Prevention. Assisted reproductive technology surveillance-United States, 2011. *Morbidity and Mortality Weekly Report. Surveillance Summaries*, 63(10):1–28, 2014.

[94] A. E. Treloar, R. E. Boynton, B. G. Behn, and B. W. Brown. Variation of the human menstrual cycle through reproductive life. *International Journal of Fertility*, 12(1 Part 2):77–126, 1967.

[95] A. Treloar. Menstrual cyclicity and the pre-menopause. *Maturitas*, 3(3-4):249–264, 1981.

[96] C. Tsai and S. Yen. The effects of ethinyl estradiol administration during early follicular phase of the cycle on the gonadotropin levels and ovarian function. *Journal of Clinical Endocrinology*, 33(6):917–923, 1971.

[97] U.S. Cancer Statistics Working Group. *United States Cancer Statistics: 1999-2011 Incidence and Mortality Web-based Report. Atlanta: U.S. Department of Health and Human Services, Centers for Disease Control and Prevention and National Cancer Institute*. www.cdc.gov/uscs. 2014 (accessed May 25, 2015).

[98] C. K. Welt, D. J. McNicholl, A. E. Taylor, and J. E. Hall. Female Reproductive Aging Is Marked by Decreased Secretion of Dimeric Inhibin. *The Journal of Clinical Endocrinology and Metabolism*, 84(1):105–111, 1999.

[99] T. Westergaard, J. Wohlfahrt, P. Aaby, and M. Melbye. Population based study of rates of multiple pregnancies in denmark, 1980-94. *BMJ*, 314(7083):775–779, 1997.

[100] E. Widmaier, H. Raff, and K. Strang. *Vander's Human Physiology: The Mechanisms of Body Function*. 12th. McGraw-Hill, 2011.

[101] D. Wolfenson, G. Inbar, Z. Roth, M. Kaim, A. Bloch, and R. Braw-Tal. Follicular dynamics and concentrations of steroids and gonadotropins in lactating cows and nulliparous heifers. *Theriogenology*, 62(6):1042–1055, 2004.

[102] M. Wright-Walters and C. Volz. Municipal Wastewater Concentrations of Pharmaceutical and Xeno-Estrogens: Wildlife and Human Health Implications. *Proceedings of the 2007 National Conference on Environmental Science and Technology*. New York, NY: Springer New York, 2009, 103–113.

[103] H. Yue, M. Brown, J. Knowles, H. Wang, D. S. Broomhead, and D. B. Kell. Insights into the behaviour of systems biology models from dynamic sensitivity and identifiability analysis: a case study of an NF-κB signalling pathway. *Molecular BioSystems*, 2(12):640–649, 2006.

[104] A. J. Zeleznik. The physiology of follicle selection. *Reproductive Biology and Endocrinology*, 2:31, 2004.

[105] A. J. Zeleznik and C. R. Pohl. Control of Follicular Development, Corpus Luteum Function, the Maternal Recognition of Pregnancy, and the Neuroendocrine Regulation of the Menstrual Cycle in Higher Primates. *Knobil and Neill's Physiology of Reproduction*. Elsevier Inc, 2006, 2449–2510.

APPENDICES

Appendix A

Data Sets

McLachlan Data and Units

The data were taken from Selgrade (2001) [91] that were rescaled after original acquisition from McLachlan, et al. (1990) [66] and are included in Table A.1. For simplicity during study, the units from the Selgrade publication were converted to parts per liter, but the scaling remained the same. Hormone units of measure are listed in the table. The error bars on the data were acquired from the McLachlan publication using *grabit* in MATLAB and the units were converted to match. Though no measurements were taken for follicular mass, note that the ovarian stages of growth are measured in μg in accordance with the units of measure for the hormones that produce them and the hormones that they in turn produce.

Welt Data and Units

Data were taken from Pasteur (2008) [78] based on the work by Welt, et al. (1999) [98]. The error bars on the data were acquired from Margolskee [62] using *grabit* in MATLAB. Note that all ovarian stages of follicle growth are measured in IU.

Table A.1 Data from McLachlan, et al. [66] as taken from Selgrade [91] and undergoing change of units. The values for the thirty-one day cycle beginning at menses at day 0 for E2, P4, IHA, FSH and LH are included.

day	**E2 (ng/L)**	**P4(μg/L)**	**IHA (U/L)**	**FSH (μg/L)**	**LH (μg/L)**
0	56.387	0.468	297.9	142.5	25.34
1	49.168	0.227	284.1	158.3	28.74
2	56.087	0.519	313.8	175.1	29.36
3	59.465	0.43	308.7	168	33.71
4	55.76	0.417	299.3	179.1	34.29
5	59.138	0.406	298.7	180.6	36.78
6	68.4	0.392	302.2	177.3	37.35
7	68.236	0.379	301.5	177	38.88
8	78.696	0.292	339.8	166.1	38.52
9	92.67	0.279	352	153.4	35.28
10	104.3	0.418	329.7	144.4	38.71
11	143.04	0.254	346.3	134.5	34.54
12	181.75	0.393	388.8	118.9	37.02
13	231.05	0.381	461.7	116.6	56.62
14	296.92	0.52	625.4	155.3	142.9
15	248.43	1.189	745.8	325.4	369.2
16	123.4	1.934	636.9	210.7	124
17	93.76	3.966	584.2	138.9	44.63
18	114.82	7.897	778.3	127.1	41.39
19	133.5	11.52	993.9	118.2	34.32
20	149.85	13.401	1279	107.3	29.18
21	155.57	15.741	1486	101.2	21.18
22	174.28	16.483	1632	86.53	17.95
23	178.83	15.486	1597	81.36	16.64
24	162.19	12.366	1440	75.29	13.38
25	149.06	10.306	1154	76.79	12.02
26	130.04	7.111	919.5	82.1	13.54
27	112.23	4.749	711.1	91.23	16.02
28	92.044	3.827	675.8	100.4	16.56
29	75.373	2.45	532.2	121.9	24.72
30	66.983	1.604	423.4	133.9	28.2

Table A.2 Data from Welt, et al. [98] as taken from Pasteur [78]. Measurements were taken from E2, P4, IHA, IHB, FSH and LH for the 28 day cycle. Here day 1 corresponds to the onset of menses.

day	**E2 (pg/mL)**	**P4 (ng/mL)**	**IHA (IU/mL)**	**IHB (pg/mL)**	**FSH (IU/L)**	**LH (IU/L)**
1	51	1.1	1	79	11.4	12
2	55	0.6	1.1	109	11.6	14
3	53	0.6	1	116	11.7	15
4	59	0.6	1.1	123	12.4	14
5	60	0.6	1.1	140	12.6	17
6	62	0.6	1	135	11.3	17
7	66	0.6	1.1	140	12.1	19
8	72	0.6	1.2	144	11.3	18
9	95	0.6	1.7	147	10	17
10	119	0.6	2.3	130	8.7	17
11	138	0.6	3.2	113	8.6	17
12	188	0.6	4.5	98	8.2	25
13	237	0.7	7.4	83	10.4	50
14	215	1.2	9.3	147	19.6	123
15	127	2	7.7	167	12.1	41
16	91	5	8.1	106	9.2	22
17	102	8.9	10.1	57	8.7	20
18	119	11.2	8.9	44	8.6	20
19	140	15.6	9.5	43	7.4	18
20	133	17.3	11.5	38	7.2	16
21	152	17.9	9.1	32	6.1	12
22	142	17.2	8.7	30	5.4	9
23	140	14.4	7.5	29	5.2	11
24	155	12.6	6.6	36	5.4	10
25	133	10.3	5.7	30	5.3	11
26	114	8.1	4.1	37	6.1	11
27	70	4.3	2.2	35	6.7	11
28	55	1.9	1.7	55	8.3	11

Appendix B

One-Wave Parameters

Before modeling the two-wave endocrine control of the menstrual cycle, parameters were optimized for the one-wave systems to ensure the systems and computer coding produced the expected results and so we have the best possible starting point. Three merged one-wave systems, the five-hormone McLachlan, the five-hormone Welt and the six-hormone Welt merged model parameters are included in the following three tables. The initial conditions for these three systems are included in Appendix C. The parameters for both Welt systems in Tables B.2 and B.3 were used to obtain the Figures 3.2, 3.2, 4.2, and 4.1.

Table B.1 Parameter results for the five-hormone, one-wave merged model fitting the McLachlan data set. All of the following optimized parameters were truncated to two significant decimal digits.

Param.	**Value**	**Units**
v_{0LH}	1327.30	μg/day
v_{1LH}	40480.61	μg/day
Km_{LH}	275.20	ng/L
$Ki_{LH,P}$	8.81	μg/L
k_{LH}	2.76	1/day
$c_{LH,P}$	0.049	L/μg
$c_{LH,E}$	1.41E-07	L/ng
d_E	0.88	Days
d_P	2.0053	Days
v_{FSH}	5386.74	μg/day
$Ki_{FSH,IHA}$	629.0064	U/L
k_{FSH}	9.21	1/day
$c_{FSH,P}$	540.21	L/μg
$c_{FSH,E}$	0.17	$(\text{L/ng})^2$
d_{IHA}	1.49	Days
α	0.77	Dimensionless
β	0.25	Dimensionless
γ	0.0066	Dimensionless
b	0.0012	L/day
c_1	0.0059	1/day

Param.	**Value**	**Units**
c_2	0.045	$(\text{L/}\mu\text{g})^{\alpha}$(1/day)
c_3	0.00093	$(\text{L/}\mu\text{g})^{\beta}$(1/day)
c_4	0.0022	(L/μg)(1/day)
c_5	1.017	$(\text{L/}\mu\text{g})^{\gamma}$(1/day)
d_1	0.85	1/day
d_2	0.60	1/day
k_1	0.67	1/day
k_2	0.90	1/day
k_3	0.99	1/day
k_4	0.73	1/day
e_0	0.096	ng/L
e_1	0.20	1/kL
e_2	0.0019	1/kL
e_3	0.48	1/kL
p_1	0.026	1/L
p_2	0.042	1/L
h_0	184.44	U/L
h_1	0.91	(U/L)/μg
h_2	0.12	(U/L)/μg
h_3	0.0024	(U/L)/μg
h_4	5.11	(U/L)/μg

Table B.2 Parameter results for the five-hormone, one-wave merged model fitting the Welt data set. All of the following optimized parameters were truncated to two significant decimal digits.

Param.	**Value**	**Units**
v_{0LH}	698.70	IU/day
v_{1LH}	6153.58	IU/day
Km_{LH}	218.20	pg/mL
$Ki_{LH,P}$	4.81	ng/mL
k_{LH}	6.92	1/day
$c_{LH,P}$	2.92	mL/ng
$c_{LH,E}$	0.20	mL/pg
d_E	0.088	Days
d_P	0.35	Days
v_{FSH}	419.87	IU/day
$Ki_{FSH,IHA}$	3.15	IU/mL
k_{FSH}	1.96	1/day
$c_{FSH,P}$	14.025	mL/ng
$c_{FSH,E}$	0.0028	$(\text{mL/pg})^2$
d_{IHA}	1.84	Days
α	0.77	Dimensionless
β	0.014	Dimensionless
γ	0.13	Dimensionless
b	0.15	L/day
c_1	0.13	(L/IU)(1/day)
c_2	0.16	$(\text{L/IU})^{\alpha}(1/\text{day})$

Param.	**Value**	**Units**
c_3	0.020	$(\text{L/IU})^{\beta}(1/\text{day})$
c_4	0.027	(L/IU)(1/day)
c_5	0.56	$(\text{L/IU})^{\gamma}(1/\text{day})$
d_1	0.58	1/day
d_2	0.40	1/day
k_1	0.59	1/day
k_2	1.00	1/day
k_3	0.73	1/day
k_4	0.72	1/day
e_0	28.40	pg/mL
e_1	0.0039	(pg/mL)/IU
e_2	0.016	(pg/mL)/IU
e_3	0.023	(pg/mL)/IU
p_0	0.45	ng/mL
p_1	2.40E-08	(ng/mL)/IU
p_2	0.0030	(ng/mL)/IU
h_0	0.46	IU/mL
h_1	8.97E-07	1/mL
h_2	0.00094	1/mL
h_3	0.00020	1/mL
h_4	0.0011	1/mL

Table B.3 Parameter results for the six-hormone, one-wave merged model fitting the Welt data set. All of the following optimized parameters were truncated to two significant decimal digits.

Param.	**Value**	**Units**
v_{0LH}	750.00	IU/day
v_{1LH}	2828.48	IU/day
Km_{LH}	192.083	pg/mL
$Ki_{LH,P}$	14.55	ng/mL
k_{LH}	1.99	1/day
$c_{LH,P}$	0.25	mL/ng
$c_{LH,E}$	0.0070	mL/pg
d_E	0.44	Days
d_P	1.0059	Days
v_{FSH}	866.40	IU/day
$Ki_{FSH,IHA}$	2.17	IU/mL
k_{FSH}	4.16	1/day
$c_{FSH,P}$	28.87	mL/ng
$c_{FSH,E}$	0.70	$(\text{mL/pg})^2$
d_{IHA}	2.31	Days
$Ki_{FSH,IHB}$	116.030	pg/mL
d_{IHB}	1.84	Days
η	8.98	Dimensionless
δ	0.98	Dimensionless
α	0.75	Dimensionless
β	0.090	Dimensionless
γ	0.065	Dimensionless
f_1	9.50	IU/L
f_2	2.56	IU/day
f_3	0.80	(L/IU)/day
f_4	0.091	$(\text{L/IU})^{\delta}(1/\text{day})$
c_1	0.19	(L/IU)/day

Param.	**Value**	**Units**
c_2	0.20	$(\text{L/IU})^{\alpha}(1/\text{day})$
c_3	0.059	$(\text{L/IU})^{\beta}(1/\text{day})$
c_4	0.03	(L/IU)/day
c_5	0.50	$(\text{L/IU})^{\gamma}(1/\text{day})$
c_6	0.81	1/day
d_1	0.66	1/day
d_2	0.55	1/day
k_1	0.51	1/day
k_2	0.57	1/day
k_3	0.77	1/day
k_4	0.88	1/day
e_0	14.11	pg/mL
e_1	0.010	(pg/mL)/IU
e_2	0.025	(pg/mL)/IU
e_3	0.063	(pg/mL)/IU
p_1	0.0055	(ng/mL)/IU
p_2	0.0015	(ng/mL)/IU
h_0	0.065	IU/mL
h_1	0.0012	1/mL
h_2	0.0018	1/mL
h_3	0.0017	1/mL
h_4	0.00071	1/mL
j_0	27.60	(pg/mL)
j_1	66.00	(pg/mL)/IU
j_2	0.0012	(pg/mL)/IU
j_3	0.020	(pg/mL)/IU

Appendix C

Initial Conditions

Initial conditions are needed for each differential equation in the system to find a solution. Six sets of initial conditions are included in this appendix. Three sets are for merged one-wave models and three sets are for merged two-wave models. In all cases, the initial conditions for FSH and LH are their respective data values for the first day of the cycle. The initial conditions for the merged two-wave models are used in conjunction with the parameters in Chapters 3 and 4 to yield their respective figures.

Table C.1 Initial conditions for the McLachlan five-hormone, one-wave merged model. Parameter values for this model can be found in Appendix B.

State	**Value**	**Units**
$RP_{\mathrm{LH}}(0)$	243.50	μg
LH(0)	25.34	μg/L
$RP_{\mathrm{FSH}}(0)$	100.60	μg
FSH(0)	142.50	μg/L
$RcF(0)$	150.00	μg
$GrF(0)$	590.00	μg
$DomF(0)$	67.80	μg
$OvF_1(0)$	145.30	μg
$OvF_2(0)$	151.50	μg
$Lut_1(0)$	176.20	μg
$Lut_2(0)$	203.20	μg
$Lut_3(0)$	233.70	μg
$Lut_4(0)$	252.10	μg

Table C.2 Initial conditions for the McLachlan five-hormone, two-wave merged model. Parameter values for this model can be found in Chapter 3.

State	**Value**	**Units**
$RP_{\mathrm{LH}}(0)$	83.43	μg
LH(0)	25.34	μg/L
$RP_{\mathrm{FSH}}(0)$	442.29	μg
FSH(0)	142.50	μg/L
$RcF(0)$	790.68	μg
$GrF(0)$	1160.43	μg
$DomF(0)$	113.01	μg
$OvF_1(0)$	24.77	μg
$OvF_2(0)$	15.19	μg
$Lut_1(0)$	14.94	μg
$Lut_2(0)$	37.76	μg
$Lut_3(0)$	104.52	μg
$Lut_4(0)$	140.12	μg

Table C.3 Initial conditions for the Welt five-hormone, one-wave merged model. Parameter values for this model can be found in Appendix B.

State	**Value**	**Units**
$RP_{\mathrm{LH}}(0)$	29.50	IU
LH(0)	12.00	IU/L
$RP_{\mathrm{FSH}}(0)$	10.60	IU
FSH(0)	11.40	IU/L
$RcF(0)$	5.25	IU
$GrF(0)$	9.25	IU
$DomF(0)$	3.50	IU
$OvF_1(0)$	3.00	IU
$OvF_2(0)$	15.00	IU
$Lut_1(0)$	44.00	IU
$Lut_2(0)$	63.00	IU
$Lut_3(0)$	76.00	IU
$Lut_4(0)$	105.00	IU

Table C.4 Initial conditions for the Welt five-hormone, two-wave merged model. Parameter values for this model can be found in Chapter 3.

State	**Value**	**Units**
$RP_{\mathrm{LH}}(0)$	25.52	IU
LH(0)	12.00	IU/L
$RP_{\mathrm{FSH}}(0)$	6.08	IU
FSH(0)	11.40	IU/L
$RcF(0)$	173.30	IU
$GrF(0)$	479.49	IU
$DomF(0)$	27.55	IU
$OvF_1(0)$	23.21	IU
$OvF_2(0)$	49.94	IU
$Lut_1(0)$	152.93	IU
$Lut_2(0)$	501.65	IU
$Lut_3(0)$	1392.90	IU
$Lut_4(0)$	2174.70	IU

Table C.5 Initial conditions for the Welt six-hormone, one-wave merged model. Parameter values for this model can be found in Appendix B.

State	**Value**	**Units**
$RP_{\mathrm{LH}}(0)$	83.00	IU
$\mathrm{LH}(0)$	12.00	IU/L
$RP_{\mathrm{FSH}}(0)$	11.49	IU
$\mathrm{FSH}(0)$	11.40	IU/L
$PrAn(0)$	0.07	IU
$SmAn(0)$	0.22	IU
$RcF(0)$	1.74	IU
$GrF(0)$	8.21	IU
$DomF(0)$	8.23	IU
$Ov1(0)$	10.79	IU
$Ov2(0)$	42.65	IU
$Ov2(0)$	208.47	IU
$Lut_1(0)$	649.37	IU
$Lut_2(0)$	1123.31	IU
$Lut_3(0)$	1191.70	IU
$Lut_4(0)$	1344.30	IU

Table C.6 Initial conditions for the Welt six-hormone, two-wave merged model. Parameter values for this model can be found in Chapter 4.

State	**Value**	**Units**
$RP_{\mathrm{LH}}(0)$	76.73	IU
$\mathrm{LH}(0)$	12.00	IU/L
$RP_{\mathrm{FSH}}(0)$	17.85	IU
$\mathrm{FSH}(0)$	11.40	IU/L
$PrAn(0)$	0.04	IU
$SmAn(0)$	0.23	IU
$RcF(0)$	42.05	IU
$GrF(0)$	344.20	IU
$DomF(0)$	277.38	IU
$Ov1(0)$	590.44	IU
$Ov2(0)$	1113.43	IU
$Ov2(0)$	1461.18	IU
$Lut_1(0)$	1590.26	IU
$Lut_2(0)$	1535.22	IU
$Lut_3(0)$	1942.47	IU
$Lut_4(0)$	2333.00	IU